Briefing for PWSRCAC Board of Directors – January 2024

ACTION ITEM

Sponsor: Danielle Verna and the Scientific Advisory Committee
Project number and name or topic: 9510 Long-Term Environmental Monitoring Program

1. **Description of agenda item:** The Board is being asked to accept the report titled "Long-Term Environmental Monitoring Program 2022–2023 Summary Report" and the accompanying 2022–2023 Technical Supplement by Dr. Morgan Bender of Owl Ridge Natural Resource Consultants, Inc., both dated December 2023. The report and technical supplement provide data and results from the 2022 and 2023 sampling excursions in Port Valdez and Prince William Sound for the Council's Long-Term Environmental Monitoring Program (LTEMP), now in its 30th year.

2. **Why is this item important to PWSRCAC:** The Oil Pollution Act of 1990 directs PWSRCAC to "devise and manage a comprehensive program of monitoring the environmental impacts of the operations of terminal facilities and crude oil tankers while operating in Prince William Sound" – LTEMP is designed to address this directive. LTEMP results are used to assess the environmental impacts of the Valdez Marine Terminal and the crude oil tankers operating in Prince William Sound, including the long-term impacts of the Exxon Valdez oil spill.

3. **Previous actions taken by the Board on this item:** The Long-Term Environmental Monitoring Program has been conducted by PWSRCAC since 1993, and many actions have been taken by the Board on this item since that time. In the interest of providing recent pertinent information, only the last five years of actions related to LTEMP are presented below. All historic actions pertaining to this agenda item are available for review upon request (for more information contact Danielle Verna).

Meeting	Date	Action
Board	5/2/2019	The Board authorized contract negotiations with Payne Environmental Consultants for sampling and analytical report work on mussels and sediments to be performed under LTEMP for FY20, at an amount not to exceed $65,866; and authorized contract negotiations with Newfields Environmental Forensics Practice for analytical laboratory work and sample storage to be performed under LTEMP for FY20 at an amount not to exceed $28,506. Authorized contract negotiations with Oregon State University for passive sample device purchase and analytical laboratory work on passive sampling devices to be performed under LTEMP for FY20, at an amount not to exceed $20,590; and authorized contract work to commence prior to the start of FY20, as approximately $20,000 of these funds will need to be expended in May and June 2019 because of the supply prerequisites and sampling timing.
Board	9/19/2019	The Board accepted the report titled "Long Term Environmental Monitoring Program: 2018 Sampling Results and Interpretations" by Dr. James R. Payne and William B. Driskell, dated July 2019 as meeting the terms of the contract and for distribution to the public.

Board	5/7/2020	The Board accepted the report titled "Long-Term Environmental Program: 2019 Sampling Results and Interpretations," by Dr. James Payne and William B. Driskell, dated March 2020, as meeting the terms and conditions of contract number 951.20.04, and for distribution to the public.
Board	5/21/2020	Approval of FY2021 Contracts for Project 9510 LTEMP - The Board approved the following: Authorizing a contract negotiation with Payne Environmental Consultants Inc., for work to be performed under LTEMP, at an amount not to exceed $115,064. Authorizing a contract negotiation with Newfields Environmental Forensics Practice, for work to be performed under LTEMP, at an amount not to exceed $95,807. Authorizing a contract negotiation with the United States Geological Survey, for work to be performed under LTEMP, at an amount not to exceed $65,371. Authorizing a contract negotiation with Oregon State University, for work to be performed under LTEMP, at an amount not to exceed $22,030. Authorizing a contract work to commence prior to the start of FY2021, as approximately $33,000 of these funds will need to be expended in May and June 2020.
Board	5/6/2021	LTEMP 2020 Sampling Results & Interpretations Report Approval: The Board accepted the reports titled "Long Term Environmental Monitoring Program: 2020 Sampling Results & Interpretations," by Dr. James R. Payne and William Driskell, dated March 2021 as meeting the terms and conditions of contract 951.21.04, and for distribution to the public.
Board	5/21/2021	Approval of FY2022 LTEMP Contractors: The Board Authorized individual contracts with NewFields Environmental Forensics Practice, Oregon State University, and the USGS with the aggregate total not to exceed the amount approved in the final FY2022 LTEMP budget (project #9510) for contract expenses, and delegated authority to the Executive Director to enter into individual contracts with the aforementioned consultants; and authorized that the contract work to commence prior to the start of FY2022 as approximately $30,000 of these funds will need to be expended in May and June 2021.
Board	1/27/2022	LTEMP FY2022 Contract Approval: The Board authorized a budget modification, adding $53,880 to Project 9510-Long-Term Environmental Monitoring Program; and authorized a contract negotiation with Owl Ridge Natural Resource Consultants, to complete the LTEMP scope of work in RFP 951.21.06, and with Payne Environmental Consultants, to support Owl Ridge's work, at a total aggregate cost not to exceed $77,000.
Board	6/21/2022	FY2023 LTEMP Contract Change Order: The Board approved an FY2023 budget modification, adding $6,478 to project #9510 – Long-Term Environmental Monitoring Program, for contract expenses; and, approved a negotiation of a contract change order, for contract #951.22.06, with Owl Ridge Natural Resource Consultants, adding $6,478 for compensation to archive the 1993-2021 LTLEMP data in the Alaska Ocean Observing System.
Board	1/26/2023	Approval Of LTEMP Budget Modification And Contract Change Order: The Board authorized an FY2023 budget modification from the contingency fund to project #9510 – Long Term Environmental Monitoring Program adding $836 for contract expenses and approval of negotiation of a contract change order, for contract #951.22.06, with Owl Ridge Natural Resource Consultants, adding $5,058 for compensation to archive the 1993-2021 LTEMP data in the Alaska Ocean Observing System and extending the term of the contract to March 31, 2023. [Note: This change order would increase the total contract amount to $68,007.]
Board	5/4/2023	Approval Of FY2024 LTEMP Contract Authorization: The Board approved the following: a) Authorization of individual contracts with Alpha Analytical and Owl Ridge Natural Resource Consultants, Inc. with the aggregate total not to exceed the amount approved in the final FY2024 LTEMP budget (Project #9510) for contract expenses, and b) Authorization of contract work to commence prior to the start of the 2024 fiscal year to accommodate timing considerations and

purchasing needs. It is estimated that up to $15,000 of the above contract work may be performed before June 30, 2023.

4. **Summary of policy, issues, support, or opposition:** None.

5. **Committee Recommendation:** The Scientific Advisory Committee has reviewed the report and technical supplement, and recommended the Board accept the material as final, at its meeting on December 5, 2023.

6. **Relationship to LRP and Budget:** Project 951 / Long Term Environmental Monitoring Program is in the approved FY2024 budget and annual work plan.

9510 – Long Term Environmental Monitoring

As of December 19, 2023

Original Budget	$173,636.79
Revised Budget	$157,372.79
Actual & Commitments	$133,054.90
Amount Remaining	$24,318.89

7. **Action Requested of the Board of Directors:** Accept the reports titled “Long-Term Environmental Monitoring Program 2022–2023 Summary Report” and “Long-Term Environmental Monitoring Program 2022–2023 Technical Supplement” by Morgan Bender of Owl Ridge Natural Resource Consultants, Inc., both dated December 2023, as meeting the terms and conditions of contract number 951.24.04, and for distribution to the public.

8. **Alternatives:** None.

9. **Attachments:**
   A) “Long-Term Environmental Monitoring Program 2022–2023 Summary Report”
   B) “Long-Term Environmental Monitoring Program 2022–2023 Technical Supplement”

This page intentionally left blank.

Final

Long-Term Environmental Monitoring Program

2022–2023 Summary Report

December 2023

Prepared for:
Prince William Sound Regional Citizens' Advisory Council
3709 Spenard Road, Suite 100
Anchorage, Alaska 99503

Prepared by:
Morgan L. Bender, Ph.D.
Owl Ridge Natural Resource Consultants, Inc.
4060 B Street, Suite 200
Anchorage, Alaska 99503
T: 907.344.3448
www.owlridgenrc.com

"The opinions expressed in this PWSRCAC commissioned report are not necessarily those of PWSRCAC. PWSRCAC Contract #951.24.04."

Document Number: PWS002-23-001F0

TABLE OF CONTENTS

ACRONYMS AND ABBREVIATIONS

ANS	Alaska North Slope
BWTF	Ballast Water Treatment Facility
EPA	U.S. Environmental Protection Agency
EVOS	Exxon Valdez Oil Spill
LTEMP	Long-Term Environmental Monitoring Program
NOAA	National Oceanic and Atmospheric Administration
PAHs	Polycyclic aromatic hydrocarbons
PPB (or ng/g)	Parts Per Billion
PWSRCAC	Prince William Sound Regional Citizens' Advisory Council
UV	Ultraviolet

ABSTRACT

To understand the environmental impact, fate, and source of hydrocarbons related to the operations of Alyeska Pipeline Service Company's Valdez Marine Terminal, hydrocarbon concentrations were monitored in sediments, in intertidal Pacific blue mussels, and in the water via passive sampling devices. In the 2022 and 2023 results, we see low levels of petroleum (petrogenic) hydrocarbons in sediments at the terminal that can be attributed to terminal operations. Passive water sampling devices and Pacific blue mussels from all sampled locations had low levels of toxic hydrocarbons. Sediment and mussels sampled from sites away from the terminal in Port Valdez contained more combustion (pyrogenic) related compounds than detected at the terminal. In 2022, mussels from the Valdez Small Boat Harbor had the highest levels of hydrocarbons, likely due to frequent small spills and heavy human activity not forensically attributed to terminal operations. In 2023, higher polycyclic aromatic hydrocarbons (PAH) levels were found in some mussel samples at Knowles Head in northeastern Prince William Sound than those in the harbor. Other mussel sites sampled in 2023 as part of the expanded sampling regime included Disk Island, Zaikof Bay, a new site in outer Zaikof Bay, Sleepy Bay, and Sheep Bay. Generally, the expanded sampling sites had comparable PAH levels to annual sampling sites (e.g., Gold Creek and sites near the terminal) with low potential hydrocarbon ecotoxicity for organisms.

In 2022 and 2023, the hydrocarbons detected by the Long-Term Environmental Monitoring Program sampling, and determined to be from the terminal and tankers, posed low potential ecotoxicological risk. Since 1993, hydrocarbon concentrations are generally low with localized spikes corresponding with spill events like the April 2020 oil spill at the terminal. Following an all-time low in the mid-2010s, hydrocarbon concentrations detected in sediments and mussels have slowly increased across all sites but are still below any threshold for adverse effects on aquatic life. Prince William Sound-wide trends in these hydrocarbon concentrations may be influenced by environmental factors such as increased freshwater input, glacial melt, and warming ocean temperatures. We recommend that future monitoring efforts maintain the current three-matrix design and attempt to preserve, economize, and modernize aspects of Prince William Sound Regional Citizens' Advisory Council's Long-Term Environmental Monitoring Program.

1. INTRODUCTION

The Long-Term Environmental Monitoring Program (LTEMP), managed by the Prince William Sound Regional Citizens' Advisory Council (PWSRCAC), is in its 30th year of monitoring hydrocarbons in the wake of the Exxon Valdez oil spill. Through LTEMP, we are able to determine the source of hydrocarbons and the potential adverse effects on the ecosystem from Alyeska Pipeline Service Company's Valdez Marine Terminal (terminal) and tanker activity. These data have been insightful in understanding the influence of terminal and non-terminal sources of hydrocarbons and environmental factors on hydrocarbon dynamics across Prince William Sound and the Gulf of Alaska.

Hydrocarbons are an extremely diverse group of compounds that make up the bulk of petroleum products like crude oil, fuel, and various maritime products like hydraulic and motor oil. However, hydrocarbons are also readily created by marine and terrestrial plants, locked up in organic sediments and rocks, and produced by combustion. Hydrocarbons in the environment undergo processes called weathering, which includes dissolution, evaporation, ultraviolet (UV) degradation, and microbial degradation. These change the physical and chemical properties of the released oil. Polycyclic aromatic hydrocarbons (PAHs) are a group of hydrocarbons in oil with varying numbers of benzene rings that are relatively resistant to degradation and toxic to living organisms. This group of chemicals tends to adsorb rapidly on suspended materials and sediments, and accumulate in biological tissues once released into the marine environment.

PAHs, as a group, are comprised of hundreds of compounds, each with its own degree of toxicity, and their mixtures can exhibit a wide range of toxicities. Specific hydrocarbons, patterns, and diagnostic compounds (i.e., chemical biomarkers) aid in the identification of specific hydrocarbon sources and are indicative of their weathering history (e.g., degree of weathering, degradation, dissolution). PAH profiles are used to identify petrogenic (of crude oil origin) or pyrogenic (of combustion origin), based on well-established pattern changes (e.g., on the ratio of parent and alkylated compounds). Chemical biomarkers, comprising the hopanes, steranes, terpenes, triaromatic, and monoaromatic steroids, are much more resistant to degrading in the environment and thus used to confirm sources (e.g., between different crude oils) even when the PAH patterns are heavily weathered. Saturated hydrocarbons (n-alkanes) are used to identify naturally occurring plant hydrocarbons and determine the degree of weathering and biodegradation.

While many aquatic organisms like fish can metabolize PAHs, marine invertebrates, such as Pacific blue mussels, are less able to efficiently metabolize these compounds, remain sedentary in a fixed location, filter particles from their immediate surroundings, and therefore serve as efficient natural samplers and indicators of overall environmental PAH exposure (Neff and Burns 1996). Toxic responses to PAHs in aquatic organisms include inhibiting reproduction, developmental effects, tissue damage, cellular stress, oxidative stress, damage to genetic material, and mortality. While the body of knowledge on the adverse effects of petroleum exposure is immense, specifics regarding PAH mixtures, exposure routes, duration and magnitude, species and life stages exposed, and other environmental factors that may act synergistically on organisms, challenge the predictive ability of any hydrocarbon study and necessitate the continued monitoring efforts of LTEMP.

The ubiquity of hydrocarbons in the environment complicates tracing sources, understanding ecotoxic thresholds, and following dynamics over time and space. Environmental samples, like sediments, can accumulate multiple hydrocarbon sources over time, resulting in a mixed or unresolved profile. Organisms such as blue mussels can accumulate, eliminate, or alter hydrocarbon compounds, which complicates the task of identifying the sources. Passive sampling devices are specifically designed to complement the biological and toxicological interpretations by measuring just the dissolved compounds available to aquatic organisms (the bioavailable fraction) but are not well suited for hydrocarbon forensics. Sources investigated for the present study are those associated with terminal operations, including Alaska North Slope (ANS) crude oil (which is pumped through the trans-Alaska pipeline and is loaded into tankers at the terminal), effluent from the Ballast Water Treatment Facility (BWTF) at the terminal, and samples from recent spills at the terminal.

The following study presents the 2022 and 2023 results from the LTEMP and aims to determine:

- The extent, if any, that the terminal and associated tankers' hydrocarbon fingerprint is present in 2022 and 2023 samples with varying ranges from the terminal.
- The potential ecotoxicological risk posed by the measured hydrocarbon contribution from the terminal and tankers.
- The historical trends, ecotoxicological risk, and hydrocarbon fingerprint from mussels collected from extended sampling sites across greater Prince William Sound in 2023.
- Other factors (e.g., environmental or anthropogenic) that may be influencing hydrocarbon presence and composition in 2022 and 2023 samples, and the ecotoxicological relevance of these results.
- Recommendations for future monitoring of petroleum hydrocarbons at the terminal and in Prince William Sound.

2. RESULTS AND DISCUSSION

Sediment, passive sampling device, and Pacific blue mussel tissue samples were collected in June of 2022 and 2023 from annual and quinquennial expanded sampling at LTEMP monitoring stations in Port Valdez and greater Prince William Sound. The sampling program investigated three matrices: sediment, Pacific blue mussels, and water quality. For 2022 and 2023 sediments were sampled at two sites –Alyeska's Valdez Marine Terminal and Gold Creek (Figure 1). In 2022, Pacific blue mussel samples were taken from four sites around the Port of Valdez with a focus on the terminal – Saw Island, Jackson Point, Gold Creek, and Valdez Small Boat Harbor entrance (RED - a site that is chemically different from the ANS terminal source signature and currently acts as a high human use, non-ANS reference site). In 2023, mussels were collected from the four standard sites in Port Valdez in addition to the quinquennial expanded sampling sites of Knowles Head, Disk Island, Zaikof Bay, a new station in outer Zaikof Bay, Sleepy Bay, and Sheep Bay. Three Gulf of Alaska stations (i.e., Aialik Bay, Windy Bay, and Shuyak Harbor) planned to be included in the five-year survey will instead be sampled in 2024 due to weather preventing sampling in 2023. Water was sampled with passive sampling devices at three sites in 2022 — Gold Creek, Jackson Point, and Saw Island. In 2023 passive sampling devices were again deployed at Gold Creek, Jackson Point, and Saw Island, and additional devices were deployed at Knowles Head and Disk Island; the Knowles Head devices could not be relocated due to a severed line and were not retrieved.

Samples were analyzed for PAHs, saturated hydrocarbons, and geochemical petroleum biomarkers using advanced analytical techniques at the NewFields (2022) and Alpha Analytical Laboratory (2023) in Mansfield, Massachusetts (sediments and tissues), and the Oregon State University Food Safety and Environmental Stewardship lab in Corvallis, Oregon (passive sampler, PAHs only). These are the same laboratories that have participated in the LTEMP effort for the last eight years. Briefly, the results continue to be of acceptable precision and accuracy and can be compared to previous years' data. Physical characteristics of sediments were also reported in laboratory results though not presented herein.

Many compounds, especially in the mussel tissues, were below or near the analytical methods detection limit or were not detected in the sample. Sediment and mussel tissue concentrations are plotted and discussed as a sum of multiple PAHs (sum PAH) either by dry weight or wet weight where appropriate. Passive sampling device concentrations have been converted by the analytical lab into the dissolved-phase water concentration, C-free concentration. By converting the concentration units, comparisons can be made across other studies, areas, and ecotoxicological effect thresholds. Concentrations below the method level of detection threshold were provided by the lab as an estimate. These estimated concentrations were plotted on PAH profile figures and included in sum calculations; compounds that were not detected in a sample or were biased by laboratory issues were not included in the sum calculations. Forensic interpretation was done using analyte profile pattern comparisons for likely petroleum sources (i.e., ANS crude, a sample of the April 2020 oil spill at the terminal, and a spring 2017 effluent sample from the BWTF) for PAH, geochemical petroleum biomarkers, and saturated hydrocarbons in sediment sample. Blue mussels and passive sampling devices tentative forensic assertions were made by qualitative ratios of parent to alkylated compounds and low and high molecular weight PAH compounds. Analytical results and calculations for all samples and all analytes, pattern profiles, forensic ratios, and laboratory blanks are presented in the Technical Summary (Owl Ridge 2023) to support the assertions made in this summary report.

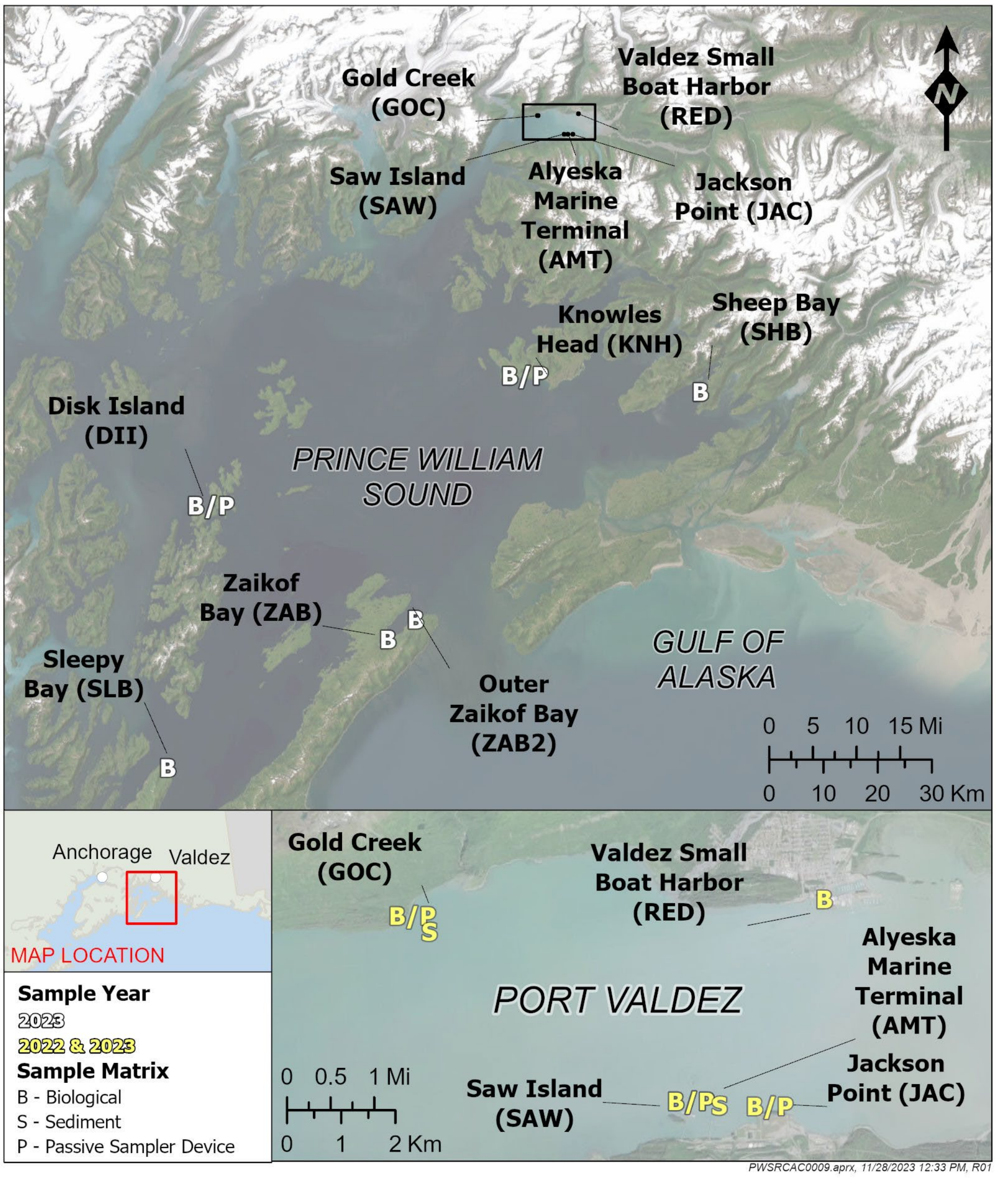

Figure 1. Map of 2022 and 2023 LTEMP sites for sediment (S), Pacific blue mussels (B), and passive sampling devices (P).

2.1. Sediments

Hydrocarbons were detected in all sediments sampled at the terminal and Gold Creek sites in the low parts per billion range (ppb or ng/g). One (1) ng/g or 1 ppb can be visualized as the concentration of 50 drops in an Olympic-sized swimming pool. In 2022, the highest sum (∑) PAH concentrations were found in the Gold Creek sediment (17.6±22.0 ng/g dry weight), while in 2023 the highest concentrations were found in the terminal sediments (41.1±5.7 ng/g dry weight) (Figure 2 and Figure 3). Naphthalenes and alkylated fluorenes, phenanthrenes, fluoranthenes/pyrenes, and chrysenes made up the bulk of PAHs at Gold Creek in 2022 and 2023 (see Figure 4 for 2023 results). At the terminal, similar compounds made up the bulk of detectable PAHs for both years but with great contribution from naphthobenzothiophenes. For comparison, PAH concentrations across both Port Valdez sites are lower than those reported in Norwegian fjords, Novia Scotia small boat harbors, and the Baltic Sea (Oen et al. 2006; Davis et al. 2018; Pikkarainen 2010). Present Port Valdez concentrations were more similar to those reported from sediments of Cook Inlet and St. Paul Island, Alaska (Nesvacil et al. 2016).

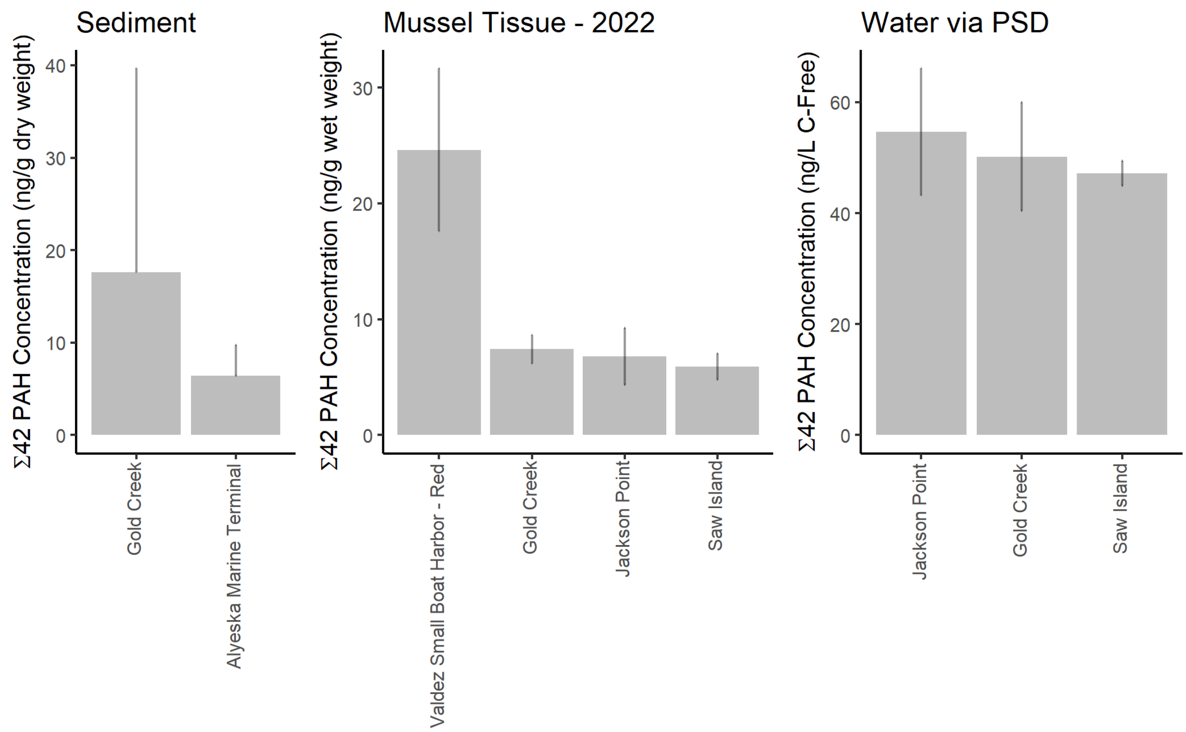

Figure 2. ∑ PAH concentrations for 2022 sediments, Pacific blue mussel tissues, and water sampled via passive sampling devices by site plotted at the mean ± 1 standard deviation. Due to large deviation between replicate samples, standard deviation was plotted only in the positive direction for sediment samples. Note difference in units between matrices (i.e., parts per billion for sediments and mussel tissues and parts per trillion for passive sampling devices).

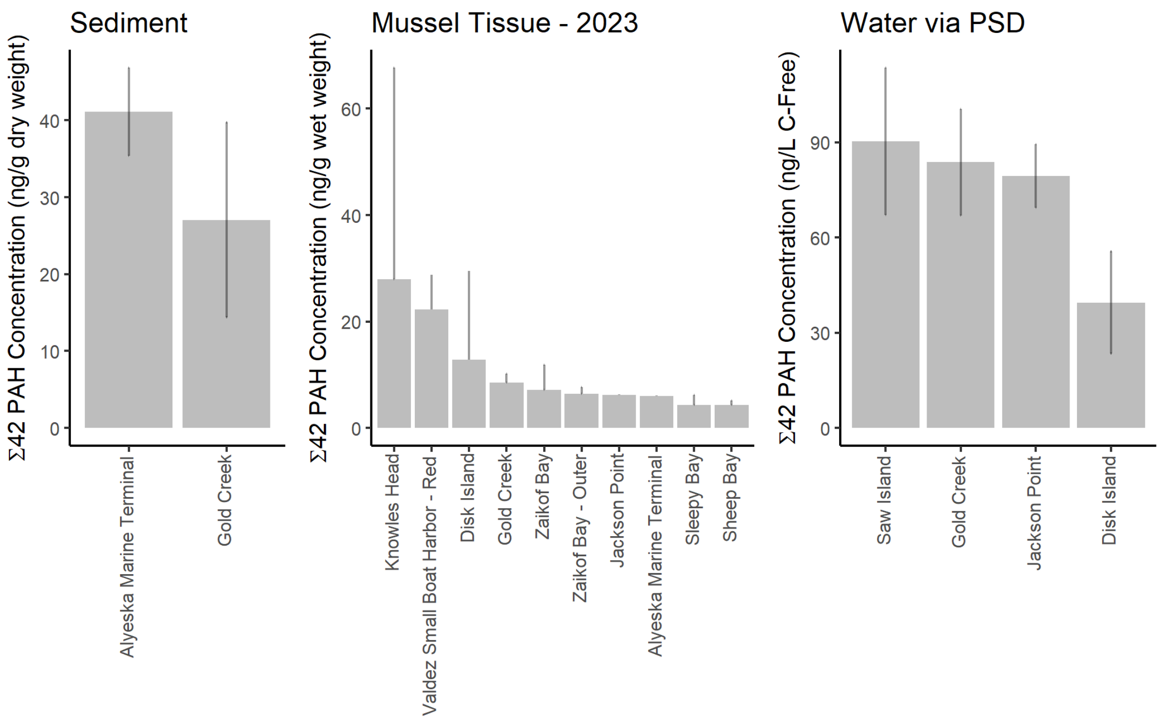

Figure 3. ∑ PAH concentrations for 2023 sediments, Pacific blue mussel tissues, and water sampled via passive sampling devices by site plotted at the mean ± 1 standard deviation. Due to a large deviation between replicate samples, standard deviation was plotted only in the positive direction for mussel samples. Note difference in units between matrices (i.e., parts per billion for sediments and mussel tissues and parts per trillion for passive sampling devices).

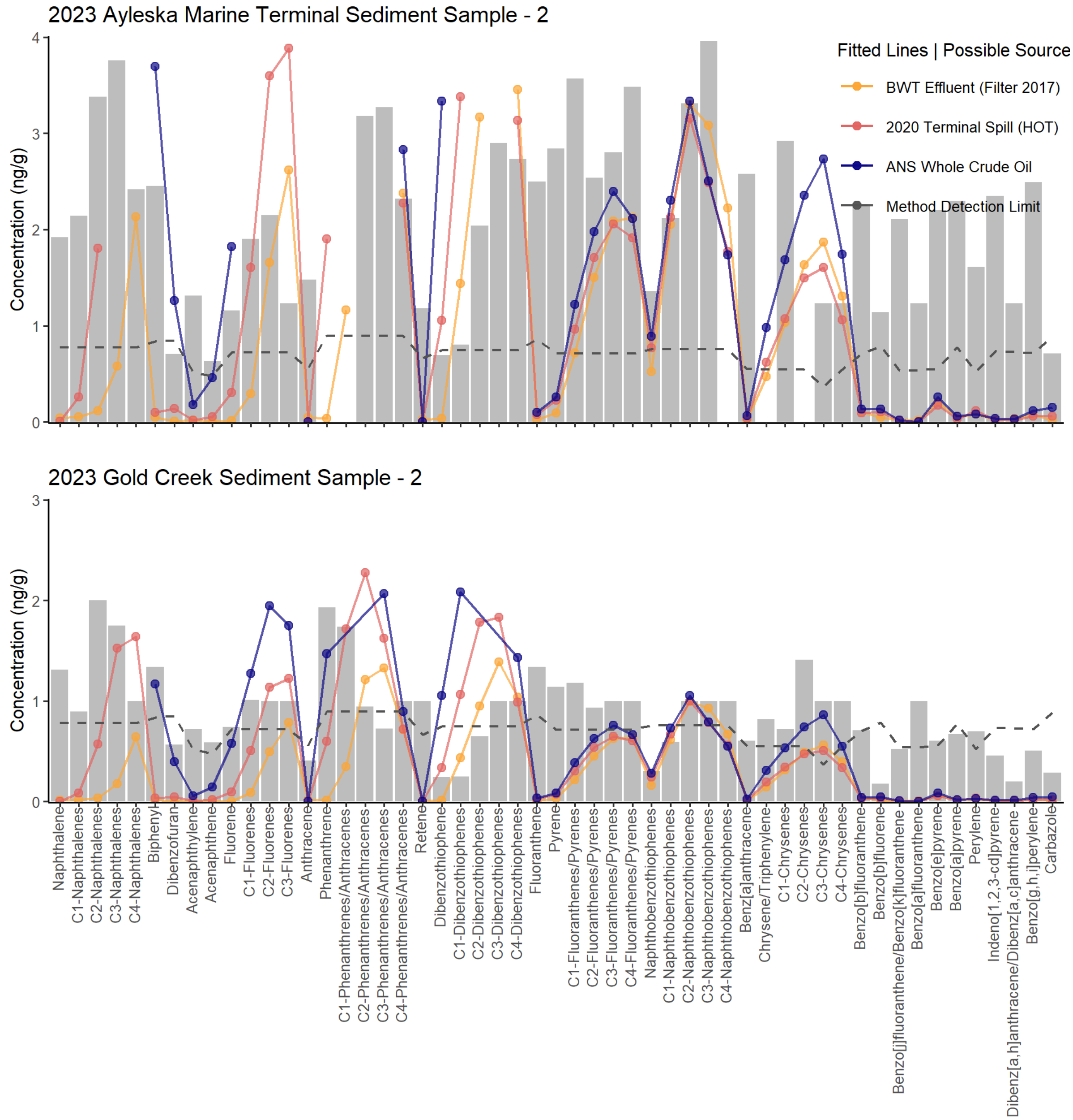

Figure 4. 2023 PAH profiles from sediments sampled at the terminal and Gold Creek site. Each plot displays a representative sample from the three replicates analyzed (note difference in y-axis scale). Possible Alaska North Slope Crude related source profiles are super imposed as different colored lines. A dashed, dark line indicated the analyte specific method detection limit.

2.1.1. Ecotoxicological Interpretation

In 2022 and 2023, individual and ∑ PAH concentrations in sediment at the terminal and Gold Creek sites pose little to no acute or chronic risk for marine organisms with concentrations of individual compounds and sums 1% or less than the U.S. Environmental Protection Agency (EPA) sediment quality PAH benchmarks for aquatic life (EPA 2016). While benthic communities adapted to the cold and sediment-rich waters of Port Valdez may not be adequately represented in these EPA benchmarks, past monitoring efforts around the terminal have indicated little to no change in the benthic community with varying PAH concentrations (Shaw and Blanchard 2021). The total organic carbon concentration in the sediment is low (0.4–0.6%), which indicates higher bioavailability of PAHs to marine organisms. High molecular weight PAHs are detected in sediments but concentrations of this group do not exceed any protective benchmarks nor are these compounds generally present in oil. Known carcinogenic PAHs are present in low concentrations at both sites.

2.1.2. Site-Specific Source Identification

Using PAH and biomarker profiles, the source of the hydrocarbons in the 2022 and 2023 terminal sediments is determined to be mostly petrogenic and derived from ANS crude oil. Biomarker patterns closely match those of previous oil spills at the terminal in 2017 and April 2020 (Payne and Driskell 2021) and particulate-phase oil in the effluent from the BWTF (Payne and Driskell 2018). The diagnostic biomarkers confirm ANS crude oil as the source. Two other patterns are also seen including a water-washing weathering of fluorenes and pyrogenic indicative phenanthrene/anthracene ratios. Accumulation of higher molecular weight alkylated PAHs, likely from local combustion sources, indicates residuals of prior PAH inputs inefficiently degraded over time, especially in 2023 samples. Saturated hydrocarbons in the terminal sediment reveal strong microbial degradation and weathering of the hydrocarbons leaving the higher molecular weight compounds (and in some cases, terrestrial plant wax compounds).

At Gold Creek, chemical biomarkers were sparse compared to those at the terminal, still petrogenic biomarker traces confirm the oil signal as a distant source. However, the PAH patterns are mixed petrogenic and pyrogenic. Gold Creek sediments are moderately weathered with a near complete loss of saturated hydrocarbons, except those contributed by terrestrial plants. In summary, relatively low hydrocarbon concentrations in the terminal sediments are linked to the terminal activities and incidents (BWTF effluent, spills, and combustion) with residues that have undergone environmental degradation and accumulated over time. Gold Creek sediments show mixed pyrogenic and lower petrogenic sources with a greater degree of weathering.

2.1.3. Historical Perspective

Hydrocarbon concentrations have varied widely throughout the LTEMP monitoring period from 1993 to the present (Figure 5). The highest sediment PAH concentrations were measured in the early 2000s at nearly 36 times the present concentrations. Since 2005, hydrocarbon concentrations have remained low with an all-time low seen in the mid-2010s. Since the low, a gradual increase in PAHs has been measured in sediments at the terminal and Gold Creek (Figure 5B). Terminal sediments have generally contained higher, more variable PAH loads than Gold Creek although considerable overlap in PAH concentration ranges between the two stations has persisted since 2008.

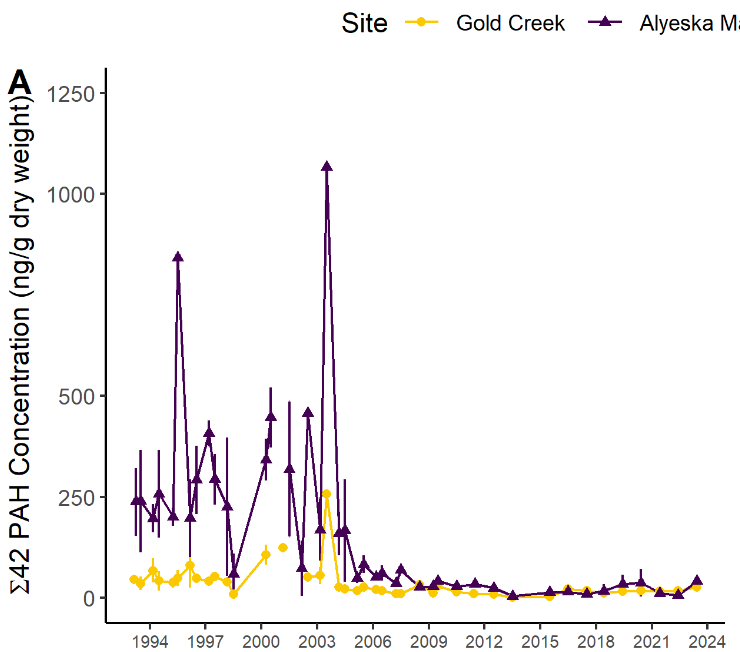

Figure 5. Sum 42 PAH concentrations in sediments (A) over the entire duration of the LTEMP and (B) since 2005 when concentrations have remained relatively low. Note the difference in scale. Colors and shapes indicate sampling site; mean values ± 1 standard deviation are plotted for each sampling event.

2.2. Pacific Blue Mussels

PAHs were detected in Pacific blue mussels (*Mytilus trossulus*) at low to moderate concentrations at all sites (Figure 2 and Figure 3). In 2022, the highest PAH concentrations were found at the Valdez Small Boat Harbor entrance, a non-ANS positive control site at the red harbor navigation light (range 18.4–32.2 ng/g wet weight; Figure 6). PAH concentrations in 2022 were similar at Gold Creek, Saw Island, and Jackson Point (range 4.7–9.5 ng/g wet weight). In 2023, mussels were collected from ten sites around the terminal, Port Valdez, and greater Prince William Sound (Figure 7). Samples were intended from the North Gulf coast of Alaska but these were not collected in 2023 due to inclement weather. The highest (and lowest) PAH levels were seen in mussels from Knowles Head in northeastern Prince William Sound (range 2.8–73.8 ng/g wet weight) although variability between replicates was high. Other relatively high PAH levels were found in mussels from the Valdez Small Boat Harbor and Disk Island.

Phenanthrene was the most abundant PAH at sites in 2022 except for the harbor where larger PAHs were more prevalent (Figure 6). In 2023, higher molecular weight PAHs were found in some replicates from Disk Island, Knowles Head, and the Valdez Small Boat Harbor, while Naphthalene and Phenanthrene were most prevalent at other Port Valdez sites, Sleepy Bay, and other Zaikof Bay sites.

The 2022 and 2023 mussel tissue PAH concentrations in Port Valdez are comparable to those found in relatively pristine locations in national parks and forests around southcentral and southeast Alaska and well below the high concentrations (>1000 ng/g dry weight (138 ng/g wet weight when using mean conversion factor from LTEMP mussel data)) found in the harbor at Skagway, Alaska

(Rider 2020). Only mussels from the Valdez Small Boat Harbor exceeded National Oceanic and Atmospheric Administration's (NOAA) national long-term monitoring status "Low Concentration" range (0–173 ng/g dry weight (0–24 ng/g wet weight)). Like the Valdez Small Boat Harbor location, fluoranthene was also the most abundant PAH in mussels in a Norwegian fjord with moderate human activity where sum PAH concentrations were otherwise comparable to this study (Schøyen et al. 2017). Mussel tissue PAH concentrations were comparable to those measured in pelagic zooplankton in Valdez Arm (Carls et al. 2006) and to mussels caged two kilometers or greater from an oil rig in the North Sea (Sundt et al. 2011).

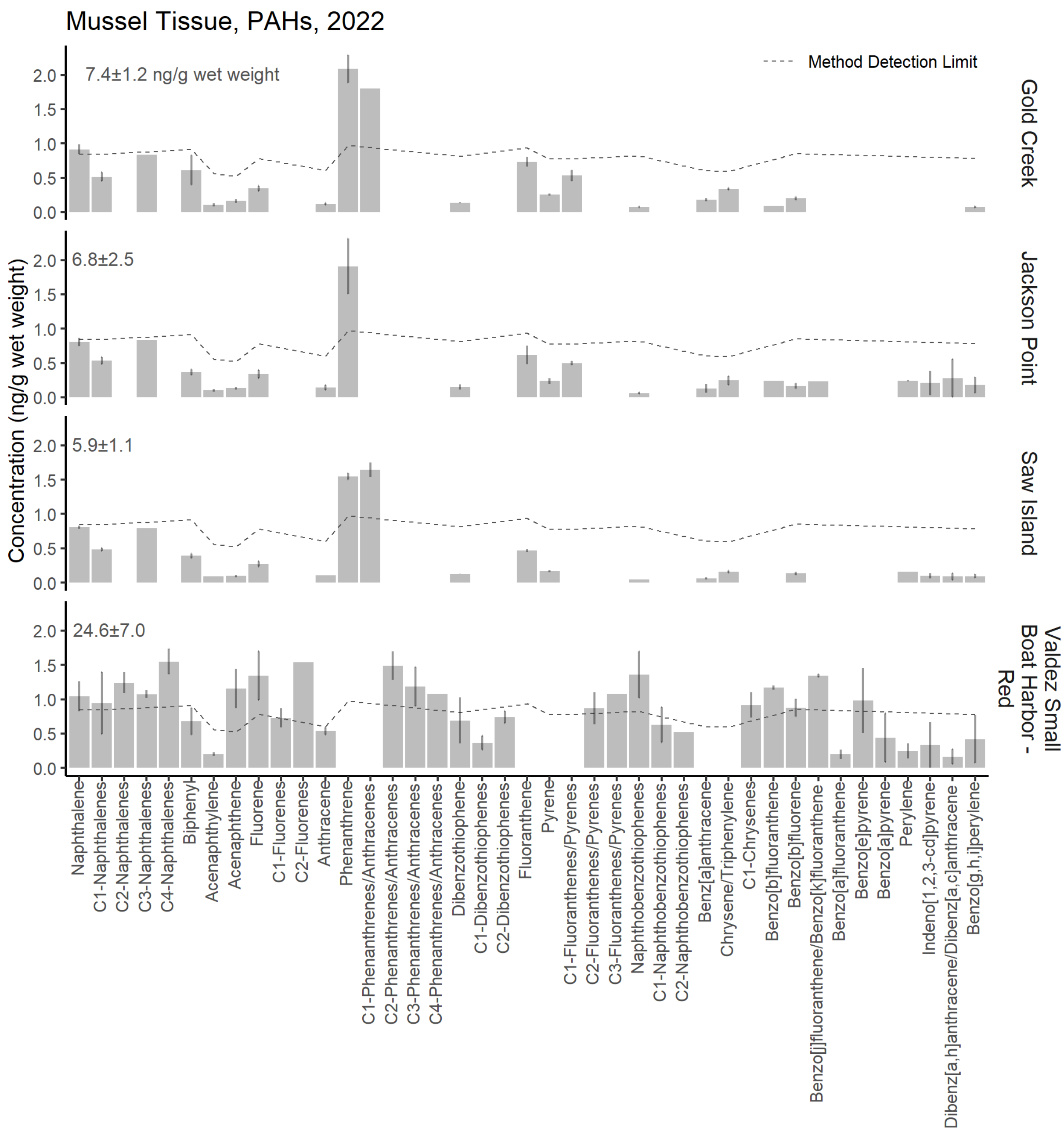

Figure 6. PAH profiles from Pacific blue mussels sampled at four sites in Port Valdez in 2022. Values represent mean ± 1 standard deviation and sum 42 PAH values are displayed in the upper left of each profile. The dashed line represents the PAH specific method detection limit.

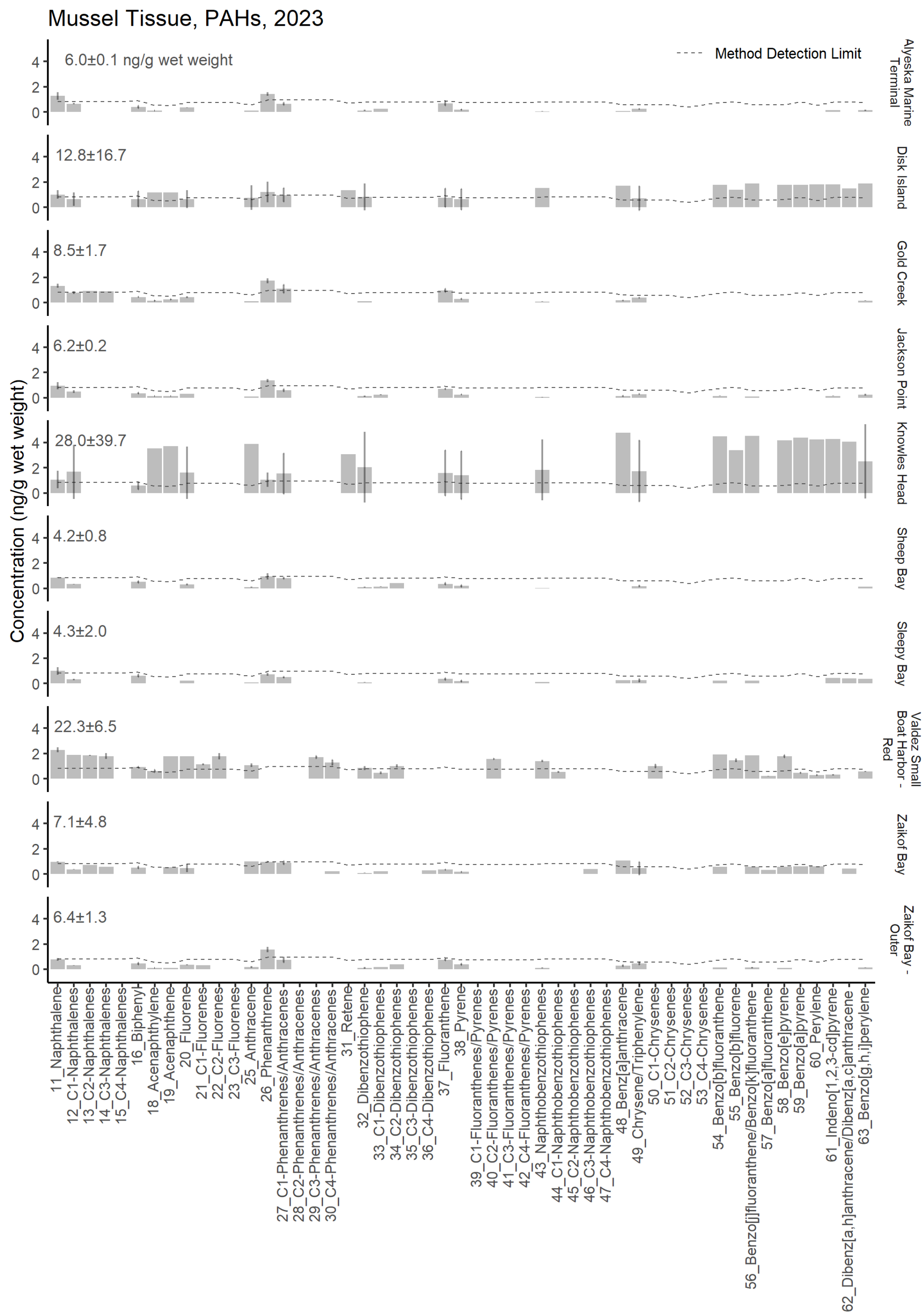

Figure 7. 2023 PAH profiles from Pacific blue mussels sampled at ten sites in Port Valdez and Prince William Sound. Values represent mean ± 1 standard deviation and sum 42 PAH values are displayed in the upper left of each profile. The dashed line represents the PAH specific method detection limit.

2.2.1. Ecotoxicological Interpretations

At the 2022 and 2023 tissue concentrations, no adverse biological effects are predicted. Considering the behavior of larger PAHs to adhere to lipids, mussel tissue concentrations are likely higher in the winter and early spring, before Pacific blue mussel spawning events (i.e., lipid-rich eggs will carry away significant amounts of PAHs). In this case, the post-spawning June sampling may represent a PAH accumulation low over the annual cycle.

Similar mussel tissue concentrations did not elicit early warning signs for genotoxicity or cellular toxicity in laboratory and field studies (Hylland et al. 2008; Sundt et al. 2011). At tissue PAH concentrations two orders of magnitude greater, laboratory studies observed reduced body size and greater cellular stress but no significant differences in gamete development in fuel-oil-exposed mussels (Ruiz et al. 2014).

Mussels accumulate more than just hydrocarbons. Across Prince William Sound and the North Gulf Coast, elevated concentrations of many metals and legacy pollutants are found locally in Pacific blue mussels (Rider 2020). While some of these concentrations are directly related to local past and present anthropogenic sources (e.g., mining, chemical storage, shipping, accidents and spills, and human activities), long-range transport of chemicals is likely a contributing factor. The potential for adverse effects on aquatic organisms from the combined stressors either through contaminant mixtures and/or environmental stressors should be highlighted but any further assertion as to the degree of injury would be speculative.

2.2.2. Site-Specific Source Identification

As tissue hydrocarbon concentrations and chemical compositions are driven by the bioavailability of compounds, environmental conditions, and physiological, cellular, and molecular processes in the mussels, which govern exposure, uptake, metabolism, and elimination, source identification analysis should be performed with caution.

In 2022, Gold Creek, Jackson Point, and Saw Island mussels exhibited similar PAH profiles with very few petroleum biomarkers detected. Saturated hydrocarbon in these samples reveal a higher relative presence of lighter saturated hydrocarbons compared to 2021 and 2023 which indicate a larger contribution of marine biogenic origin hydrocarbons (e.g., n-C15, n-C17, and pristane). The PAH profile at the harbor shows a greater contribution of pyrogenic sources with a lesser pyrogenic signature at sites around the terminal (i.e., Saw Island and Jackson Point). Gold Creek had so few PAHs detected but can tentatively be assessed as more petrogenic in origin whereas the other sites are more mixed source in origin. The ratio of n-C17/Pristane was greater than one at the Valdez Small Boat Harbor indicating a less biodegraded hydrocarbon source. At the other Port Valdez sites this ratio was less than one and thus reveals greater biodegradation.

In 2023, many sites exhibited detectable presence of higher molecular weight PAHs, indicative of bioavailable pyrogenic PAH and/or selective accumulation and retention of these compounds. Very few petroleum biomarkers were seen in the Knowles Head, Sheep Bay, and Sleepy Bay samples, thus exposure of these mussels to petroleum compounds is likely very low. At Disk Island and Knowles Head, high molecular weight PAHs were observed at relatively high concentrations in a single replicate. In both instances these high levels were not supported by the presence of petroleum biomarkers indicating a specific source. Similar patterns and sources attributed were seen in Port Valdez sites in 2023 as in 2022.

2.2.3. Historical Perspective

Historical trends in Pacific blue mussel tissue PAH concentrations are variable, reflecting known oil spill incidents in 2004 at Gold Creek, and 2017 and April 2020 spills at the terminal, and mirroring high concentrations found in sediments pre-2005 (Figure 8). Within the larger trend, PAH variability and mean tissue concentrations have stabilized since ~2010 in the absence of known spills (Figure 8B). In non-spill conditions, mussel tissue concentrations have remained below < 1,000 ng/g wet weight, indicating the mussels are likely not under PAH exposure-induced stress. However, high values have been recorded following spill incidents (e.g., 244,000 ng/g wet weight after the April 2020 terminal spill, not shown), a value likely to induce adverse effects at the molecular to the individual level for organisms (Figure 8A). Expanded sampling stations (e.g., Disk Island, Knowles Head, Sheep Bay, Sleepy Bay, and Zaikof Bay) show less variability in recent years, likely due to them being less exposed to recent spill events and the bias of less frequent sampling. Overall, 2022 and 2023 represent years with one of the lowest PAH concentrations found in mussels in LTEMP's 30-year history. However, this should be interpreted with caution as analytical methods are at the lower limits of detection and as such many compounds are considered an estimation in sum calculations.

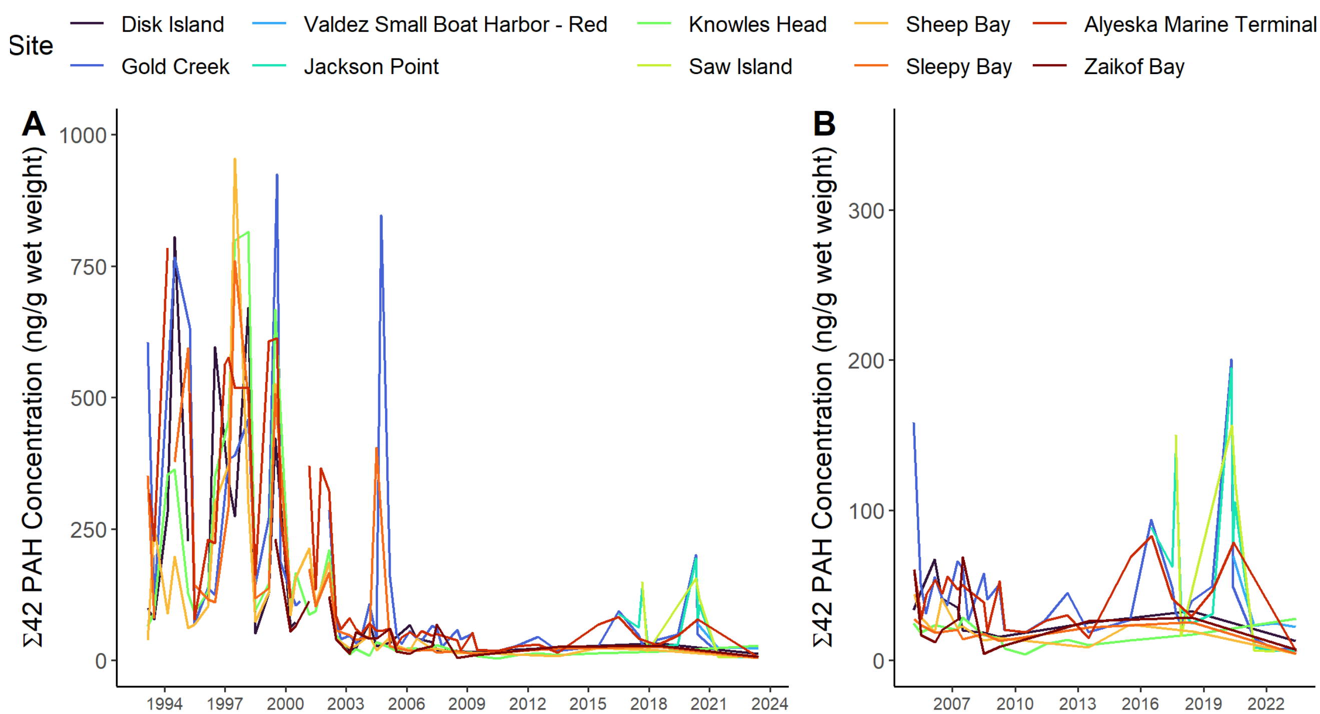

Figure 8. Total PAH concentrations in Pacific blue mussel tissue (A) over the entire duration of the LTEMP; note concentrations > 1000 ng/g wet weight (i.e., known spill events) were removed for clarity even though max post spill concentration >200 000 ng/g wet weight, and (B) over the last 18 years and excluding concentrations >350 ng/g wet weight for clarity. Colors indicate sampling site and mean values are plotted for each sampling event.

The range of the 2022 and 2023 PAH concentrations in Port Valdez mussel tissues is within the historical range of locations with limited human use and not oiled during the Exxon Valdez oil spill (Boehm et al. 2004).

2.3. Water sampled via Passive Sampling Devices

Hydrocarbons were found at low concentrations in water sampled via passive sampling devices in 2022, at sites in Port Valdez (47–54 ng/L sum 42 PAHs) (Figure 2) and in Port Valdez and greater Prince William Sound in 2023 (38–83 ng/L sum 42 PAHs) (Figure 3). These concentrations represent the dissolved constituents (C-free) and are not traditional total water concentrations, but in this report the passive sampling device C-free concentrations are used as a proxy for water concentrations of PAHs. In 2022, the highest relative passive sampling device-derived water concentrations were measured at Jackson Point (54±11 ng/L) closely followed by Gold Creek (49±9 ng/L) and Saw Island (47±2 ng/L). In 2023, Port Valdez trends were reversed with Saw Island reporting the highest relative PAH concentration (84±19 ng/L) followed by Gold Creek (81±17 ng/L), Jackson Point (78±10 ng/L) and the extended sampling site in central western Prince William Sound, Disk Island, (38±16 ng/L). A passive sampling device was deployed at Knowles Head in 2023, but could not be located for retrieval.

In both years, dissolved and heavily water-washed naphthalenes made up the majority of the PAH bulk across all samples and sites (see Figure 9 for 2023 PAH profile). Smaller, 2–3 ring PAHs made up 99% of the sum concentrations, indicative of the more readily water-soluble fraction. Other PAHs that were detected at lower concentrations at all sites were fluorenes, fluoranthenes, dibenzothiophenes, phenanthrenes, and anthracenes. Concentrations of alkylated compounds were greater than those of parent compounds at Disk Island indicating a water-washed oil source, evaporative transfer of dissolved compounds into the atmosphere, or weathering of a surface oil film before it was entrained into near-surface water and dissolved to an appreciable extent. At Port Valdez sites a petrogenic pattern was seen in parent and alkylated fluorenes. While direct comparison of the passive sampling data to other environmental hydrocarbon studies is challenging due to methodological differences, present dissolved PAH concentrations from the passive sampling devices are comparable to water concentrations at unoiled sites and sites with medium human activity around Prince William Sound (Short et al. 2008; Lindeberg et al. 2017). The present passive sampling device-derived water concentrations in Port Valdez and at Disk Island were all at least two to three orders of magnitude below published water quality standards and below those of polluted areas across the United States (EPA 2002).

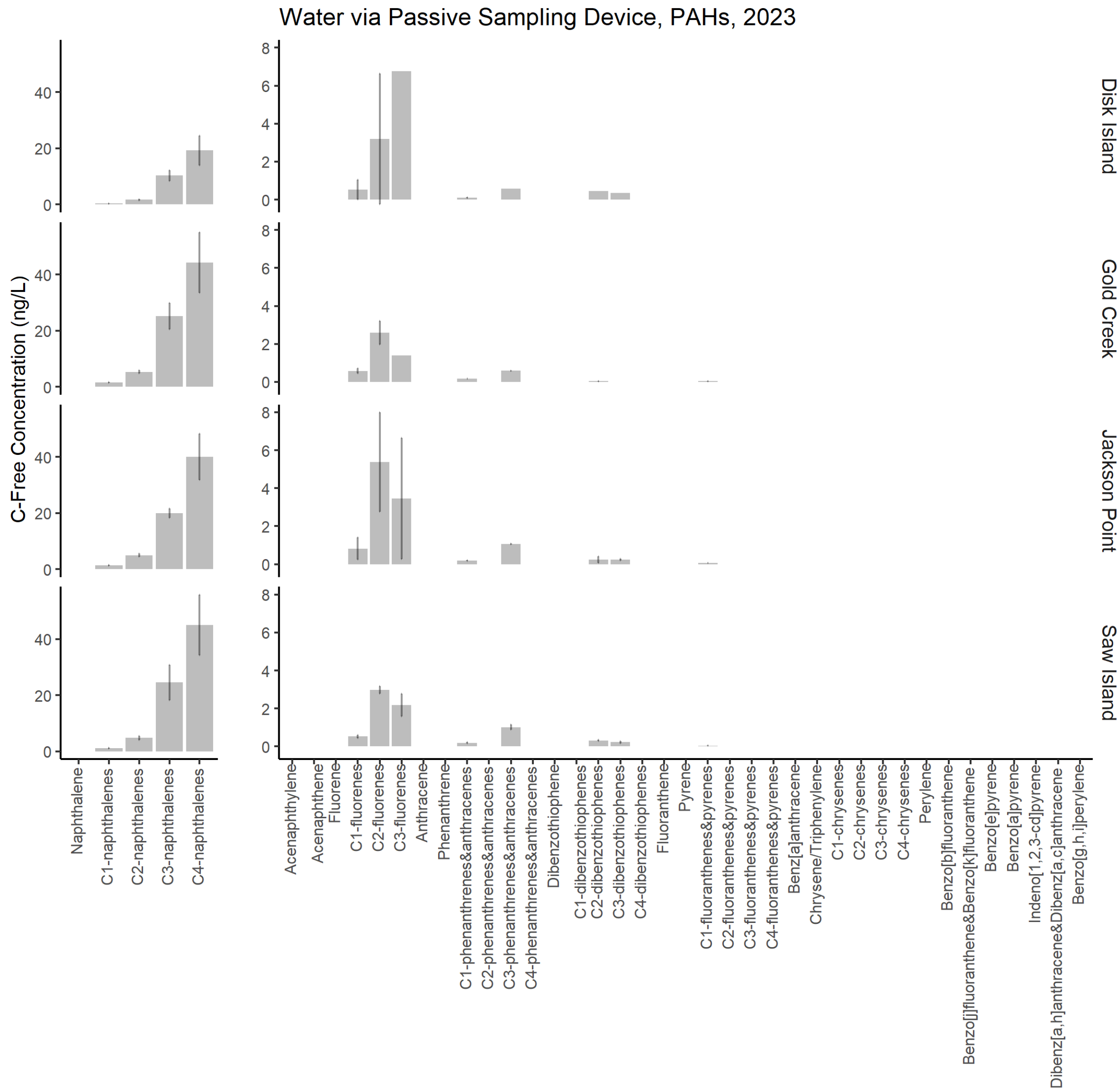

Figure 9. PAH Profiles in 2023 water sampled via passive sampling devices placed at Gold Creek, Jackson Point, and Saw Island. Values represent mean ± standard deviation for the three replicates.

2.3.1. Ecotoxicological Interpretations

Concentrations reported in the Port Valdez passive sampling device-derived water concentrations are below those reported to cause adverse effects even in the most sensitive of life stages for marine organisms. The 2022 and 2023 PAH concentrations in the parts per trillion range (i.e., one drop in 20 Olympic-sized swimming pools) are an order of magnitude lower than those reported to cause developmental and delayed effects in herring and salmon early life stages (Incardona et al. 2015), although no analytical lower limit measured from water or tissues has been identified for developmental cardiac effects in herring (Incardona et al. 2023). Studies on Arctic cod embryos, a Bering Sea species not present in Prince William Sound, report malformations and reduced survival at concentrations similar to those measured by the passive samplers; however, the analytic methods and exposure PAH composition differs with the Arctic cod study using whole crude oil (Bender et al. 2021). Naphthalene, while present at greater concentrations than other PAHs, is of low toxicological concern at present concentrations and is not a carcinogen.

2.3.2. Site-Specific Source Identification

Though not the focus of the passive sampling device, which measures the dissolved and bioavailable fraction (C-free concentrations) in the water, PAH profiles can be used conservatively for source identification and forensic analysis. One striking observation is the large naphthalene peak with ascending alkylation, indicative of a water-washed and weathered petrogenic source present in all samples. Similar patterns are seen in the fluorenes in all 2022 samples; however, the pattern is more petrogenic in 2023 at Gold Creek and Saw Island.

2.3.3. Historical Perspective

PAH concentrations in passive samplers have remained low since the 2016 inclusion of passive sampling device-derived water concentrations into LTEMP (Figure 10). A peak in PAH levels is seen at the terminal adjacent site, Jackson Point, following the 2020 terminal spill. Passive sampler PAH profiles over time have also remained consistent with high naphthalene spikes dominating PAH profiles as noted in previous LTEMP reports (Payne and Driskell 2021).

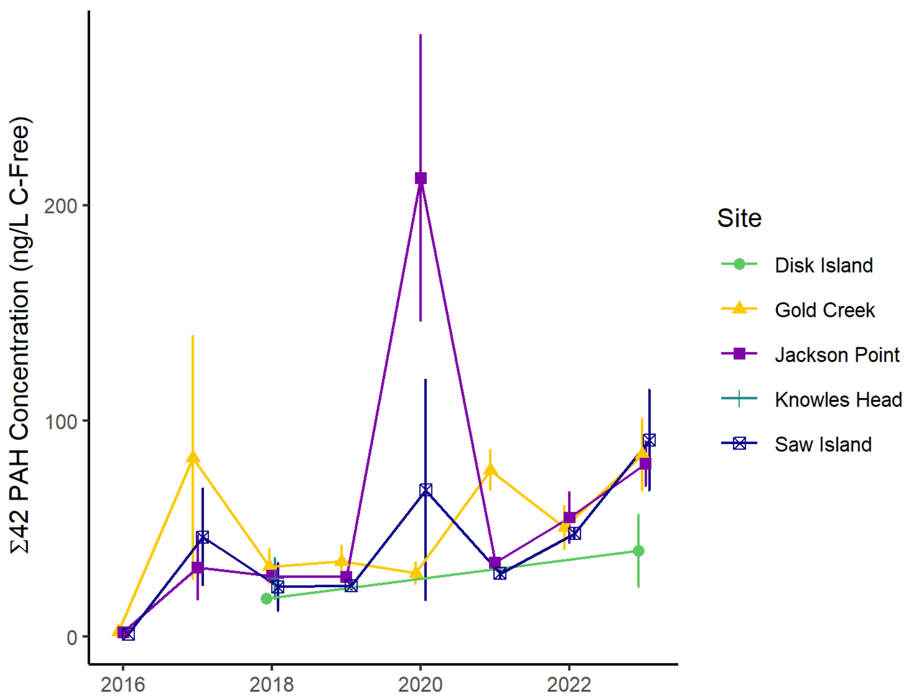

Figure 10. Sum 42 PAH concentrations in passive sampling device-derived water concentrations at five sites for 2016–2023. Sites are distinguished by color and shape and plotted by mean ± 1 standard deviation. Note that 2016 values only include parent PAHs, no alkylated PAHs were quantified in 2016.

2.4. Holistic Interpretation

In 2022, we saw agreement on low-level PAHs at similar concentrations across the three standard LTEMP stations in Port Valdez (i.e., Gold Creek, Saw Island, and Jackson Point). Mussel PAH levels found at the Valdez Small Boat Harbor were higher than other stations but could not be confirmed by sediment or passive sampler results as these samples were not taken. In 2023, the standard LTEMP stations in Port Valdez reported similar PAH concentrations and similarities to one another as in 2022. Surprisingly, the expanded LTEMP stations of Knowles Head and Disk Island had average PAH concentrations more similar to the Valdez Small Boat Harbor. Other expanded LTEMP mussel sites of the Zaikof Bay (both inner and outer), Sleepy Bay, and Sheep Bay had low PAH concentrations similar to those around the terminal. The passive sampling device deployed and retrieved at Disk Island did not corroborate the relative increased abundance of PAHs found in mussels at Disk Island but rather reported a concentration of water-soluble PAHs below that of the Port Valdez sites. Both mussels and passive sampling devices from Disk Island had considerable variability between replicates compared to other sites so the ranking of hydrocarbon contaminant between sites should be done with caution. Even greater variability between replicates was seen in the Knowles Head mussel samples which may indicate a difference in the sampling for these expanded efforts may have impacted sample agreement (e.g., holding time, sample quality, cross contamination procedures). However, both locations from the remote site of Zaikof Bay had relatively good agreement so other factors may contribute to the variability (e.g., site specific heterogeneity in mussel community or habitat).

Looking across time both sediments and mussel PAH concentrations have varied over time (Figure 11) with both matrices experiencing peaks and troughs in PAH concentrations. Relatively low R-squared values, which reflect the amount of variation in the data explained by the 3rd order polynomial log transformed model, are expected for this type of environmental chemistry data, however these values indicate that other factors besides time likely influence PAH concentrations (e.g., environmental changes in Port Valdez such as increased glacial melt/freshwater runoff (Campbell 2018), recent spills). Although sampling locations for sediments and mussels are not identical in all years, more recent PAH peaks are seen in mussels compared to sediments. This is likely due to the shorter response time mussels have to spill events, something highlighted in LTEMP adjacent studies (e.g., Bowen et al. 2021) which investigated the transcriptomic response of mussels exposed to the April 2020 spill at the terminal.

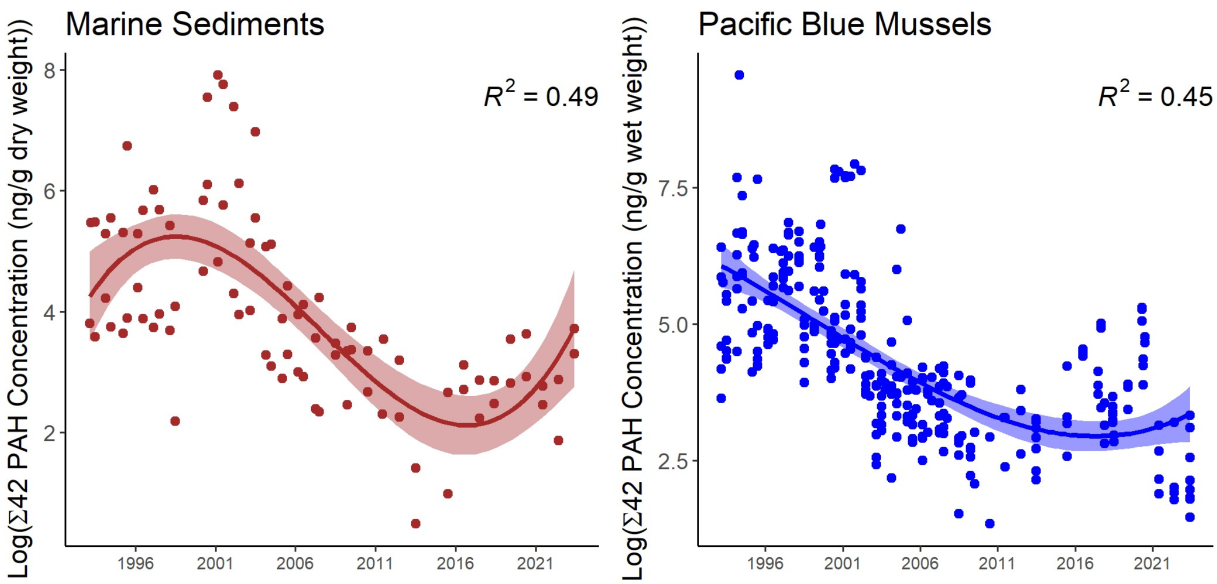

Figure 11. Polynomial trend line (3rd order) with standard error trend line fit to log transformed marine sediment (left) and Pacific Blue mussel tissue (right) PAH levels since 1993 for the sites sampled in 2023.

The forensic agreement between 2022 and 2023 samples is consistent with the mixed source petrogenic signal closer to the terminal and pyrogenic signal of stations further away. Again, string pyrogenic and mixed sources contribute to blue mussel hydrocarbons profiles at the Valdez Small Boat Harbor. As blue mussel tissues do not provide robust forensic data (e.g., few biomarkers of detection) interpretation of the expanded LTEMP sampling locations is limited. In a recent published study by Short and Maselko (2023) analyzing intertidal sediment oil samples from 2006 in western Prince William Sound, including Disk Island, crude oil from Exxon Valdez oil spill (EVOS) was determined to be the primary PAH contributor even when considering historical and ongoing human activities (e.g., mining, logging, fish processing, and fish hatcheries), and natural disasters such as the hydrocarbon pollution resulting from the 1964 earth quake and subsequent tank ruptures, and past forest fires.

The ecotoxicological risk to organisms from the hydrocarbon levels present in the sediments, mussel tissue, and dissolved in the water from 2022 and 2023 was low. Previous work focusing on how low levels of hydrocarbon exposure can influence ecologically and commercially important fish species in Prince William Sound has found profound effects on heart development (Incardona et al. 2021). In fact, recent herring research reveals that analytical chemistry with detection levels in the sub parts per billion level (ng/g) is not sensitive enough to distinguish between exposure and background concentrations in water or embryo tissue even when crude oil-induced effects on heart development and PAH-induced enzymatic response were detected (Incardona et al. 2023). Rather enzymatic induction related to nominal crude oil exposure (e.g., CYP1A induction) is directly related to cardiac deformities in herring and may provide a more sensitive assessment of injury at the low end of PAH exposure levels (Incardona et al. 2023). Targeted laboratory experiments have yet to confirm the link between early life stage oil exposure and sensitivity to pathogens later in life, which is the latest ecotoxicological hypothesis for the post-EVOS herring collapse (Whitehead et al. nd).

Current herring dynamics research has shifted focus away from hydrocarbon-induced direct effects and on to how ocean climate, freshwater input, and changes in timing of spawning have influenced survival of herring (Dias et al. 2022). Recent survey results indicate that herring may be rebounding with strong age classes observed in 2021 (Pegau et al. 2023).

3. FUTURE PERSPECTIVE

Recent work done by Harsha and Podgorski (2023) on hydrocarbon oxidation products and heavy metals in the BWTF and effluent has highlighted the presence and potential environmental risk of compounds not captured by the current LTEMP monitoring scheme. This work also argues that the assumption that stormwater and runoff from the terminal is "uncontaminated," is a finding supported from LTEMP sampling of sediments and blue mussels in the absence of spill events. Specifically, assessing the risk of toxic effects from the bioaccumulation of heavy metals, zinc, and arsenic, from BWTF effluent not removed in the filtration and biodegradation process has not been carried out in LTEMP or Alyeska pollution discharge permitting (i.e., APDES) monitoring (Shaw and Blanchard, 2021). In fact, the recent 2019 ADEC report cites that the biggest water quality concerns from the terminal BWTF effluent is zinc, total aromatic hydrocarbons, and whole effluent toxicity (ADEC 2019).

Heavy metal monitoring is routinely done in other petroleum and hydrocarbon monitoring efforts including in forensic studies in marine sediments and offshore petroleum industry monitoring efforts although typically focusing on mercury, lead, cadmium, and barium (e.g., Norwegian Environmental Agency, 2020).

Frequent reanalysis of LTEMP's aims and methodology is necessary to maintain the utility of such a powerful monitoring program even in its 30th year. While maintaining the integrity of the program with the three matrix approaches, efforts must be taken to ensure that future monitoring and reporting is conducted in a manner that guarantees comparability to previous analysis. The following represents a list of potential additions, subtractions, and alterations in methodology that could be considered for future LTEMP cycles.

1. Alter forensic analysis from its current and recent historical qualitative profile analysis to a quantitative statistical analysis using multidimensional scaling to allow greater comparative power over time, space, and between studies.
2. Place a passive sampling device at the Valdez Small Boat Harbor to allow for direct comparability for mussels sampled from this site.
3. Work with existing laboratories to expand analytical power to include emerging contaminants of environmental concern (e.g., PFAS, per- and polyfluoroalkyl substances, or the magnitude of the unresolved complex mixture which may include oxygenated products).
4. Perform a comprehensive evaluation of LTEMP in light of international environmental marine monitoring standards for planning, implementation, analysis, and reporting while still tailoring LTEMP to the needs of PWSRCAC.

5. Execute a “rat hunt” to explore the utility of the current and past LTEMP analyte and sampling regime. For example, assessing if running full hydrocarbon forensic analysis on blue mussels is necessary as a high frequency of geochemical biomarkers analytes are not detectable and therefore not useful in forensic analysis.
6. Investigate the potential to include additional biological information to reduce potential variability between biological samples including assessing spawning status, size, and condition in Pacific blue mussels.
7. Expand biological sampling. (1) Include PAH analysis in liver and bile of wild caught resident fish species (e.g., sculpin); (2) expand BWTF effluent testing as whole effluent testing reveals concerning toxicity (suggestion by Harsha and Podgorski 2023); and (3) include hydrocarbon specific biomarkers of PAH exposure and injury with mussel sampling.
8. Consider all phases of LTEMP in the current era of rapid environmental change, demand for scientific transparency, and environmental justice.

At this point in time many options mentioned above have not been fully investigated as this would require additional analysis. This list is intended for discussion purposes amongst the PWSRCAC Scientific Advisory Committee. Modernizing LTEMP could involve inclusion of biosensors for real time monitoring as was suggested by Harsha and Podgorski (2023) in their work on the hydrocarbon oxidation products in the BWTF effluent (Gavrilas et al. 2022) or remote sensing environmental monitoring of oil pollution using satellites, an emerging technique for remote areas with rapid environmental change and human activity (Sizov et al. 2014).

.

4. CONCLUSION

In the 30th year of the LTEMP run by PWSRCAC, two years of data were analyzed for the concentration, source, and potential ecotoxicological effects of hydrocarbons in marine subtidal sediments, Pacific blue mussels, and dissolved in the nearshore waters via passive sampling devices. The hydrocarbon fingerprints in the 2022 and 2023 samples vary by site with those at or near the Valdez Marine Terminal revealing ANS crude and its associated products (i.e., BWTF effluent) as the primary source for hydrocarbons. Hydrocarbons found in Pacific blue mussels from Gold Creek, Knowles Head, Disk Island, Sheep Bay, Sleepy Bay, Zaikof Bay, and the Valdez Small Boat Harbor cannot be linked directly to the terminal operations although these samples revealed a mix of sources. Low potential environmental and toxicological risk is posed by hydrocarbons contributed by the terminal and tankers in 2022 and 2023. Surprisingly, concentrations of toxic hydrocarbons were similar at the remote sites of Knowles Head and Disk Island and the Valdez Small Boat Harbor, a site of high human activity and potential chronic petroleum pollution. Passive sampling devices continue to report low levels of bioavailable hydrocarbons in the water column with higher concentration within Port Valdez compared to the remote, historically EVOS oiled site of Disk Island. Since 1993, hydrocarbon concentrations in Prince William Sound are generally low with localized spikes corresponding with spill events like the April 2020 oil spill at the terminal. Following an all-time low in the mid-2010s, hydrocarbon concentrations in sediments and mussels have slowly increased across all sites but are still below any threshold for adverse effects on aquatic life. Several suggestions have been made to expand, economize, and modernize LTEMP.

5. REFERENCES

Alaska Department of Environmental Conservation (ADEC). 2019. Alaska Pollutant Discharge Elimination System Permit - Alyeska Pipeline Service Company, Valdez Marine Terminal. In *AK0023248*, edited by Alaska Department of Environmental Conservation.

Alaska Department of Environmental Conservation (ADEC). 2022. Division of Spill Prevention and Response. PPR Spills Database. April 1, 2022. https://dec.alaska.gov/Applications/SPAR/PublicMVC/PERP/SpillSearch

Bender, M. L., J. Giebichenstein, R.N. Teisrud, J. Laurent, M. Frantzen, J. P. Meador, L. Sørensen, B. H. Hansen, H. C. Reinhardy, B. Laurel, and J. Nahrgang. 2021. Combined Effects of Crude Oil Exposure and Warming on Eggs and Larvae of an Arctic Forage Fish. *Scientific Reports* 11 (1): 8410. https://doi.org/10.1038/s41598-021-87932-2

Boehm, P.D., D.S. Page, J.S. Brown, J.M. Neff, and W.A. Burns. 2004. Polycyclic Aromatic Hydrocarbon Levels in Mussels from Prince William Sound, Alaska, USA, Document the Return to Baseline Conditions. *Environmental Toxicology and Chemistry* 23 (12): 2916–29. https://doi.org/10.1897/03-514.1

Bowen, L., W. B. Driskell, J.R. Payne, A. Love, E. Litman, and B. Ballachey. 2021. Mussel Oiling and Genetic Response to the April 2020 Valdez Marine Terminal Spill: Executive Summary 6.

Campbell, R.W. 2018. Hydrographic Trends in Prince William Sound, Alaska, 1960–2016. *Deep Sea Research Part II: Topical Studies in Oceanography*, Spatial And Temporal Ecological Variability In The Northern Gulf Of Alaska: What Have We Learned Since The Exxon Valdez Oil Spill?, 147 (January): 43–57. https://doi.org/10.1016/j.dsr2.2017.08.014

Carls, M.G., J.W. Short, and J. Payne. 2006. Accumulation of Polycyclic Aromatic Hydrocarbons by Neocalanus Copepods in Port Valdez, Alaska. *Marine Pollution Bulletin* 52 (11): 1480–89. https://doi.org/10.1016/j.marpolbul.2006.05.008

Davis, E., T. R. Walker, M. Adams, and R. Willis. 2018. Characterization of Polycyclic Aromatic Hydrocarbons (PAHs) in Small Craft Harbour (SCH) Sediments in Nova Scotia, Canada. *Marine Pollution Bulletin* 137 (December): 285–94. https://doi.org/10.1016/j.marpolbul.2018.10.043

Dias, B.S., D.W. McGowan, R. Campbell, T.A. Branch. 2022. Influence of environmental and population factors on Prince William Sound herring spawning phenology. 696 https://doi.org/10.3354/meps14133

Gavrilaș, S., C.Ș. Ursachi, S. Perța-Crișan, F.D. Munteanu. 2022. Recent Trends in Biosensors for Environmental Quality Monitoring. Sensors (Basel). Feb 15; 22(4):1513. doi: 10.3390/s22041513. PMID: 35214408; PMCID: PMC8879434.

Harsha, M.L., and D.C. Podgorski. 2023 Examining the Effectiveness of Ballast Water Treatment Processes: Insights into Hydrocarbon Oxidation Product Formation and Environmental Implications. Report to PWSRCAC 08-01-2023.

Incardona J.P., T.L. Linbo, J.R. Cameron, B.L. French, J.L. Bolton, J.L. Gregg, C.E. Donald, P.K. Hershberger, and N.L. Scholz. Environmental Science & Technology 2023 57 (48), 19214-19222, DOI: 10.1021/acs.est.3c04122

Incardona J.P., T.L. Linbo, B.L. French, J. Cameron, K.A. Peck, C.A. Laetz, M.B. Hicks, G, Hutchinson S.E. Allan, D.T. Boyd, G.M. Ylitalo, N.L. Scholz. 2021. Low-level embryonic crude oil exposure disrupts ventricular ballooning and subsequent trabeculation in Pacific herring. Aquat Toxicol. 2021 Jun; 235:105810. doi: 10.1016/j.aquatox.2021.105810. Epub 2021 Mar 22. PMID: 33823483.

Incardona, J P., M.G. Carls, L. Holland, T.L. Linbo, D.H. Baldwin, M.S. Myers, K. A. Peck, M. Tagal, S.D. Rice, and N.L. Scholz. 2015. Very Low Embryonic Crude Oil Exposures Cause Lasting Cardiac Defects in Salmon and Herring. *Scientific Reports* 5 (1): 13499. https://doi.org/10.1038/srep13499

Lehtonen, K.K., G. d'Errico, S. Korpinen, F. Regoli, H. Ahkola, T. Kinnunen, and A. Lastumäki. 2019. Mussel Caging and the Weight of Evidence Approach in the Assessment of Chemical Contamination in Coastal Waters of Finland (Baltic Sea). *Frontiers in Marine Science* 6. https://doi.org/10.3389/fmars.2019.00688

Lindeberg, M., J. Maselko, R. Heintz, C. Fugate, and L. Holland. 2017. Conditions of Persistent Oil on Beaches in Prince William Sound 26 Years after the Exxon Valdez Spill. *Deep Sea Research Part II: Topical Studies in Oceanography* 147 (July). https://doi.org/10.1016/j.dsr2.2017.07.011

Norwegian Environment Agency. 2020. Guidelines for environmental monitoring of petroleum activities on the Norwegian continental shelf. https://www.miljodirektoratet.no/globalassets/publikasjoner/M408/M408.pdf

Neff, J., and W. Burns. 1996. Estimation of Polycyclic Aromatic Hydrocarbon Concentrations in the Water Column Based on Tissue Residues in Mussels and Salmon: An Equilibrium Partitioning Approach. *Environmental Toxicology and Chemistry* 15 (December): 2240–53. https://doi.org/10.1002/etc.5620151218

Nesvacil, K., M. Carls, L. Holland, and S. Wright. 2016. Assessment of Bioavailable Hydrocarbons in Pribilof Island Rock Sandpiper Fall Staging Areas and Overwintering Habitat. *Marine Pollution Bulletin* 110 (1): 415–23. https://doi.org/10.1016/j.marpolbul.2016.06.032

Oen, A.M. P., G. Cornelissen, and G. D. Breedveld. 2006. Relation between PAH and Black Carbon Contents in Size Fractions of Norwegian Harbor Sediments. *Environmental Pollution* 141 (2): 370–80. https://doi.org/10.1016/j.envpol.2005.08.033

Payne, J.R., W.B. Driskell, J.F. Braddock, J. Bailey, J. W. Short, L. Ka'aihue, and T.H. Kuckertz. 2005. From Tankers to Tissues – Tracking the Degradation and Fate of Oil Discharges in Port Valdez, Alaska.

Payne, J.R., and W.B. Driskell. 2018. Long-Term Environmental Monitoring Program: 2017 sampling results and interpretations, 66.

Payne, J.R., and W.B. Driskell. 2021. Long-Term Environmental Monitoring Program: 2020 sampling results and interpretations, 104.

Pegau et al. 2023. Herring Research and Monitoring. https://pwssc.org/herring/. Accessed 10/19/2023

Whitehead et al. nd. Exposure to Oil Limits Herring Fitness. https://pwssc.org/exposure-to-oil-limits-herring-fitness/. accessed 10/19/2023

Pikkarainen, A. L. 2010. Polycyclic aromatic hydrocarbons in Baltic Sea sediments. *Polycyclic Aromatic Compounds*, August. https://doi.org/10.1080/10406630490472293

Rider, M. 2020. A Synthesis of Ten Years of Chemical Contaminants Monitoring in National Park Service - Southeast and Southwest Alaska Networks, a Collaboration with the NOAA National Mussel Watch Program. https://doi.org/10.25923/DBYQ-7Z17

Ruiz, P., M. Ortiz-Zarragoitia, A. Orbea, S. Vingen, A. Hjelle, T. Baussant, and M.P. Cajaraville. 2014. Short- and Long-Term Responses and Recovery of Mussels Mytilus Edulis Exposed to Heavy Fuel Oil No. 6 and Styrene. *Ecotoxicology* 23 (5): 861–79. https://doi.org/10.1007/s10646-014-1226-6

Schøyen, M., I.J. Allan, A. Ruus, J. Håvardstun, D. Ø. Hjermann, and J. Beyer. 2017. Comparison of Caged and Native Blue Mussels (Mytilus Edulis Spp.) for Environmental Monitoring of PAH, PCB and Trace Metals. *Marine Environmental Research* 130 (September): 221–32. https://doi.org/10.1016/j.marenvres.2017.07.025

Sizov, O., A. Agoltsov, N. Rubtsova. 2014. Methodological Issues of Elaborating and Implementing Remote Environmental Monitoring of Oil and Gas Exploration Applying Satellite Images: The Priobskoye Oil Field (Yugra, Russia), Energy Procedia,Volume 59, Pages 51-58, ISSN 1876-6102, https://doi.org/10.1016/j.egypro.2014.10.348.

Shaw, D.G., and A.L. Blanchard. 2021. Environmental sediment monitoring in Port Valdez, Alaska: 2021. 110.

Short, J.W., and J.M. Maselko. 2023. A Quantitative Comparison of Oil Sources on Shorelines of Prince William Sound, Alaska, 17 Years After the *Exxon Valdez* Oil Spill. *Arch Environ Contam Toxicol* 85, 140–146 (2023). https://doi.org/10.1007/s00244-023-01019-9

Short, J.W., K.R. Springman, M.R. Lindeberg, L.G. Holland, M.L. Larsen, C.A. Sloan, C. Khan, P.V. Hodson, and S.D. Rice. 2008. Semipermeable Membrane Devices Link Site-Specific Contaminants to Effects: PART II - A Comparison of Lingering Exxon Valdez Oil with Other Potential Sources of CYP1A Inducers in Prince William Sound, Alaska. *Marine Environmental Research* 66 (5): 487–98. https://doi.org/10.1016/j.marenvres.2008.08.007

U.S. Environmental Protection Agency (EPA). 2002. National Recommended Water Quality Criteria: 2002. https://www.epa.gov/wqc/national-recommended-water-quality-criteria-aquatic-life-criteria-table

U.S. Environmental Protection Agency (EPA). 2016. Sediment Benchmarks. Sediment Benchmarks for Aquatic Life. 2016. https://archive.epa.gov/emergency/bpspill/web/html/sediment-benchmarks.html#anthracenes.

Final

Long-Term Environmental Monitoring Program

2022–2023 Technical Supplement

December 2023

Prepared for:
Prince William Sound Regional Citizens' Advisory Council
3709 Spenard Road, Suite 100
Anchorage, Alaska 99503

Prepared by:
Morgan L. Bender, Ph.D.
Owl Ridge Natural Resource Consultants, Inc.
4060 B Street, Suite 200
Anchorage, Alaska 99503
T: 907.344.3448
www.owlridgenrc.com

Document Number: PWS002-23-002F0

TABLE OF CONTENTS

List of Tables

<u>List of Figures</u>

ACRONYMS AND ABBREVIATIONS

°C	Degrees Celsius
AMT	Alyeska Marine Terminal [officially known as the Valdez Marine Terminal]
ANS	Alaska North Slope [Crude Oil]
BWTF	Ballast Water Treatment Facility
cm	Centimeter
CV	Calibration Verification
DII	Disk Island
DQO	Data Quality Objective
EPA	U.S. Environmental Protection Agency
FID	Flame Ionization Detector [FID chromatogram]
FSES	Food Safety and Environmental Stewardship [Oregon State University lab]
GC/MS	Gas Chromatography/Mass Spectrometry
GOC	Gold Creek
HOT	Site of the April 2020 oil spill at the Valdez Marine Terminal
HMW	High Molecular Weight [PAH]
JAC	Jackson Point
KNH	Knowles Head
LMW	Low Molecular Weight [PAH]
LTEMP	Long-Term Environmental Monitoring Program
m	Meter
mL	Milliliter
MDL	Method Detection Limit
ng/g	Nanogram per Gram
OSU	Oregon State University
PAH	Polycyclic Aromatic Hydrocarbons
pg/µL	Picogram per Microliter
PSD	Passive Sampling Device
PWSRCAC	Prince William Sound Regional Citizens' Advisory Council
QC	Quality Control
RED	Valdez Small Boat Harbor Entrance [red light]
SAW	Saw Island
SHB	Sheep Bay
SHC	Saturated Hydrocarbons
SIM	Specific Ion Monitoring
SLB	Sleepy Bay
SOP	Standard Operating Procedure
ZAB	Zaikof Bay

EXECUTIVE SUMMARY

This technical supplement contains information on field sampling, and analytical and data analysis methods used to monitor and assess environmental hydrocarbons and their potential environmental risk in Prince William Sound Regional Citizens' Advisory Council's (PWSRCAC) Long-Term Environmental Monitoring Program (LTEMP). Here we have plotted and summarized all sediment, Pacific blue mussel tissue, and passive samples collected in the 2022 campaign in Port Valdez and the 2023 campaign in Port Valdez and greater Prince William Sound. This document should function as an aid to the assertions made in the 2023 Long-Term Environmental Monitoring Program Summary Report (Owl Ridge 2023).

1. METHODS

1.1. Field Methods

1.1.1. Sediments and Mussel Tissue

In 2022, sediment sampling at Valdez Marine Terminal (Alyeska Marine Terminal (AMT)) took place on June 3 and at Gold Creek (GOC) on June 1 (Table 1, Figure 1). In 2023, sample dates were June 3 and 4 for GOC and AMT, respectively. Samples were collected using a modified Van Veen grab and deployed to a depth of 65–67 meters (m) at AMT and 26–27 m at GOC from a small research vessel. For each replicate, a ~ 250 milliliters (mL) sample of the surface 1–5 mL was collected at each site, placed in a hydrocarbon-free jar, and frozen for hydrocarbons and total organic carbon analysis. Samples were sent frozen to the lab for analysis.

The 2022 Pacific blue mussel sampling was performed at GOC, Jackson Point (JAC), and Saw Island (SAW) on June 1 and at the Valdez Small Boat Harbor – RED (RED) on June 3. In 2023, mussels were collected from Port Valdez station on June 3, RED on June 5, Disk Island and Knowles Head on June 6, and Sleepy Bay, Sheep Bay, and Zaikof Bay (2 sites) on June 7. Three replicates of ~30 large mussels were collected by hand at each site. Sample replicates are usually taken from multiple locations spaced along 30 m of shoreline. Mussel samples were wrapped in aluminum foil and double bagged in plastic zip-locks, frozen and shipped to the laboratory where they remained frozen until analysis. Dissections were performed by the analytical lab as a whole mussel including all internal organs.

1.1.2. Passive Sampling Devices

In 2022, the Passive Sampler Devices (PSDs) were retrieved June 1 at sites GOC, JAC, and SAW. In 2023, PSDs were deployed May 6 and retrieved June 3. The PSDs used are a low density polyethylene membrane submerged in shallow water to absorb passing hydrocarbons. The PSD is intended to only sample a fraction of the total hydrocarbon analytes present, namely, freely dissolved compounds and labile complexes that diffuse into the membrane that, for biota, are the most bioavailable hydrocarbons. As a critical part of the method, various deuterated surrogate compounds are pre-infused into the membrane prior to deployment. The PSDs were deployed in 4–7 m of water, attached to new polypropylene rope with hydrocarbon-free steel cables and shackles, anchored to a concrete cinder block at each location. At each site, three replicates of 5 PSDs were deployed such that they floated approximately 1 m above the seafloor. The PSDs were collected from stations and were transferred to hydrocarbon-free Teflon bags, sealed, and stored at room temperature following LTEMP field protocols (2019 LTEMP PSD SOP). A deployment field blank and a retrieval field blank was included in each annual analysis. Samples were sent to the Oregon State University Food Safety and Environmental Stewardship (FSES) lab in Corvallis, Oregon, for analysis and frozen at -20°C upon arrival.

1.2. Analytical Methods

1.2.1. Sediments and Mussel Tissue

Tissue and sediment samples were analyzed for semi-volatiles, biomarkers, and saturated hydrocarbons analytes at Alpha Analytical (previously NewFields 2022) lab in Mansfield, Massachusetts. Extractions used the ALPHA OP-018 method for tissues and ALPHA OP-013 method for sediments. The usual hydrocarbon data reported polycyclic aromatic hydrocarbons (PAH), sterane/triterpene biomarkers, and saturated hydrocarbons (SHC). Semi-volatile compounds, the PAH, alkylated PAH, and petroleum biomarkers, are analyzed using selected ion monitoring gas chromatography/mass spectrometry (SIM GC/MS) via a modified U.S. Environmental Protection Agency (EPA) Method 8270 (aka 8270M). This analysis provides the concentration of 1) approximately 80 PAH, alkylated PAH homologues, individual PAH isomers, and sulfur-containing aromatics, and 2) approximately 50 tricyclic and pentacyclic triterpenes, regular and rearranged steranes, and triaromatic and monoaromatic steroids. Complete lists of PAH, SHC, and biomarkers analytes are presented in Table 2, Table 3, and Table 4.

Using a modified EPA Method 8015B, SHC in sediments are quantified as total extractable materials (C_9-C_{44}), and as concentrations of n-alkanes (C_9-C_{40}) and selected (C_{15}-C_{20}) acyclic isoprenoids (e.g., pristane and phytane). A high-resolution gas chromatography-flame ionization detector (GC/FID) fingerprint of the sediment and tissue samples is also provided. Petroleum samples were diluted but not extracted. At the lab's discretion, extracts may be fractionated (F1) to improve the discrimination of biomarkers.

Surrogates are novel or deuterated compounds added in known amounts to each raw sample to assess, by their final percent recovery, the efficiency of extraction and analysis. Surrogate recoveries are considered acceptable if they are between 50-130%. Surrogate percent recovery concentrations are acceptable across all analytes analyzed. One lab-performance quality control (QC) measure is the EPA-formulated, statistically derived, analyte-specific, Method Detection Limit (MDL) that EPA defines as "the minimum measured concentration of a substance that can be reported with 99 percent confidence that the measured concentration is distinguishable from method blank results." Alpha Analytics Laboratory's MDLs for hydrocarbons exceed the performance of most commercial labs, falling within the accepted stricter concentrations for forensic purposes. Duplicates sediment and tissue samples were run for method quality control and to assess precision.

1.2.2. Passive Sampling Device

To remove any biofouling (e.g., periphyton or particulates), the PSD strips were cleaned in the laboratory by light scrubbing and sequential washing in 1 N HCl, 18 MΩ*cm water, and twice with isopropanol, then dried. PSDs were extracted twice at room temperature with 200 mL n-hexane before the volume was reduced. Briefly, 62 PAHs were quantified on a modified Agilent 7890 gas chromatograph (GC) and Agilent 7000 triple quadrupole mass spectrometer. The internal standard, Perylene-D12, was added to each sample or parallel aliquots of bioassay samples immediately prior to analyses. Calculation of freely dissolved water concentration of organic compounds was done following the lab specific standard operating procedure (SOP). Continuing calibration verification

(CV) analysis was performed at the start and end of every analytical batch (maximum of 15 samples). CVs met FSES data quality objectives (DQOs) with an average of 93% of the target analytes being within 30% of the known value. Instrument blanks were analyzed after each CV, and in all cases, FSES DQOs were met for all target analytes. To demonstrate instrument accuracy an over-spike analysis was performed where the sample was spiked with target compounds post extraction. The average percent recovery was 85%, meeting FSES DQO's. To demonstrate instrument precision, a duplicate analysis was performed. The average relative percent difference was 3.1%, meeting FSES DQO's. Field blanks are presented in pg/μL extract as time calculated C-free concentrations are not applicable.

1.3. Data Analysis

Data analysis and data management was done using the R statistical program (R Core Team 2021). Briefly, data were reformatted to allow for individual locations and analytes to be accessed. For summary purposes all data with concentrations reported as "non-detect" by Alpha Analytics were removed though detected values under the method detection concentration were retained if no other issues were reported with the value. Any sample with matrix interference (i.e., "G" lab flag) was removed for matrix interference. For Sediment analysis, samples with negative detection and matrix interference were plotted for forensic determination. Only a select group of commonly used analytes were plotted to ease interpretation at the author's discretion and ordered using previously used LTEMP standards when possible. Method detection concentrations were plotted for sediment and tissue samples. Corrections for dry weight, total organic carbon, and lipid content are reported in the tables and text when appropriate. Data from multiple labs were merged to allow for historical data comparison (Auke Bay Lab, NewFields / Alpha Analytical, and GERG).

Passive sampling device data were extracted and merged into a single dataset. A group of PAHs aimed at forensic determinations was used to gather toxicological information and Oregon State University (OSU)-produced ratios were plotted for potential source determination. Common lab flags were "B" for background corrected and applied broadly to Naphthalene and Fluorene and "J" which is close to the detection level and therefore estimated.

1.4. Source Identification, Petroleum Fingerprinting, and Biomarker Analysis

Source identification through petroleum fingerprinting and biomarker analysis was performed using the following sources: Alaska North Slope (ANS) whole crude oil run as laboratory standard with 2022 and 2023 samples, filtered (0.7 μm glass fiber filter) Ballast Water Treatment Facility (BWTF) effluent collected in March 2017, oil/water sample collected from the April 2020 spill at the terminal (HOT), 2016 terminal spill (Barge), a weathered diesel spill in Port Chalmers from 2006 and a crude oil sample from Cook Inlet. The first three respective sources are displayed for each replicate sediment sample to avoid a single snapshot in time of a potential ANS source. Two additional non-ANS sources were investigated to provide an outside reference including a Cook Inlet whole crude oil sample and a heavily weathered diesel fuel spill collected opportunistically from Port Chalmers, Prince William Sound, in 2006, but not displayed in figures. Profiles were scaled to C2-naphthobenzothiophenes for PAHs, n-heptacosane (C27) for saturated hydrocarbons, and T19-hopane for biomarkers when possible, to aid in interpretation. Profiles were visually evaluated for the best match between individual replicates and potential sources using expertise outlined in previous LTEMP reports (Payne and Driskell 2021; Wang et al. 2014; Stout and Wang 2016).

1.5. Toxicological Interpretations

Multiple avenues were used to investigate the possibility of toxicological effects as no single standard exists and development in the field of ecotoxicology is rapid. The most commonly accepted methods are through summing a select group of PAHs. This includes 42, 16, and other specific PAHs, referred to as summed (∑) PAHs due to the variety of methods used. This metric is similar to the Total PAH metric used prior to the BP Deepwater Horizon oil spill in 2010, but accounts for the complex mixture and multitude of calculations that can be used. Calculations were made of the relative proportion on low (2–3 ring) and high (4–6 ring) molecular weight PAHs as well as sum totals of known carcinogenic PAHs (i.e., benzo(a)pyrene, benz(a)anthracene, chrysene, benzo(b)fluoranthene, benzo(k)fluoranthene, dibenzo(a,h)anthracene, and indeno(1,2,3-c,d)pyrene). Furthermore, these values were adjusted for dry weight and lipid weight for mussel tissues to aid in cross study comparisons. Sediment values were compared to acute and chronic EPA sediment-quality benchmarks and tissue concentrations were compared against the most recently available published literature and concentration-of-concern guidelines, as appropriate. Concentrations were compared to other field measurements across similar environments (sub-arctic, temperate fjord systems), areas with moderate human activity converted for wet or dry weight in tissues as appropriate, other lab studies with analogous aims as LTEMP (e.g., monitoring of ongoing petroleum operations, sublethal effects, chronic exposure).

Saturated hydrocarbons and biomarkers were not a focus of toxicological interpretations as they are not known to have specific modes of toxic action.

2. RESULTS

2.1. Sediments

2.1.1. Analytical Results and Source Identification

In the sediments, we detect hydrocarbons in all stations and replicates. Summed PAH levels between AMT and GOC alternate in ranking between 2022 and 2023 (Table 5; Figure 2). PAH profile patterns are largely petrogenic at AMT and some pyrogenic at GOC with some weathered/water washed petrogenic patterns at GOC. When overlaid with ANS related sources (i.e., ANS whole crude, BWTF filter effluent from spring 2017, and recovered oil/water from the April 2020 spill at AMT (HOT) there is good agreement between the PAH profiles (Figure 3 7). Elevated concentrations of higher molecular weight PAHs at both sites are indicative of combustion sources and could be related to exhaust, stormwater, or runoff (Figure 5–Figure 7). Sediments were moderately weathered with a near-complete loss of saturated hydrocarbons, except those present in terrestrial plants (i.e., C27, C29, C31, C33) at both sites in both years (Figure 8–Figure 10).

In the biomarkers, the ratio of T15-Norhopane and T19-Hopane indicates a crude oil source for AMT in both years (Table 9) but not GOC, which further supports the forensic differences found in the PAH pattern analysis (Figure 14–Figure 16).

2.1.2. A Note on Toxicity

The potential toxicity of hydrocarbons in the sediments was calculated using total organic matter conversions for 35 individual PAHs with EPA Sediment Benchmarks for Aquatic Life (Table 5; https://archive.epa.gov/emergency/bpspill/web/html/sediment-benchmarks.html#anthracenes).

Results show that no single PAH measured in AMT or GOC sites exceeded the chronic Potency Divisor, which represents the amount of an individual chemical (i.e., phenanthrene), by itself, that can cause an adverse effect. Correcting samples for total organic carbon content accounts for the difference in bioavailability between samples. These benchmarks are meant to be used for screening purposes only; they are not regulatory standards, site-specific cleanup levels, or remediation goals. These screening benchmarks are presented with the EPA data to help the public understand the condition of the environment as it relates to the oil spill. Additional research on PAH sediment levels from polluted and pristine areas are comparable to those found at AMT and GOC in 2022 and 2023 (see LTEMP Summary Report, Owl Ridge 2023).

2.2. Pacific Blue Mussel Tissues

Relatively few compounds were detected in the mussel tissue sampled from different locations in Port Valdez in 2022, and Port Valdez and Prince William Sound in 2023. The majority of the concentrations of PAHs, saturated hydrocarbons, and biomarkers were at or below the method level of detection (Table 6; Figure 20–Figure 25). PAH profiles, while sparse, do suggest a petrogenic source at JAC, SAW/AMT and GOC while mostly pyrogenic source at all other sites. High variability in PAH profiles and concentrations between duplicates from Knowles Head and Disk Island may require further investigation.

Biomarker ratios indicate more fresh pyrogenic sources in the Valdez Small Boat Harbor while greater biogenic sources are found at other stations (Table 6, Table 9; Figure 36, Figure 37).

Saturated hydrocarbons were similar in concentration across mussels from all sites (Table 9; Figure 38, Figure 39). GOC and JAC mussels had greater representation of larger C23-32 compounds, showing greater weathering of sources while the Valdez Small Boat Harbor, Sheep Bay, and Sleepy Bay had greater concentrations of lower molecular weight saturated hydrocarbons compared to the other sites indicating a less weathered and more recent source. Figures for laboratory blanks PAH, biomarkers, and SHC compounds show good laboratory quality control methods although higher PAH contaminant is found for 2023 samples compared to 2022 (Figure 40, Figure 41).

2.3. Water via Passive Sampling Device

Many compounds in the 2022 and 2023 passive sampling devices were not detected (Table 7, Table 8). However, naphthalene and alkylated naphthalenes were detected at all four sites in all years. Non-naphthalene PAH levels in 2022 Port Valdez stations were low (<0.1 ng/L) and in line with 2021 concentrations, while 2023 non-naphthalene PAHs were an order of magnitude higher especially at

Disk Island and Jackson Point (6–8 ng/L) (Figure 42–Figure 50). PAH patterns were generally water washed petrogenic and did not contain many higher molecular weight compounds. Laboratory calculated ratios developed for passive sampler forensics show petrogenic signal for all 2022 sites (P0/A0 > 30) (Stogiannidis and Laane 2015). No ratio was calculated for 2023 results, but PAH profiles indicate petrogenic sources for 2023 samples.

3. REFERENCES

Owl Ridge Natural Resource Consultants, Inc. 2023. Final Long-Term Environmental Monitoring Program. 2022-2023 Summary Report. December.

Passive Sampling of LTEMP SOP. May 2019. 1–6

Payne, J.R., and W.B Driskell. 2021. "Long-Term Environmental Monitoring Program" 104.

R Core Team. 2021. R: A Language and Environment for Statistical Computing. Vienna Austria: R Foundation for Statistical Computing. https://www.r-project.org/.

Stogiannidis, E., and R. Laane. 2015. "Source Characterization of Polycyclic Aromatic Hydrocarbons by Using Their Molecular Indices: An Overview of Possibilities." Reviews of Environmental Contamination and Toxicology 234: 49–133. https://doi.org/10.1007/978-3-319-10638-0_2.

Stout, S., and Z. Wang. 2016. Standard Handbook Oil Spill Environmental Forensics: Fingerprinting and Source Identification. Second. Academic Press. https://doi.org/10.1016/B978-0-12-809659-8.00008-5.

Wang, Z., C. Yang, J.L. Parrott, R.A. Frank, Z. Yang, C.E. Brown, and B.P. Hollebone. 2014. "Forensic Source Differentiation of Petrogenic, Pyrogenic, and Biogenic Hydrocarbons in Canadian Oil Sands Environmental Samples." *Journal of Hazardous Materials* 271 (April): 166–77. https://doi.org/10.1016/j.jhazmat.2014.02.021.

TABLES

Table 1. Long-Term Monitoring Program sites sampled in 2022 and 2023 for subtidal marine sediments, Pacific blue mussels and deployment/retrival of the passive sampling devices.

2022	2023	Site	Latitude	Longitude	Datum	Matrix
X	X	AMT-S	61.09056	-146.3928	WGS84	Sediment
X	X	GOC-S	61.12417	-146.4906	WGS84	Sediment
X	X	RED	61.123719	-146.35315	WGS84	Pacific Blue Mussel Tissue
X	X	JAC-B	61.090051	-146.375706	WGS84	Pacific Blue Mussel Tissue
X	X	GOC-B	61.1243682	-146.4961415	WGS84	Pacific Blue Mussel Tissue
X	X	GOC-PSD	61.1242561	-146.4946931	WGS84	Passive Sampler Device
X	X	SAW-B	61.0903062	-146.4091853	WGS84	Pacific Blue Mussel Tissue
X	X	JAC-PSD	61.0906991	-146.3757111	WGS84	Passive Sampler Device
X	X	SAW-PSD	61.0913844	-146.4091726	WGS84	Passive Sampler Device
	X	DII-B	60.49861	-147.6586	WGS84	Pacific Blue Mussel Tissue
	X	DII-PSD	60.49886	-147.66	WGS84	Passive Sampler Device
	X	SHP-B	60.64722	-145.995	WGS84	Pacific Blue Mussel Tissue
	X	SLB-B	60.0675	-147.8319445	WGS84	Pacific Blue Mussel Tissue
	X	KNH-B	60.69055	-146.5833	WGS84	Pacific Blue Mussel Tissue
	X	ZAB-B	60.26583	-147.08445	WGS84	Pacific Blue Mussel Tissue
	X	ZAB2-B	60.298926	-147.00218	WGS84	Pacific Blue Mussel Tissue

Table 2. Analytes reported for 2022 and 2023 sediments and mussel tissue samples.

Saturated Hydrocarbons	
Nonane (C9)	
Decane (C10)	
Undecane	
Dodecane (C12)	
Tridecane	
2,6,10 Trimethyldodecane (1380)	
n-Tetradecane (C14)	
2,6,10-Trimethyltridecane (1470)	
n-Pentadecane (C15)	
n-Hexadecane (C16)	
Norpristane (1650)	
n-Heptadecane (C17)	
Pristane	
n-Octadecane (C18)	
Phytane	
n-Nonadecane (C19)	
n-Eicosane (C20)	
n-Heneicosane (C21)	
n-Docosane (C22)	
n-Tricosane (C23)	
n-Tetracosane (C24)	
n-Pentacosane (C25)	
n-Hexacosane (C26)	
n-Heptacosane (C27)	
n-Octacosane (C28)	
n-Nonacosane (C29)	
n-Triacontane (C30)	
n-Hentriacontane (C31)	
n-Dotriacontane (C32)	
n-Tritriacontane (C33)	
n-Tetratriacontane (C34)	
n-Pentatriacontane (C35)	
n-Hexatriacontane (C36)	
n-Heptatriacontane (C37)	
n-Octatriacontane (C38)	
n-Nonatriacontane (C39)	
n-Tetracontane (C40)	
Total Petroleum Hydrocarbons (C9-C44)	Laboratory Calculation
Total Saturated Hydrocarbons	Laboratory Calculation
o-terphenyl	Surrogate
d50-Tetracosane	Surrogate

Table 2. Analytes reported for 2022 and 2023 sediments and mussel tissue samples.

PAHs
cis/trans-Decalin
C1-Decalins
C2-Decalins
C3-Decalins
C4-Decalins
Naphthalene
C1-Naphthalenes
C2-Naphthalenes
C3-Naphthalenes
C4-Naphthalenes
Benzothiophene
C1-Benzo(b)thiophenes
C2-Benzo(b)thiophenes
C3-Benzo(b)thiophenes
C4-Benzo(b)thiophenes
Biphenyl
Dibenzofuran
Acenaphthylene
Acenaphthene
Fluorene
C1-Fluorenes
C2-Fluorenes
C3-Fluorenes
Dibenzothiophene
C1-Dibenzothiophenes
C2-Dibenzothiophenes
C3-Dibenzothiophenes
C4-Dibenzothiophenes
Phenanthrene
C1-Phenanthrenes/Anthracenes
C2-Phenanthrenes/Anthracenes
C3-Phenanthrenes/Anthracenes
C4-Phenanthrenes/Anthracenes
Retene
Anthracene
Carbazole
Fluoranthene
Benzo[b]fluorene
Pyrene
C1-Fluoranthenes/Pyrenes
C2-Fluoranthenes/Pyrenes
C3-Fluoranthenes/Pyrenes
C4-Fluoranthenes/Pyrenes
Naphthobenzothiophenes
C1-Naphthobenzothiophenes
C2-Naphthobenzothiophenes
C3-Naphthobenzothiophenes
C4-Naphthobenzothiophenes
Benz[a]anthracene
Chrysene/Triphenylene
C1-Chrysenes
C2-Chrysenes
C3-Chrysenes
C4-Chrysenes
Benzo[b]fluoranthene
Benzo[j]fluoranthene/Benzo[k]fluoranthene
Benzo[a]fluoranthene
Benzo[e]pyrene
Benzo[a]pyrene
Perylene
Indeno[1,2,3-cd]pyrene
Dibenz[a,h]anthracene/Dibenz[a,c]anthracene
Benzo[g,h,i]perylene
2-Methylnaphthalene
1-Methylnaphthalene
2,6-Dimethylnaphthalene
2,3,5-Trimethylnaphthalene
4-Methyldibenzothiophene(4MDT)
2/3-Methyldibenzothiophene(2MDT)
1-Methyldibenzothiophene(1MDT)
3-Methylphenanthrene
2-Methylphenanthrene (2MP)
2-Methylanthracene (2MA)
9/4-Methylphenanthrene (9MP)
1-Methylphenanthrene

Surrogates
Naphthalene-d8
Phenanthrene-d10
Benzo(a)pyrene-d12
5B(H)Cholane

Table 2. Analytes reported for 2022 and 2023 sediments and mussel tissue samples.

Geochemical Petroleum Biomarkers	
Hopane (T19)	14b,17b-20R-Methylcholestane (S22)
C23 Tricyclic Terpane (T4)	14b,17b-20S-Methylcholestane (S23)
C24 Tricyclic Terpane (T5)	14b(H),17b(H)-20R-Ethylcholestane (S26)
C25 Tricyclic Terpane (T6)	14b(H),17b(H)-20S-Ethylcholestane (S27)
C24 Tetracyclic Terpane (T6a)	C20 Pregnane
C26 Tricyclic Terpane-22S (T6b)	C21 20-Methylpregnane
C26 Tricyclic Terpane-22R (T6c)	C22 20-Ethylpregnane (a)
C28 Tricyclic Terpane-22S (T7)	C22 20-Ethylpregnane (b)
C28 Tricyclic Terpane-22R (T8)	C26,20S TAS
C29 Tricyclic Terpane-22S (T9)	C26,20R+C27,20S TAS
C29 Tricyclic Terpane-22R (T10)	C28,20S TAS
18a-22,29,30-Trisnorneohopane-TS (T11)	C27,20R TAS
C30 Tricyclic Terpane-22S	C28,20R TAS
C30 Tricyclic Terpane-22R	C29,20S TAS
17a(H)-22,29,30-Trisnorhopane-TM	C29,20R TAS
17a/b,21b/a 28,30-Bisnorhopane (T14a)	5b(H)-C27 (20S) MAS+
17a(H),21b(H)-25-Norhopane (T14b)	5b(H)-C27 (20R) MAS+
30-Norhopane (T15)	5a(H)-C27 (20S) MAS
18a(H)-30-Norneohopane-C29Ts (T16)	5b(H)-C28 (20S) MAS+
17a(H)-Diahopane (X)	5a(H)-C27 (20R) MAS
30-Normoretane (T17)	5a(H)-C28 (20S) MAS
18a(H)&18b(H)-Oleananes (T18)	5b(H)-C28 (20R) MAS+
Moretane (T20)	5b(H)-C29 (20S) MAS+
30-Homohopane-22S (T21)	5a(H)-C29 (20S) MAS
30-Homohopane-22R (T22)	5a(H)-C28 (20R) MAS
Gammacerane/C32-Diahopane	5b(H)-C29 (20R) MAS+
30,31-Bishomohopane-22S (T26)	5a(H)-C29 (20R) MAS
30,31-Bishomohopane-22R (T27)	
30,31-Trishomohopane-22S (T30)	
30,31-Trishomohopane-22R (T31)	**Surrogates**
Tetrakishomohopane-22S (T32)	Naphthalene-d8
Tetrakishomohopane-22R (T33)	Phenanthrene-d10
Pentakishomohopane-22S (T34)	Benzo[a]pyrene-d12
Pentakishomohopane-22R (T35)	5B(H)Cholane
13b(H),17a(H)-20S-Diacholestane (S4)	
13b(H),17a(H)-20R-Diacholestane (S5)	
13b,17a-20S-Methyldiacholestane (S8)	
14b(H),17b(H)-20R-Cholestane (S14)	
14b(H),17b(H)-20S-Cholestane (S15)	**Other**
17a(H)20SC27/C29dia	Total Organic Carbon (Rep1)
17a(H)20rc27/C29dia	Total Organic Carbon (Rep2)
Unknown Sterane (S18)	Total Organic Carbon (Average)
13a,17b-20S-Ethyldiacholestane (S19)	Percent Lipids
14a,17a-20S-Methylcholestane (S20)	Moisture
14a,17a-20R-Methylcholestane (S24)	
14a(H),17a(H)-20S-Ethylcholestane (S25)	
14a(H),17a(H)-20R-Ethylcholestane (S28)	

Table 3. 2022 Analytes quantified in water samples via passive sampling device.

#	Analytes	#	Analytes
1	1,2-dimethylnaphthalene	48	Dibenzo[e,l]pyrene
2	1,4-dimethylnaphthalene	49	Dibenzothiophene
3	1,5-dimethylnaphthalene	50	Fluoranthene
4	1,6and1,3-Dimethylnaphthalene	51	Fluorene
5	1,8-dimethylnaphthalene	52	Indeno[1,2,3-cd]pyrene
6	1-methylnaphthalene	53	Naphthalene
7	1-methylphenanthrene	54	Naphtho[1,2-b]fluoranthene
8	1-methylpyrene	55	Naphtho[2,3-a]pyrene
9	2,3-dimethylanthracene	56	Naphtho[2,3-b]fluoranthene
10	2,6-diethylnaphthalene	57	Naphtho[2,3-e]pyrene
11	2,6-dimethylnaphthalene	58	Naphtho[2,3-j]andNaphtho[1,2-k]fluoranthene
12	2-ethylnaphthalene	59	Naphtho[2,3-k]fluoranthene
13	2-methylanthracene	60	Perylene
14	2-methylnaphthalene	61	Phenanthrene
15	2-methylphenanthrene	62	Pyrene
16	3,6-dimethylphenanthrene	63	Retene
17	5-methylchrysene	64	Triphenylene
18	6-methylchrysene	65	A0/PA0
19	7,12-dimethylbenz[a]anthracene	66	BaA/228
20	9,10-dimethylanthracene	67	BaA/Ch0
21	9-methylanthracene	68	C1-benz[a]anthracenes&chrysenes&triphenylenes
22	Acenaphthene	69	C1-dibenzothiophenes
23	Acenaphthylene	70	C1-fluoranthenes&pyrenes
24	Anthanthrene	71	C1-fluorenes
25	Anthracene	72	C1-naphthalenes
26	Benz[a]anthracene	73	C1-phenanthrenes&anthracenes
27	Benz[j]and[e]aceanthrylene	74	C2-benz[a]anthracenes&chrysenes&triphenylenes
28	Benzo[a]chrysene	75	C2-dibenzothiophenes
29	Benzo[a]fluorene	76	C2-fluoranthenes&pyrenes
30	Benzo[a]pyrene	77	C2-fluorenes
31	Benzo[b]fluoranthene	78	C2-naphthalenes
32	Benzo[b]fluorene	79	C2-phenanthrenes&C2-anthracenes
33	Benzo[b]perylene	80	C3-dibenzothiophenes
34	Benzo[c]fluorene	81	C3-fluorenes
35	Benzo[e]pyrene	82	C3-naphthalenes
36	Benzo[ghi]perylene	83	C3-phenanthrenes&anthracenes
37	Benzo[j]fluoranthene	84	C4-naphthalenes
38	Benzo[k]fluoranthene	85	C4-phenanthrenes&C4-anthracenes
39	Chrysene	86	FL0/FLPY
40	Coronene	87	FL0/PY0
41	Cyclopenta[cd]pyrene	88	FLP1/FLPY0
42	Dibenzo[a,e]fluoranthene	89	FLP1/PY0
43	Dibenzo[a,e]pyrene	90	FLPY/(P2+P3+P4)
44	Dibenzo[a,h]anthracene	91	FLPY0/FLPY01
45	Dibenzo[a,h]pyrene	92	P0/A0
46	Dibenzo[a,i]pyrene	93	PA0/PA01
47	Dibenzo[a,l]pyrene	94	PA1/PA0

Table 4. 2023 Analytes quantified in water samples via passive sampling device.

#	Analyte	#	Analyte
1	1,2-dimethylnaphthalene	48	Dibenzo[e,l]pyrene
2	1,4-dimethylnaphthalene	49	Dibenzothiophene
3	1,5-dimethylnaphthalene	50	Fluoranthene
4	1,6and1,3-Dimethylnaphthalene	51	Fluorene
5	1,8-dimethylnaphthalene	52	Indeno[1,2,3-cd]pyrene
6	1-methylnaphthalene	53	Naphthalene
7	1-methylphenanthrene	54	Naphtho[1,2-b]fluoranthene
8	1-methylpyrene	55	Naphtho[2,3-a]pyrene
9	2,3-dimethylanthracene	56	Naphtho[2,3-b]fluoranthene
10	2,6-diethylnaphthalene	57	Naphtho[2,3-e]pyrene
11	2,6-dimethylnaphthalene	58	Naphtho[2,3-j]andNaphtho[1,2-k]fluoranthene
12	2-ethylnaphthalene	59	Naphtho[2,3-k]fluoranthene
13	2-methylanthracene	60	Perylene
14	2-methylnaphthalene	61	Phenanthrene
15	2-methylphenanthrene	62	Pyrene
16	3,6-dimethylphenanthrene	63	Retene
17	5-methylchrysene	64	Triphenylene
18	6-methylchrysene	65	C1-benz[a]anthracenes&chrysenes&triphenylenes
19	7,12-dimethylbenz[a]anthracene	66	C1-dibenzothiophenes
20	9,10-dimethylanthracene	67	C1-fluoranthenes&pyrenes
21	9-methylanthracene	68	C1-fluorenes
22	Acenaphthene	69	C1-naphthalenes
23	Acenaphthylene	70	C1-phenanthrenes&anthracenes
24	Anthanthrene	71	C2-benz[a]anthracenes&chrysenes&triphenylenes
25	Anthracene	72	C2-dibenzothiophenes
26	Benz[a]anthracene	73	C2-fluoranthenes&pyrenes
27	Benz[j]and[e]aceanthrylene	74	C2-fluorenes
28	Benzo[a]chrysene	75	C2-naphthalenes
29	Benzo[a]fluorene	76	C2-phenanthrenes&C2-anthracenes
30	Benzo[a]pyrene	77	C3-benz[a]anthracenes&chrysenes&triphenylenes
31	Benzo[b]fluoranthene	78	C3-dibenzothiophenes
32	Benzo[b]fluorene	79	C3-fluorenes
33	Benzo[b]perylene	80	C3-naphthalenes
34	Benzo[c]fluorene	81	C3-phenanthrenes&anthracenes
35	Benzo[e]pyrene	82	C4-benz[a]anthracenes&chrysenes&triphenylenes
36	Benzo[ghi]perylene	83	C4-dibenzothiophenes
37	Benzo[j]fluoranthene	84	C4-fluorenes
38	Benzo[k]fluoranthene	85	C4-naphthalenes
39	Chrysene	86	C4-phenanthrenes&C4-anthracenes
40	Coronene		
41	Cyclopenta[cd]pyrene		
42	Dibenzo[a,e]fluoranthene		
43	Dibenzo[a,e]pyrene		
44	Dibenzo[a,h]anthracene		
45	Dibenzo[a,h]pyrene		
46	Dibenzo[a,i]pyrene		
47	Dibenzo[a,l]pyrene		

Table 5. 2022 and 2023 Sediment PAH loads and toxicity comparisons.

	2022 Sediment Samples									2023 Sediment Samples						**Acute Toxicity Threshold (ng/g)***	**Chronic Toxicity Threshold (ng/g)***
Analyte (ng/g dry weight)	GOC-S-22-1	GOC-S-22-2	GOC-S-22-3	GOC-SAND-22	AMT-S-22-1	AMT-S-22-2	AMT-S-22-3	AMT-SAND-22	GOC-S-22-1-DUP	GOC-S-23-1	GOC-S-23-2	GOC-S-23-3	AMT-S-23-1	AMT-S-23-2	AMT-S-23-3		
Naphthalene	1.77	2.5	2.87	0.319	2.69	1.96	2.57	0.249	2.05	1.46	1.31	1.24	2.34	1.92	2.12	1600000	385000
C1-Naphthalenes	1.46	1.79	2.02	0.242	2.38	1.89	2.55	0.304	1.65	1.26	0.893	0.878	2	2.14	2.02	1850000	444000
C2-Naphthalenes	2.3	2.94	3.12	0.841	4.44	3.25	4.14	0.836	2.58	2.42	2	1.69	4.11	3.38	3.75	2120000	510000
C3-Naphthalenes	1.97	2.72	2.83	0.841	3.71	2.95	3.9	0.836	1.92	2.3	1.75	1.38	3.92	3.76	3.74	2420000	581000
C4-Naphthalenes	1.56	2.25	1.85	0.841	3.12	2.37	2.91	0.836	1.54	1.42	0.996	1.34	1.35	2.42	2.17	2730000	657000
Acenaphthylene	0.257	0.278	0.332	0.841	0.196	0.214	0.381	0.836	0.587	1.71	0.719	0.739	1.1	1.31	1.09	1880000	452000
Acenaphthene	0.569	0.714	0.663	0.841	0.517	0.559	1.26	0.836	0.724	0.636	0.586	0.519	0.785	0.629	0.624	2040000	491000
Fluorene	1.22	1.56	1.61	0.084	1.48	1.27	1.97	0.093	1.13	0.728	0.738	0.669	1.05	1.16	1.27	2240000	538000
C1-Fluorenes	1.38	2.04	2.36	0.841	2.75	2.12	2.68	0.836	1.43	1.22	1.01	0.955	1.91	1.9	2.12	2540000	611000
C2-Fluorenes	1.95	2.47	2.27	0.841	3.42	2.59	2.91	0.836	1.98	1.42	0.996	1.34	1.35	2.15	2.89	2850000	686000
C3-Fluorenes	1.56	1.13	1.11	0.841	5.43	5.35	10.8	0.836	1.54	1.42	0.996	1.34	1.35	1.23	5.91	3200000	769000
Dibenzothiophene	0.447	0.548	0.568	0.035	0.608	0.568	1.1	0.04	0.405	0.311	0.241	0.208	0.535	0.694	0.612	-	-
C1-Dibenzothiophenes	0.626	0.696	0.541	0.841	1.09	0.82	1.2	0.242	0.576	0.316	0.246	0.302	0.895	0.802	0.743	-	-
C2-Dibenzothiophenes	1.27	1.13	1.34	0.841	2.54	2.15	2.86	0.836	1.19	0.822	0.646	0.704	2.48	2.04	2.2	-	-
C3-Dibenzothiophenes	1.56	1.13	1.11	0.841	3.14	2.68	3.5	0.836	1.54	1.42	0.996	1.34	3.3	2.9	2.86	-	-
C4-Dibenzothiophenes	1.56	1.13	1.11	0.841	3.02	2.21	3.38	0.836	1.54	1.42	0.996	1.34	11.3	2.73	2.81	-	-
Phenanthrene	3.71	5.17	5.22	0.151	5.12	4.51	11.8	0.184	3.67	2.45	1.93	1.63	3.55	4.19	4.06	2480000	596000
C1-Phenanthrenes/Anthracenes	6.67	6.6	4.87	0.294	5.84	3.6	6.47	0.306	5.96	2.16	1.74	1.4	4.2	4.54	4.24	2790000	670000
C2-Phenanthrenes/Anthracenes	1.59	1.97	2.05	0.841	4.33	3.16	4.68	0.836	1.83	2.22	0.942	1.26	3.62	3.18	3.55	3100000	746000
C3-Phenanthrenes/Anthracenes	1.08	1.46	1.37	0.841	3.82	2.72	3.7	0.836	1.21	1.15	0.724	0.804	3.87	3.27	2.69	3450000	829000
C4-Phenanthrenes/Anthracenes	1.56	0.786	0.993	0.841	2.35	2.3	2.79	0.836	1.54	0.93	0.996	1.34	3.61	2.32	2.48	3790000	912000
Anthracene	0.618	0.666	0.678	0.841	0.594	0.681	1.78	0.836	0.525	0.781	0.405	0.359	0.934	1.48	1.28	2470000	594000
Fluoranthene	2.96	5.27	6.81	0.065	3.8	3.77	22.1	0.1	5.1	1.96	1.34	1.04	1.83	2.5	2.58	2940000	707000
Pyrene	1.81	3.34	4.25	0.053	2.81	2.68	9.67	0.071	4.71	1.81	1.14	0.885	1.78	2.84	2.82	2900000	697000
C1-Fluoranthenes/Pyrenes	1.91	2.43	2.79	0.841	3.2	2.85	4.78	0.836	3.08	2.68	1.18	1.22	3.52	3.57	3.11	3200000	770000
C2-Fluoranthenes/Pyrenes	1.32	1.92	1.83	0.841	3.32	3.12	5.77	0.836	1.99	1.35	0.932	0.731	2.14	2.54	2.58	-	-
C3-Fluoranthenes/Pyrenes	1.56	1.51	1.54	0.841	3.31	3.09	4.74	0.836	1.54	1.42	0.996	1.34	2.75	2.8	3.05	-	-
C4-Fluoranthenes/Pyrenes	1.56	1.13	1.11	0.841	4.26	3.84	5.31	0.836	1.54	1.42	0.996	1.34	2.89	3.48	3.71	-	-
Benz[a]anthracene	0.714	1.15	1.09	0.026	0.86	1.16	1.02	0.029	1.4	1.97	0.606	0.324	1.29	2.58	1.88	3500000	841000
Chrysene/Triphenylene	1.44	1.96	1.78	0.072	2.08	2.42	5.37	0.076	1.86	2.78	0.819	0.524	2.02	5.31	2.62	3510000	844000
C1-Chrysenes	0.657	1.17	0.944	0.841	2.1	1.83	2.42	0.836	1.19	1.54	0.719	0.663	2.35	2.92	2.9	3870000	929000
C2-Chrysenes	2.94	2.21	1.77	0.841	3.46	3.26	4.37	0.836	2.13	1.42	1.41	1.34	3.79	4.13	4.95	4200000	1010000
C3-Chrysenes	1.56	1.13	1.11	0.841	8.1	1.23	8.83	0.836	1.54	1.42	0.996	1.34	1.35	1.23	1.34	4620000	1110000
C4-Chrysenes	1.56	1.13	1.11	0.841	1.18	1.23	1.23	0.836	1.54	1.42	0.996	1.34	1.35	1.23	1.34	5030000	1210000
Benzo[b]fluoranthene	0.769	1.34	1.17	0.085	1.36	1.38	2.52	0.836	1.77	2.09	0.71	0.348	1.22	2.24	1.87	4070000	979000
Benzo[j]fluoranthene/Benzo[k]fluoranthene	0.609	1.1	0.859	0.841	0.775	1.06	1.15	0.836	1.44	2.12	0.521	0.313	1.11	2.11	1.64	4080000	981000
Benzo[e]pyrene	0.616	1.09	0.919	0.841	1.24	1.22	1.56	0.836	1.3	1.84	0.603	0.426	1.24	2.2	2.08	4020000	967000
Benzo[a]pyrene	0.432	0.934	0.719	0.841	0.822	1.19	0.689	0.836	1.48	1.94	0.67	0.348	1.17	2.3	1.8	4020000	965000
Indeno[1,2,3-cd]pyrene	0.448	0.545	0.426	0.841	0.59	0.63	0.548	0.836	0.872	1.96	0.455	0.312	1.16	2.35	1.85	4620000	1110000
Dibenz[a,h]anthracene/Dibenz[a,c]anthracene	0.261	0.18	0.15	0.841	0.126	0.222	0.172	0.836	0.256	1.14	0.2	0.11	0.468	1.23	0.878	4660000	1120000
Benzo[g,h,i]perylene	0.5	0.78	0.593	0.841	1.18	1.04	1.04	0.836	1.08	2	0.503	0.391	1.32	2.49	1.96	4540000	1090000

Table 5. 2022 and 2023 Sediment PAH loads and toxicity comparisons.

	2022 Sediment Samples									2023 Sediment Samples						Acute Toxicity Threshold (ng/g)*	Chronic Toxicity Threshold (ng/g)*
Analyte (ng/g dry weight)	GOC-S-22-1	GOC-S-22-2	GOC-S-22-3	GOC-SAND-22	AMT-S-22-1	AMT-S-22-2	AMT-S-22-3	AMT-SAND-22	GOC-S-22-1-DUP	GOC-S-23-1	GOC-S-23-2	GOC-S-23-3	AMT-S-23-1	AMT-S-23-2	AMT-S-23-3		
Total Organic Carbon (%)	0.459	0.629	0.601	NA	0.487	0.463	0.547	NA	0.491	0.509	0.56	0.452	0.626	0.52	0.596		
Ratio of Acute Benchmark to TOC	3.8E-05	3.6E-05	3.8E-05	-	6E-05	5.1E-05	8.4E-05	-	4.4E-05	3.6E-05	2E-05	2.3E-05	3.7E-05	5.2E-05	4.6E-05		
Risk for Acute Toxic Effects	Low	Low	Low	-	Low	Low	Low	-	Low	Low	Low	Low	Low	Low	Low		
Ratio of Chronic Benchmark to	0.00016	0.00015	0.00016	-	0.00025	0.00021	0.00035	-	0.00018	0.00015	8.3E-05	9.6E-05	0.00016	0.00022	0.00019		
Risk for Chronic Toxic Effects	Low	Low	Low	-	Low	Low	Low	-	Low	Low	Low	Low	Low	Low	Low		
Sum 42 PAHs	60.3	72.0	71.9	26.7	107.2	87.1	162.6	26.8	72.9	64.3	37.6	37.1	94.3	100.2	100.2		
Sum 16 PAHs	18.1	27.5	29.2	7.6	25.0	24.7	64.0	8.3	28.7	27.5	12.7	9.8	23.1	36.6	30.3		
Low Molecular weight PAH[1]	36.7	41.7	40.9	14.6	62.6	49.9	79.3	14.0	37.1	30.0	21.9	22.8	59.6	50.1	55.2		
High Molecular weight PAH[2]	23.6	30.3	31.0	12.1	44.6	37.2	83.3	12.8	35.8	34.3	15.8	14.3	34.7	50.1	45.0		
%LMW PAH	60.8	57.9	56.9	54.7	58.4	57.3	48.8	52.1	50.9	46.6	58.1	61.4	63.2	50.0	55.1		
%HMW PAH	39.2	42.1	43.1	45.3	41.6	42.7	51.2	47.9	49.1	53.4	41.9	38.6	36.8	50.0	44.9		
Sum of Carcinogenic PAHs [3]	4.7	7.2	6.2	3.5	6.6	8.1	11.5	4.3	9.1	14.0	4.0	2.3	8.4	18.1	12.5		

* EPA Sediment Toxicity Benchmarks : https://archive.epa.gov/emergency/Bpspill/web/html/sediment-Benchmarks.html

[1] Low Molecular Weight PAHs : naphthalenes - phenanthrenes (2-3-ring PAH)

[2] High Molecular weight PAHs: fluoranthene - Benzo (g,h,i)perylene (3-6 ring PAH)

[3] Carcinogenic PAHs: Benz[a]anthracene, Chrysene/Triphenylene, Benzo[b]fluoranthene, Benzo[j]fluoranthene/Benzo[k]fluoranthene, Benzo[a]pyrene, Indeno[1,2,3-cd]pyrene, Dibenz[a,h]anthracene/Dibenz[a,c]anthracene

Table 6. 2022 and 2023 tissue samples PAH summaries.

Sample	Sum 42 PAH (wet weight)	Sum 42 PAH (dry weight)	Sum 42 PAH (lipid weight)	Sum 16 PAH[1] (wet weight)	Sum 16 PAH (dry weight)	Sum low molecular weight PAH[2]	Sum high molecular weight PAH[3]	% low molecular weight PAH	% high molecular weight PAH	Sum of carcin-ogenic PAH4
JAC-B-22-1	9.60	55.15	278.95	7.45	42.83	5.71	3.89	59.51	40.49	1.60
JAC-B-22-2	5.72	46.90	301.16	4.59	37.61	3.73	1.99	65.24	34.76	0.46
JAC-B-22-3	5.05	34.60	237.14	4.43	30.34	3.75	1.30	74.26	25.74	0.40
SAW-B-22-1	7.01	57.01	381.09	3.88	31.54	5.93	1.09	84.53	15.47	0.29
SAW-B-22-2	4.75	32.95	227.03	4.16	28.89	3.46	1.28	72.96	27.04	0.39
SAW-B-22-3	5.99	44.70	290.78	3.81	28.44	4.95	1.04	82.67	17.33	0.25
GOC-B-22-1	7.05	45.20	284.31	5.74	36.78	4.80	2.26	68.00	32.00	0.53
GOC-B-22-2	6.38	45.92	320.75	5.23	37.61	4.22	2.16	66.11	33.89	0.55
GOC-B-22-3	8.78	65.54	513.57	5.08	37.87	6.77	2.02	77.06	22.94	0.58
RED-B-22-1	23.24	173.43	1408.48	7.77	57.97	18.28	4.97	78.64	21.36	0.50
RED-B-22-2	15.93	136.11	925.87	7.30	62.43	10.73	5.20	67.35	32.65	2.70
RED-B-22-3	18.38	159.83	1038.47	5.88	51.16	14.38	4.01	78.21	21.79	1.18
RED-B-22-2-DUP	16.33	120.05	850.36	7.33	53.90	11.02	5.31	67.48	32.52	2.72
JAC-B-23-1	6.30	-	-	4.91	-	4.25	2.04	67.56	32.44	0.69
JAC-B-23-2	6.30	42.58	263.68	5.01	33.85	4.75	1.56	75.33	24.67	0.40
JAC-B-23-3	6.04	35.30	183.50	4.56	26.69	4.03	2.01	66.74	33.26	0.59
AMT-B-23-1	6.15	39.69	232.15	4.60	29.70	4.80	1.35	78.01	21.99	0.27
AMT-B-23-2	6.03	35.45	171.71	4.32	25.44	5.03	1.00	83.47	16.53	0.23
AMT-B-23-3	5.90	34.10	174.56	4.57	26.40	4.41	1.49	74.71	25.29	0.33
GOC-B-23-1	7.42	43.65	234.84	5.61	33.02	5.66	1.76	76.32	23.68	0.54
GOC-B-23-2	7.59	43.59	226.42	5.92	34.05	5.58	2.00	73.61	26.39	0.55
GOC-B-23-3	10.44	56.42	278.35	6.11	33.04	8.48	1.96	81.26	18.74	0.55
DII-B-23-1	32.14	158.33	728.80	27.98	137.83	12.98	19.16	40.39	59.61	10.48
DII-B-23-2	3.43	17.31	-	2.40	12.12	2.80	0.63	81.56	18.44	0.15
DII-B-23-3	2.85	-	115.85	2.53	-	2.19	0.66	76.98	23.02	0.18
KNH-B-23-1	7.24	43.62	274.28	5.83	35.13	4.98	2.26	68.80	31.20	0.50
KNH-B-23-2	2.85	18.50	175.86	2.08	13.47	2.28	0.57	79.85	20.15	0.18
KNH-B-23-3	73.76	501.77	-	62.20	423.13	26.70	47.06	36.20	63.80	26.77
SLB-B-23-1	6.47	38.28	306.59	5.45	32.23	3.45	3.02	53.39	46.61	1.49
SLB-B-23-2	3.50	21.89	152.30	2.63	16.46	2.83	0.68	80.65	19.35	0.21
SLB-B-23-3	2.92	17.19	135.32	2.15	12.65	2.33	0.59	79.71	20.29	0.17
RED-B-23-1	17.54	110.30	759.18	7.01	44.08	12.05	5.49	68.71	31.29	0.43
RED-B-23-2	29.73	203.65	1327.37	13.98	95.73	20.36	9.37	68.48	31.52	4.27
RED-B-23-3	19.58	123.11	755.79	7.71	48.48	13.50	6.08	68.96	31.04	0.52
ZAB-B-23-1	4.04	23.22	171.23	2.85	16.35	3.34	0.70	82.68	17.32	0.17
ZAB-B-23-2	4.71	32.06	157.63	3.01	20.48	4.07	0.65	86.31	13.69	0.13
ZAB-B-23-3	12.63	66.85	473.18	9.58	50.70	7.35	5.28	58.21	41.79	4.34
ZAB2-B-23-1	5.79	40.47	208.17	4.37	30.57	4.07	1.72	70.30	29.70	0.59
ZAB2-B-23-2	5.47	36.25	316.36	5.09	33.69	3.20	2.28	58.41	41.59	1.14
ZAB2-B-23-3	7.92	48.61	257.24	6.06	37.17	5.31	2.61	67.07	32.93	1.06
SHB-B-23-1	3.84	22.60	199.07	2.56	15.06	3.12	0.72	81.18	18.82	0.15
SHB-B-23-2	3.78	22.76	119.56	2.57	15.48	3.38	0.40	89.33	10.67	0.00
SHB-B-23-3	5.24	29.76	256.76	3.40	19.33	4.27	0.97	81.56	18.44	0.21

[1] 16 EPA Priority PAHs - naphthalene, acenaphthylene, acenaphthene, fluorene, phenanthrene, anthracene, fluoranthene, pyrene, benzo[a]anthracene, chrysene, benzo[b]fluoranthene, benzo[k]fluoranthene , benzo[a]pyrene, benzo[g,h,i]perylene, indeno[1,2,3-c,d]pyrene, and dibenz[a,h]anthracene

[2] Low molecular weight PAHs : naphthalenes - phenanthrenes (2-3-ring PAH)

[3] High molecular weight PAHs: fluoranthene - benzo (g,h,i)perylene (3-6 ring PAH)

[4] Carcinogenic PAHs: benzo[a]pyrene, benz[a]anthracene, benzo[b]fluoranthene, benzo[k]fluoranthene, chrysene, dibenz[a,h]anthracene, indeno[1,2,3-cd]pyrene

Table 7. 2022 Water PAH concentrations quantified via passive sampling device.

Analyte (ng/L C-Free)	GOC 01	GOC 02	GOC 03	SAW 01	SAW 02	SAW 03	JAC 01	JAC 02	JAC 03	Field Blk SAW	Field Blk JAC	Trip Blk Deploy	Trip Blk Retrieve
Naphthalene	1.12	1.41	1.15	-	-	-	-	-	-	7.1	7.3	-	7.2
C1-naphthalenes	-	-	-	-	-	-	-	-	-	22.9	29	-	17.5
C2-naphthalenes	2.57	3.42	3.67	4.57	3.61	4.13	3.38	3.84	4.22	16.6	21.4	-	9.41
C3-naphthalenes	11.9	15	17.4	18.4	20.2	16.9	14.9	21.2	19.7	-	-	-	-
C4-naphthalenes	23.6	24.1	34.9	21.9	18.7	25.7	20.9	32.6	34.1	-	-	-	-
Acenaphthylene	-	-	-	-	-	-	-	-	-	-	-	-	-
Acenaphthene	0.176	0.265	0.223	0.00489	0.0699	0.0409	0.0834	0.0851	0.0847	1.07	1.07	1.07	1.07
Fluorene	0.14	0.174	0.19	0.0891	0.0851	0.0939	0.082	0.119	0.134	1.55	0.81	-	-
C1-fluorenes	0.112	0.147	0.179	0.115	0.0925	0.148	0.0828	0.181	0.152	8.86	5.77	-	-
C2-fluorenes	0.452	0.0216	0.605	0.347	0.34	0.3	0.359	0.68	0.555	-	-	-	-
C3-fluorenes	0.638	0.664	0.706	0.522	0.426	0.491	0.443	0.764	0.776	-	-	-	-
Anthracene	0.00106	0.00125	0.00123	0.0134	0.0157	0.00209	0.00155	0.00208	0.00216	1.05	1.05	1.05	1.05
Phenanthrene	0.271	0.392	0.384	0.162	0.163	0.185	0.155	0.25	0.279	-	-	-	-
C1-phenanthrenes&anthracenes	0.1	0.156	0.148	0.14	0.137	0.155	0.108	0.195	0.191	-	-	-	-
C3-phenanthrenes&anthracenes	-	-	-	0.77	0.444	0.625	0.364	0.614	-	-	-	-	-
Dibenzothiophene	0.0128	0.018	0.017	0.011	0.0121	0.0128	0.00866	0.0135	0.0157	0.75	0.24	0.24	0.33
C1-dibenzothiophenes	0.018	0.0234	0.0223	0.0419	0.0328	0.0444	0.028	0.0469	0.0377	-	-	-	-
C2-dibenzothiophenes	0.0179	0.02	0.025	0.0503	0.0381	0.041	0.0324	0.0527	0.0549	-	-	-	-
C3-dibenzothiophenes	-	-	-	-	-	-	-	-	0.153	-	-	-	-
Fluoranthene	0.106	0.216	0.201	0.0678	0.062	0.0704	0.0672	0.12	0.131	0.54	0.54	0.54	0.54
Pyrene	0.0223	0.0404	0.0402	0.014	0.012	0.0158	0.0123	0.0252	0.0216	0.42	0.42	0.42	0.42
C1-fluoranthenes&pyrenes	0.0219	0.0443	0.0265	0.0366	-	-	-	-	-	-	-	-	-
C2-fluoranthenes&pyrenes	-	-	-	-	-	-	-	-	-	-	-	-	-
Benz[a]anthracene	0.00206	0.00488	0.00425	0.000998	0.000978	0.00105	0.000669	0.00104	0.00109	0.75	0.75	0.75	0.75
Perylene	0.000332	0.000635	0.00061	0.00158	0.00155	0.00166	0.00106	0.00164	0.00173	1	1	1	1
Benzo[b]fluoranthene	0.00102	0.00226	0.00194	0.000495	0.000485	0.00052	0.000331	0.000514	0.000541	0.37	0.37	0.37	0.37
Benzo[e]pyrene	0.000871	0.000494	0.000474	0.00123	0.00121	0.0013	0.000822	0.00128	0.00135	0.71	0.71	0.71	0.71
Benzo[a]pyrene	0.000373	0.000713	0.000685	0.00177	0.00174	0.00186	0.00118	0.00184	0.00194	1.18	1.18	1.18	1.18
Indeno[1,2,3-cd]pyrene	0.000109	0.000209	0.00020	0.000521	0.00051	0.000548	0.000348	0.000542	0.00057	0.26	0.26	0.26	0.26
Sum 42 PAHs[1]	41.284	46.122	59.896	47.262	44.447	48.962	41.012	60.795	60.615	65.110	71.870	7.590	41.790
Sum 42 PAH w/o Naphthalene	2.094	2.192	2.776	2.392	1.937	2.232	1.832	3.155	2.595	18.510	14.170	7.590	7.680
Sum 16 PAHs[2]	1.841	2.508	2.198	0.358	0.414	0.415	0.406	0.608	0.660	16.000	15.460	7.350	14.550
Sum low molecular weight PAH[3]	41.129	45.812	59.621	47.137	44.366	48.869	40.928	60.643	60.455	59.880	66.640	2.360	36.560
Sum high molecular weight PAH[4]	0.155	0.310	0.276	0.125	0.080	0.093	0.084	0.152	0.160	5.230	5.230	5.230	5.230
Percent low molecular weight PAH	0.996	0.993	0.995	0.997	0.998	0.998	0.998	0.997	0.997	0.920	0.927	0.311	0.875
Percent high molecular weight PAH	0.004	0.007	0.005	0.003	0.002	0.002	0.002	0.003	0.003	0.080	0.073	0.689	0.125
Sum of Carcinogenic PAHs [5]	0.004	0.008	0.007	0.004	0.004	0.004	0.003	0.004	0.004	2.560	2.560	2.560	2.560
Analyte Count	24	24	24	24	23	23	23	23	23	16	16	11	14
Percent Naphthalene	0.949	0.952	0.954	0.949	0.956	0.954	0.955	0.948	0.957	0.716	0.803	0.000	0.816

[1] All PAHs listed

[2] 16 EPA Priority PAHs - naphthalene, acenaphthylene, acenaphthene, fluorene, phenanthrene, anthracene, fluoranthene, pyrene, benzo[a]anthracene, chrysene, benzo[b]fluoranthene, benzo[k]fluoranthene , benzo[a]pyrene, benzo[g,h,i]perylene, indeno[1,2,3-c,d]pyrene, and dibenz[a,h]anthracene

[3] Low molecular weight PAHs:napthalenes - phenanthrenes (2-3-ring PAH)

[4] High molecular weight PAHs: fluoranthene - benzo (g,h,i)perylene (3-6 ring PAH)

[5] Carcinogenic PAHs: benzo[a]pyrene, benz[a]anthracene, benzo[b]fluoranthene, benzo[k]fluoranthene, chrysene, dibenz[a,h]anthracene, indeno[1,2,3-cd]pyrene

Table 8. 2023 Water PAH concentrations quantified via passive sampling device

Analyte (ng/L C-Free)	GOC_PSD _23_1 F23-06	GOC_PSD _23_2 F23-06	GOC_PSD _23_3 F23-06	DII_PSD _23_1 F23-06	DII_PSD_ 23_2 F23-06	DII_PSD_ 23_3 F23-06	JAC_PSD _23_1 F23-06	JAC_PSD _23_2 F23-06	JAC_PSD _23_3 F23-06	SAW_PSD _23_1 F23-06	SAW_PSD _23_2 F23-06	SAW_PSD _23_3 F23-06	F23-06 trip blank 1	F23-06 trip blank - 02	F23-06 field blank 5/6/23	F23-06 field blank 6/3/23
Naphthalene	2.47	2.31	1.83	1.6	0.936	1.25	1.18	1.67	1.84	12.2	5.4	3.2	23.5	23.5	48.9	17.2
C1-naphthalenes	1.67	1.46	1.68	0.403	0.276	0.368	1.49	1.45	1.08	1.31	1.01	1.03	15.7	15	30.7	11.3
C2-naphthalenes	5.69	4.6	5.72	1.44	1.75	1.92	4.94	4.43	5.54	5.65	4.6	4.11	26.2	25	38.5	26.6
C3-naphthalenes	23.9	21.3	30.4	12.6	9.12	9.26	20.8	17.9	21	31.8	21.8	20	41.8	37.8	67.6	43
C4-naphthalenes	39.2	36.9	56.7	25.4	16	16.4	35	35.5	49.5	57.3	40.9	36.8	-	-	-	-
Acenaphthylene	-	-	-	-	-	-	-	-	-	-	-	-	-	-	-	-
Acenaphthene	0.245	0.204	0.261	-	-	-	0.181	-	-	-	-	-	-	-	-	-
Fluorene	0.0905	0.0907	-	-	-	-	0.0668	0.0651	0.101	0.15	0.0926	0.0956	-	-	-	-
C1-fluorenes	0.605	0.704	0.43	1.13	0.283	0.156	0.502	1.5	0.457	0.617	0.478	0.479	-	-	-	-
C2-fluorenes	1.99	2.57	3.22	7.16	1.15	1.24	2.76	8	5.37	3.04	3.13	2.76	-	-	-	-
C3-fluorenes	-	-	1.4	6.77	-	-	1.42	7.15	1.81	2.15	1.6	2.8	-	-	-	-
Anthracene	-	-	-	-	-	-	-	-	-	-	-	-	-	-	-	-
Phenanthrene	0.242	0.254	0.264	0.0711	0.0684	0.0937	0.267	0.248	0.313	0.284	0.22	0.255	-	-	-	-
C1-phenanthrenes&anthracenes	0.159	0.166	0.172	0.122	0.0677	0.101	0.166	0.206	0.197	0.23	0.161	0.198	-	-	-	-
C3-phenanthrenes&anthracenes	0.598	0.577	0.581	0.583	-	-	-	1.05	1.09	1.16	0.984	0.886	-	-	-	-
Dibenzothiophene	0.012	0.0109	0.012	0.0218	-	-	0.00963	0.0253	0.0222	0.024	0.0202	0.024	-	-	-	-
C1-dibenzothiophenes	0.0353	0.0417	0.0441	0.215	0.0191	0.0261	0.0417	0.225	0.176	0.191	0.158	0.189	0	0	0	3.39
C2-dibenzothiophenes	0.0381	0.0267	0.0427	0.46	-	-	0.0486	0.364	0.306	0.36	0.285	0.312	-	-	-	-
C3-dibenzothiophenes	-	-	-	0.348	-	-	-	0.283	0.206	0.287	0.176	0.213	-	-	-	-
C4-dibenzothiophenes	-	-	-	-	-	-	-	-	-	-	-	-	-	-	-	-
Fluoranthene	0.136	0.129	0.14	0.016	0.0127	0.0175	0.115	0.124	0.142	0.0975	0.0742	0.0893	-	-	-	-
Pyrene	0.0295	0.0305	0.0313	-	-	-	0.0198	0.019	0.0294	0.0151	0.0123	0.0159	-	-	-	-
C1-fluoranthenes&pyrenes	0.0474	0.0371	0.0298	-	-	-	-	0.0617	0.057	0.0575	0.0278	0.0483	-	-	-	-
C2-fluoranthenes&pyrenes	-	-	-	-	-	-	-	-	-	-	-	-	-	-	-	-
Benz[a]anthracene	-	-	-	-	-	-	-	-	-	-	-	-	-	-	-	-
Perylene	-	-	-	-	-	-	-	-	-	-	-	-	-	-	-	-
Benzo[b]fluoranthene	-	-	-	-	-	-	-	-	-	-	-	-	-	-	-	-
Benzo[e]pyrene	-	-	-	-	-	-	-	-	-	-	-	-	-	-	-	-
Benzo[a]pyrene	-	-	-	-	-	-	-	-	-	-	-	-	-	-	-	-
Indeno[1,2,3-cd]pyrene	-	-	-	-	-	-	-	-	-	-	-	-	-	-	-	-
Sum 42 PAHs[1]	77.1578	71.4116	102.9579	58.3399	29.6829	30.8323	69.00753	80.2711	89.2366	116.9231	81.1291	73.5051	107.2	101.3	185.7	101.49
Sum 42 PAH w/o Naphthalene	4.228	4.842	6.628	16.897	1.601	1.634	5.598	19.321	10.277	8.663	7.419	8.365	0.000	0.000	0.000	3.390
Sum 16 PAHs[2]	3.213	3.018	2.526	1.687	1.017	1.361	1.830	2.126	2.425	12.747	5.799	3.656	23.500	23.500	48.900	17.200
Sum low molecular weight PAH[3]	76.945	71.215	102.757	58.324	29.670	30.815	68.873	80.066	89.008	116.753	81.015	73.352	107.200	101.300	185.700	101.490
Sum high molecular weight PAH[4]	0.213	0.197	0.201	0.016	0.013	0.018	0.135	0.205	0.228	0.170	0.114	0.154	0.000	0.000	0.000	0.000
Percent low molecular weight PAH	0.997	0.997	0.998	1.000	1.000	0.999	0.998	0.997	0.997	0.999	0.999	0.998	1.000	1.000	1.000	1.000
Percent high molecular weight PAH	0.003	0.003	0.002	0.000	0.000	0.001	0.002	0.003	0.003	0.001	0.001	0.002	0.000	0.000	0.000	0.000
Sum of Carcinogenic PAHs[5]	0.000	0.000	0.000	0.000	0.000	0.000	0.000	0.000	0.000	0.000	0.000	0.000	0.000	0.000	0.000	0.000
Analyte Count	18	18	18	16	11	11	17	19	19	19	19	19	5	5	5	5
Percent Naphthalene	0.945	0.932	0.936	0.710	0.946	0.947	0.919	0.759	0.885	0.926	0.909	0.886	1.000	1.000	1.000	0.967

[1] All PAHs listed
[2] 16 EPA Priority PAHs - naphthalene, acenaphthylene, acenaphthene, fluorene, phenanthrene, anthracene, fluoranthene, pyrene, benzo[a]anthracene, chrysene, benzo[b]fluoranthene, benzo[k]fluoranthene , benzo[a]pyrene, benzo[g,h,i]perylene, indeno[1,2,3-c,d]pyrene, and dibenz[a,h]anthracene
[3] Low molecular weight PAHs: naphthalenes - phenanthrenes (2-3-ring PAH)
[4] High molecular weight PAHs: fluoranthene - benzo (g,h,i)perylene (3-6 ring PAH)
[5] Carcinogenic PAHs: benzo[a]pyrene, benz[a]anthracene, benzo[b]fluoranthene, benzo[k]fluoranthene, chrysene, dibenz[a,h]anthracene, indeno[1,2,3-cd]pyrene

Table 9. Saturated hydrocarbon (SHC) totals and diagnostic ratios of sediment and mussel tissues sampled in 2022 and 2023.

		Saturated Hydrocarbons (µg/g)		Diagonistic Ratios			
	Sample ID	Total Petroleum Hydrocarbons (C9-C44)	Total Saturated Hydrocarbons	Ratio of T15/T19[1]	Ratio of Pristane/ Phytane[2]	Ratio of Pristane/ C17[3]	Ratio of Phytane/ C18[4]
Sediments	GOC-S-22-1	5.25	1.75	1.005	0.857	0.500	0.636
	GOC-S-22-2	21.6	2.7	0.615	1.833	0.846	0.667
	GOC-S-22-3	22.6	2.38	0.713	1.833	0.786	0.667
	GOC-SAND-22	0.213	0.052	-	-	-	-
	AMT-S-22-1	38.6	2.41	0.648	2.700	1.350	0.714
	AMT-S-22-2	28.5	1.43	0.569	0.917	0.423	0.857
	AMT-S-22-3	33.3	2.38	0.528	3.636	2.222	1.100
	AMT-SAND-22	-	0.052	-	-	-	-
	GOC-S-22-1-DUP	5.57	1.68	0.608	1.400	0.778	0.625
	GOC-S-23-1	19.1	2.18	-	-	0.818	-
	GOC-S-23-2	32.2	3.27	0.681	4.667	1.167	0.500
	GOC-S-23-3	21.5	1.63	-	-	0.500	-
	AMT-S-23-1	69.6	2.1	0.540	1.154	0.214	1.444
	AMT-S-23-2	44.4	1.66	0.542	1.500	0.191	0.667
	AMT-S-23-3	63	2.08	0.527	1.100	0.183	1.000
Pacific Blue Mussel Tissue*	JAC-B-22-1	1.45	0.92	-	14.286	1.887	0.304
	JAC-B-22-2	-	0.689	-	15.250	1.794	0.222
	JAC-B-22-3	-	0.586	-	20.667	2.000	0.231
	SAW-B-22-1	-	0.677	-	9.800	1.690	0.294
	SAW-B-22-2	-	0.607	-	12.250	1.400	0.235
	SAW-B-22-3	-	0.685	-	22.000	1.467	0.231
	GOC-B-22-1	0.488	0.768	-	10.500	1.400	0.400
	GOC-B-22-2	-	0.716	-	10.800	1.256	0.294
	GOC-B-22-3	6.09	0.646	-	8.800	1.100	0.357
	RED-B-22-1	13.5	0.786	-	3.556	0.696	0.529
	RED-B-22-2	8.75	0.467	-	4.167	0.926	0.667
	RED-B-22-3	12.2	0.692	-	3.750	0.732	0.500
	RED-B-22-2-DUP	11.4	0.582	-	3.250	0.765	0.667
	JAC-B-23-1	8.88	2.9	-	41.400	4.929	0.385
	JAC-B-23-2	3.73	1.65	-	29.500	3.218	0.545
	JAC-B-23-3	3.16	1.57	0.774	32.500	3.250	0.308
	AMT-B-23-1	7.41	4.11	0.361	29.600	2.596	0.385
	AMT-B-23-2	0.961	1.59	-	35.600	3.179	0.357
	AMT-B-23-3	2.44	1.41	0.866	-	2.940	-
	GOC-B-23-1	3.6	3.64	-	14.500	2.109	0.667
	GOC-B-23-2	0.64	1.73	0.740	21.429	2.586	0.778
	GOC-B-23-3	1.92	1.88	-	29.857	2.155	0.778
	DII-B-23-1	3.19	3.64	-	-	3.533	-
	DII-B-23-2	10.1	2.73	-	114.500	5.089	0.154
	DII-B-23-3	7.02	2.38	0.570	-	4.556	-
	KNH-B-23-1	17.8	3.32	-	-	0.658	-
	KNH-B-23-2	7.62	1.77	-	-	0.904	-

Table 9. Saturated hydrocarbon (SHC) totals and diagnostic ratios of sediment and mussel tissues sampled in 2022 and 2023.

	Saturated Hydrocarbons (µg/g)		Diagonistic Ratios			
Sample ID	Total Petroleum Hydrocarbons (C9-C44)	Total Saturated Hydrocarbons	Ratio of T15/T19[1]	Ratio of Pristane/ Phytane[2]	Ratio of Pristane/ C17[3]	Ratio of Phytane/ C18[4]
KNH-B-23-3	18.9	5.61	-	-	0.836	-
SLB-B-23-1	-	2.91	-	-	43.429	-
SLB-B-23-2	-	1.69	-	-	19.921	-
SLB-B-23-3	-	1.68	-	-	17.400	-
RED-B-23-1	3.35	1.48	1.107	2.085	2.722	3.615
RED-B-23-2	4.1	1.73	0.860	2.214	3.263	4.000
RED-B-23-3	4.91	1.49	0.741	2.313	2.581	4.364
ZAB-B-23-1	9.91	3.32	-	-	1.353	-
ZAB-B-23-2	7.35	3.27	-	-	1.294	-
ZAB-B-23-3	9.1	3.51	-	-	1.432	-
ZAB2-B-23-1	1.07	3.41	-	-	9.667	-
ZAB2-B-23-2	12.3	3.07	-	-	10.383	-
ZAB2-B-23-3	9.81	3.34	-	-	10.542	-
SHB-B-23-1	5.57	1.41	-	8.333	0.284	0.300
SHB-B-23-2	5.75	1.42	-	5.750	0.295	0.308
SHB-B-23-3	9.16	1.63	-	8.000	0.296	0.235
Whole ANS Crude Oil	563000	77351.80	0.557	1.729	0.863	0.578

* Wet weight
[1] T15-Norhopane to T19-Hopane is a diagnostic ratio that identifies crude oil presence
[2] Higher values are indicative of greater marine biogenic sources over oil
[3] Higher values are indicative of greater weathering for oil and biogenic mixtures
[4] Higher values are indicative of oil-derived material and microbial degradation of the straight-chain alkanes

FIGURES

Figure 1. Long-Term Environmental Monitoring Program sites from 2022 and 2023 campaign.

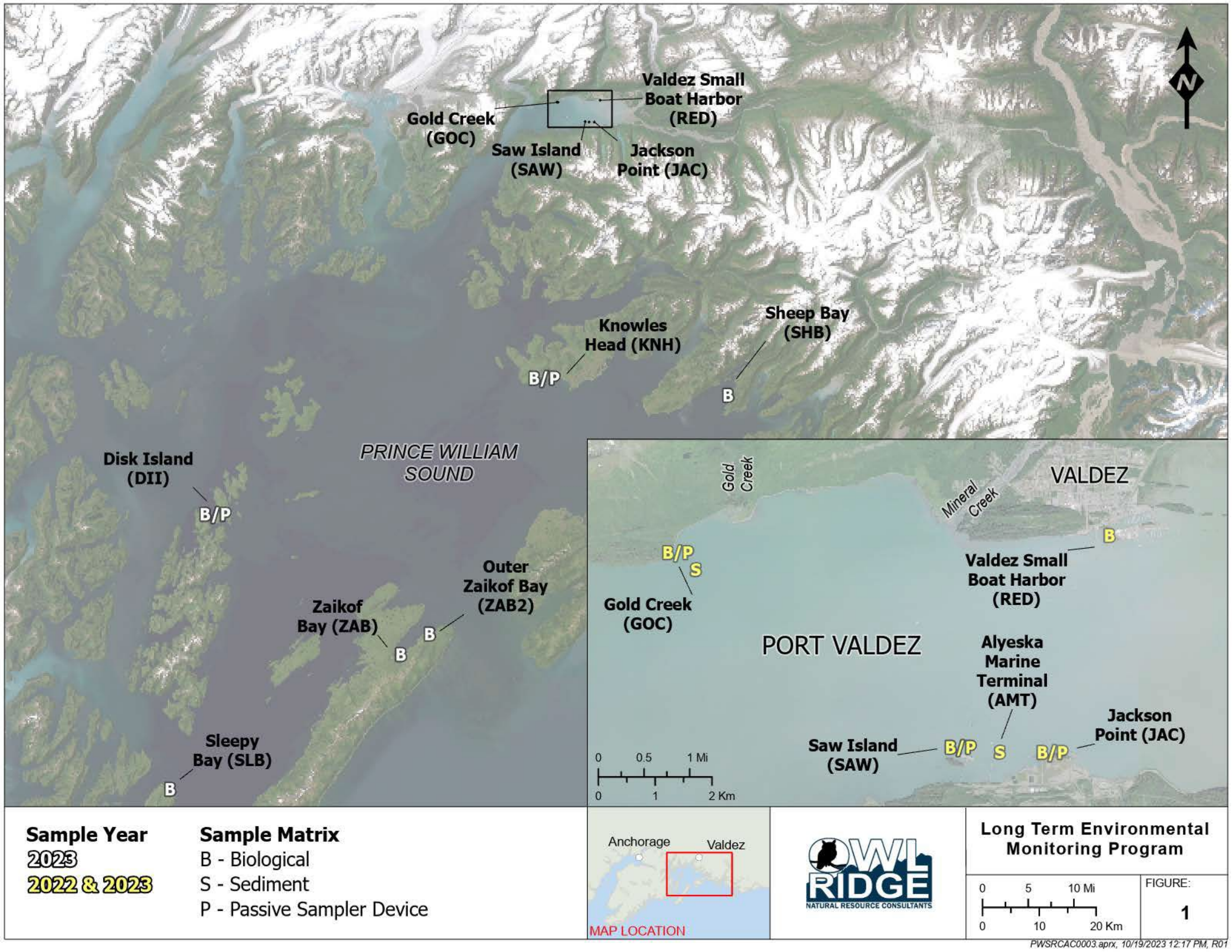

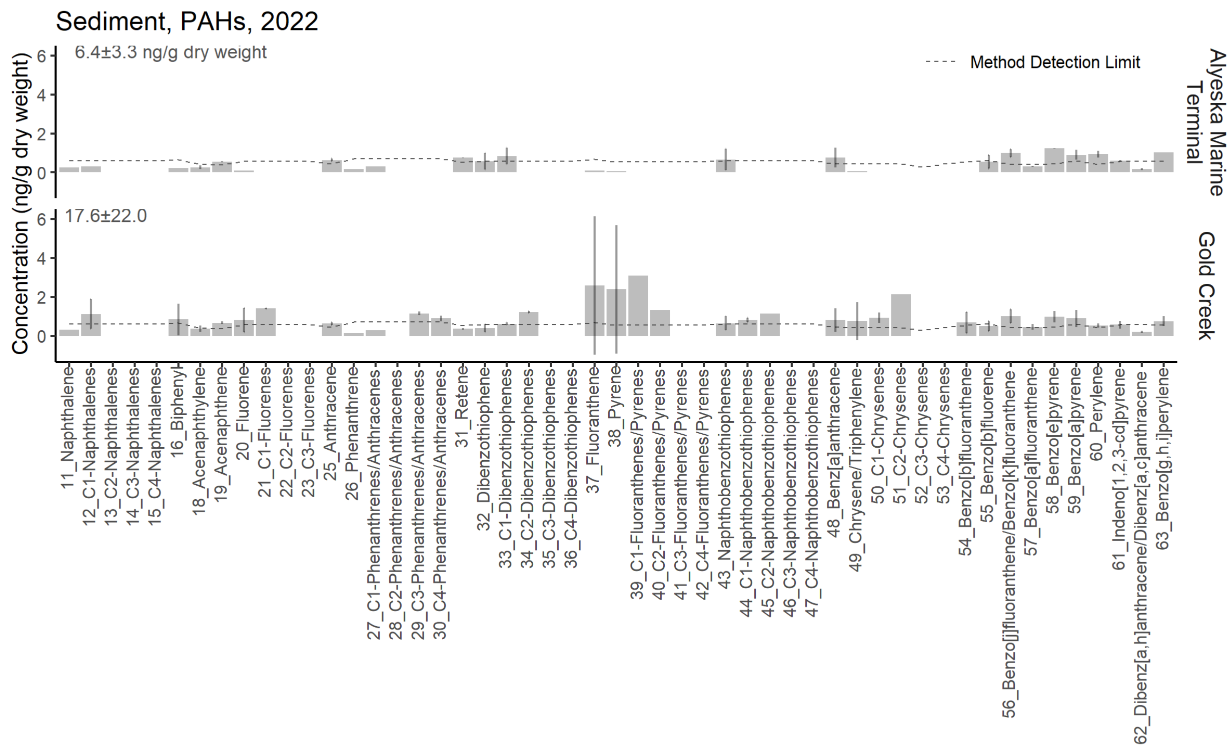

Figure 2. PAH profiles from 2022 sediment samples plotted by mean ± 1 standard deviation. The analyte-specific method detection limit is superimposed as a dashed line. Sum 43 PAH values (mean ± 1 standard deviation) are found in the upper left corner of each site profile.

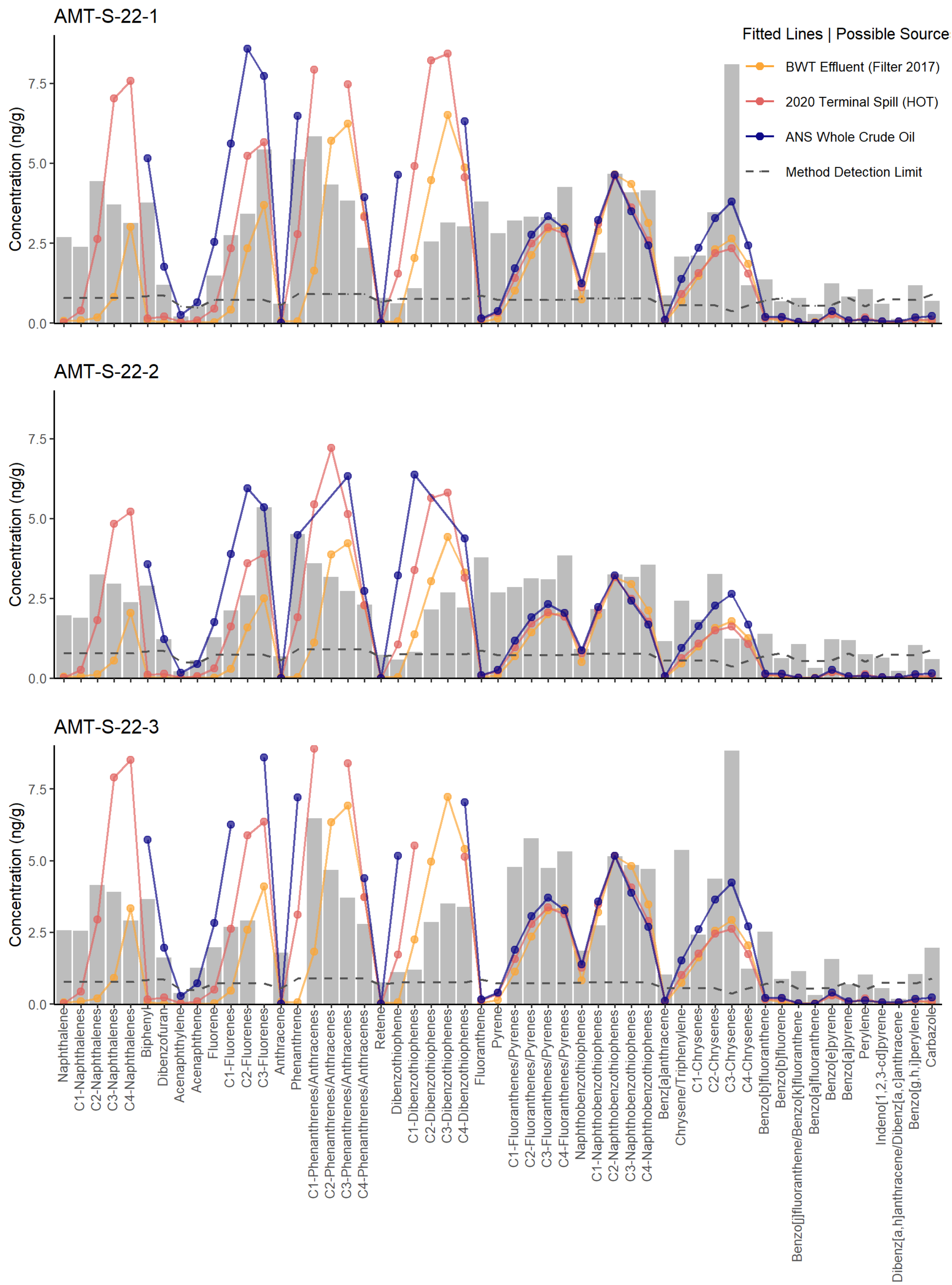

Figure 3. 2022 PAH profiles from individual sediment samples at the Valdez Marine Terminal (AMT) with three possible ANS-related source profiles and the analyte specific method detection limit superimposed as different lines.

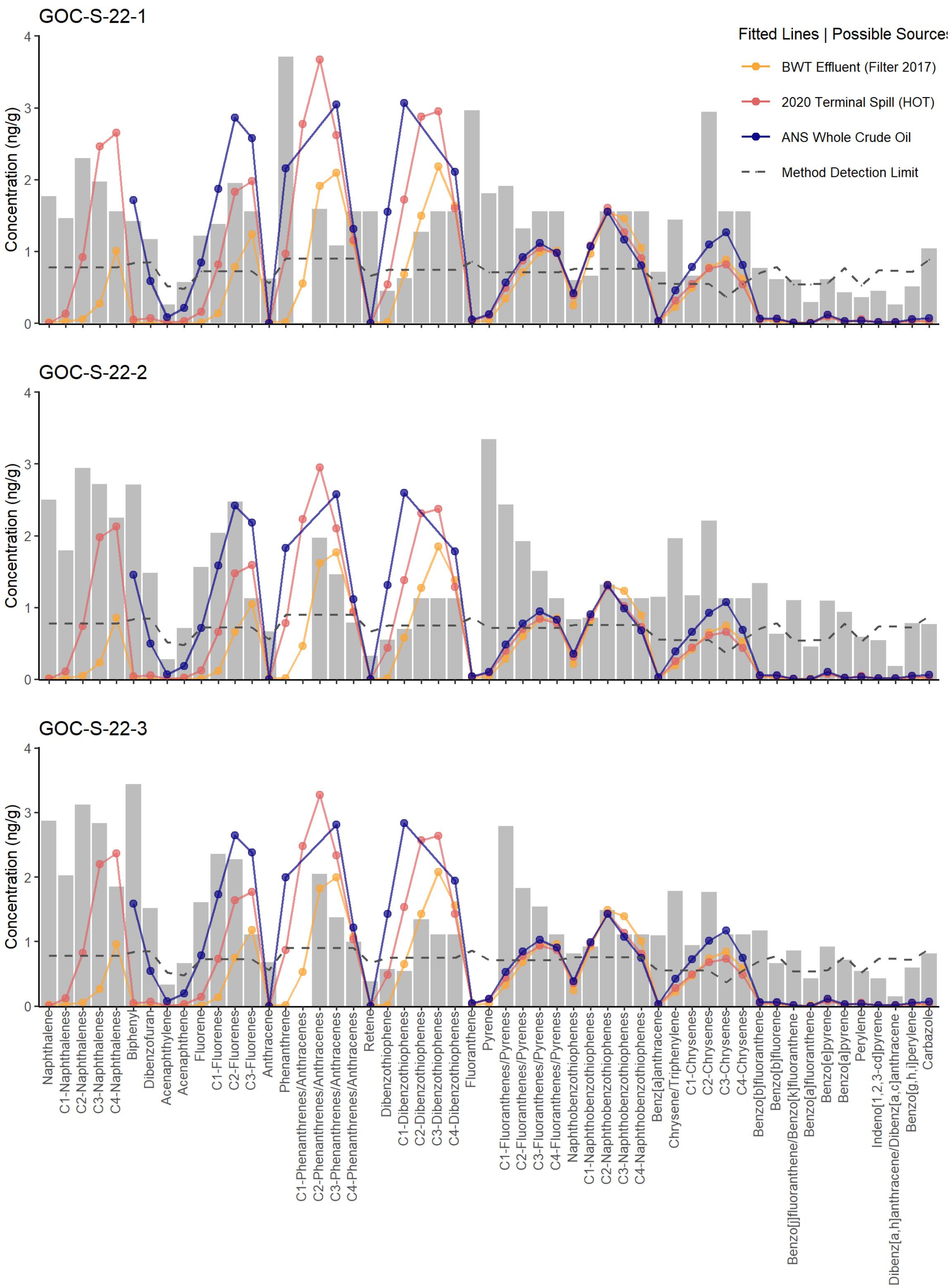

Figure 4. 2022 PAH profiles from individual sediment samples at Gold Creek (GOC) with the three possible ANS-related source profiles and the analyte specific method detection limit superimposed as different lines.

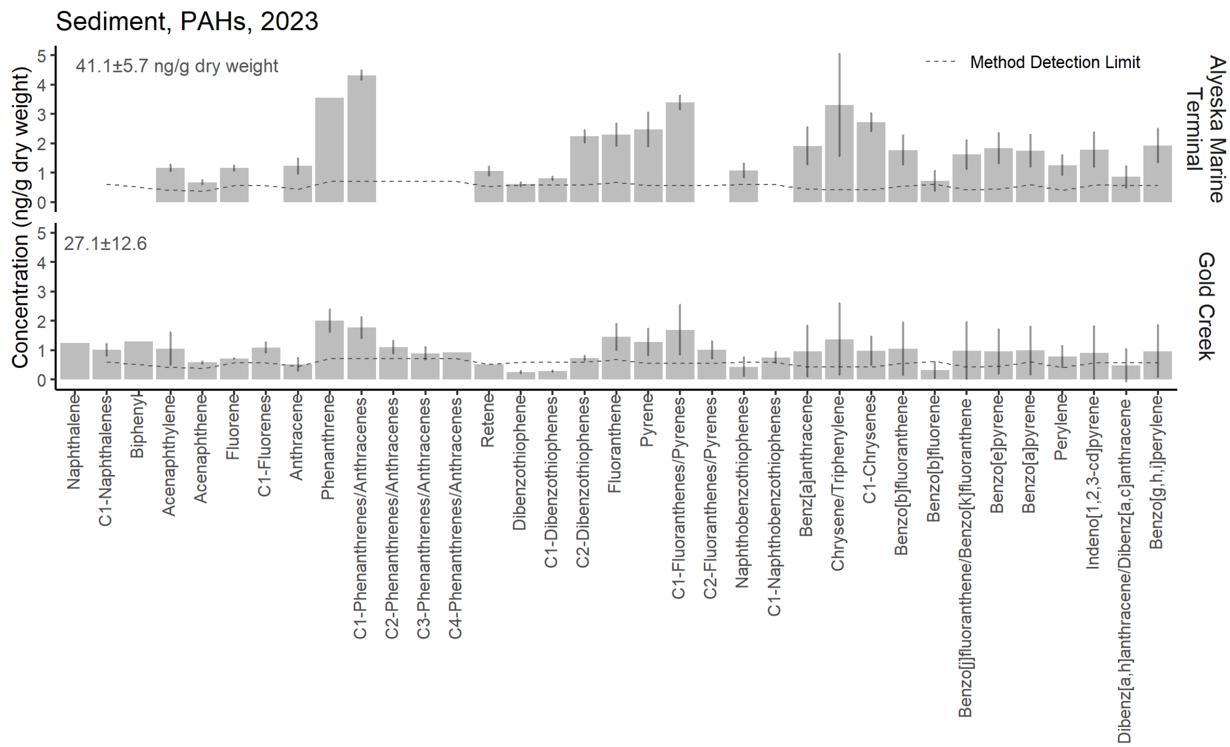

Figure 5. PAH profiles from 2023 sediment samples plotted by mean ± 1 standard deviation. The analyte-specific method detection limit is superimposed as a dashed line. Sum 43 PAH values (mean ± 1 standard deviation) are found in the upper left corner of each site profile.

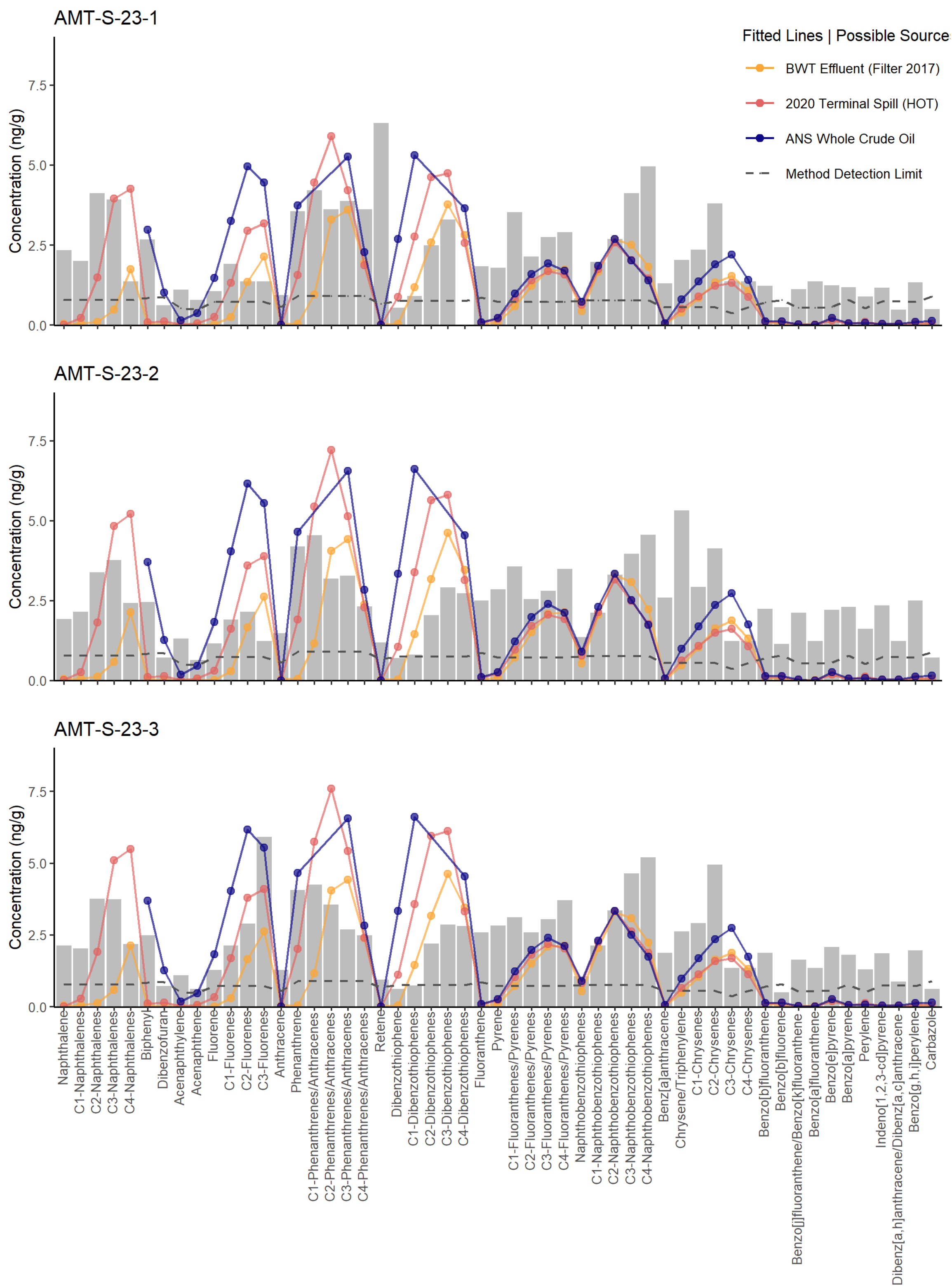

Figure 6. 2023 PAH profiles from individual sediment samples at Valdez Marine Terminal (AMT) with the three possible ANS-related source profiles and the analyte specific method detection limit superimposed as different lines.

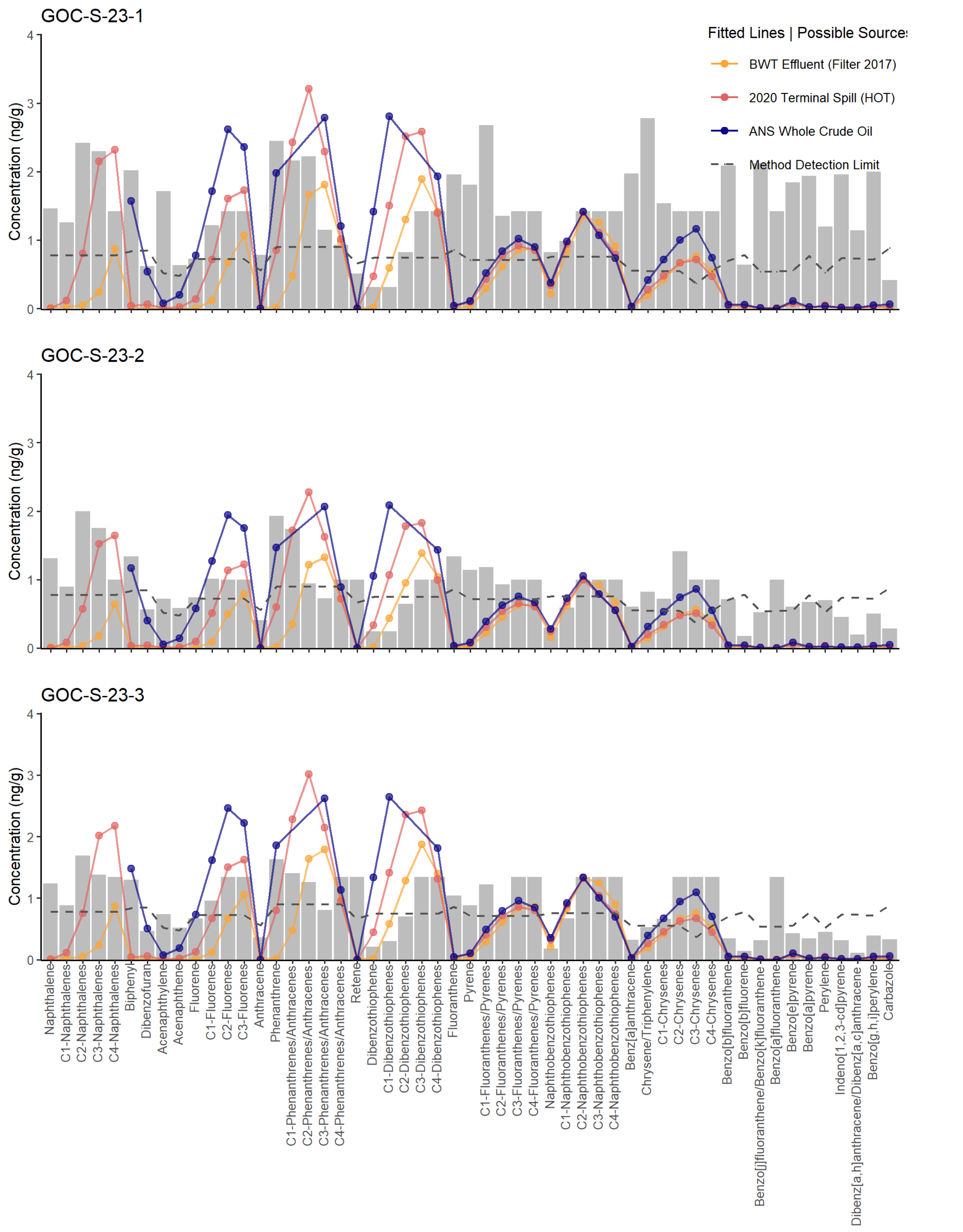

Figure 7. 2023 PAH profiles from individual sediment samples at Gold Creek (GOC) with the three possible ANS-related source profiles and the analyte specific method detection limit superimposed as different lines.

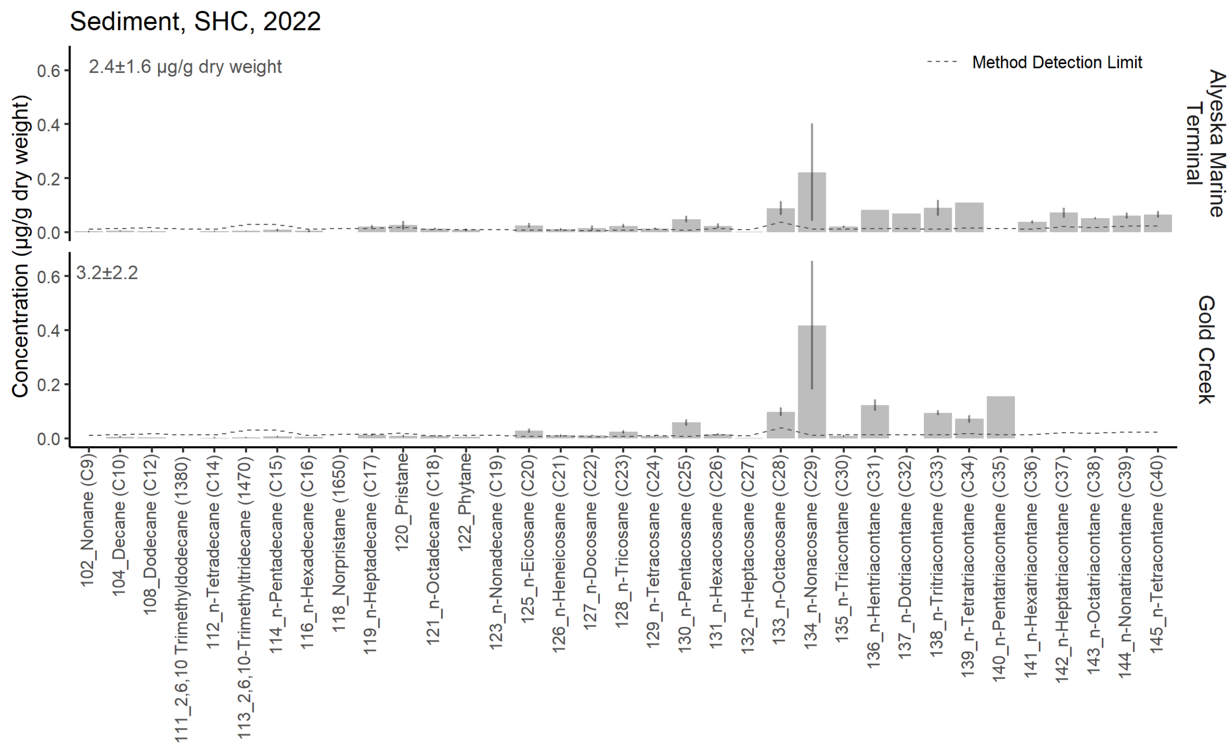

Figure 8. 2022 Saturated hydrocarbons (SHC) profiles from sediment samples plotted by mean ± 1 standard deviation. The analyte specific method detection limit is superimposed as a dashed line. Sum SHC values (mean ± 1 standard deviation) are found in the upper left corner of each site profile.

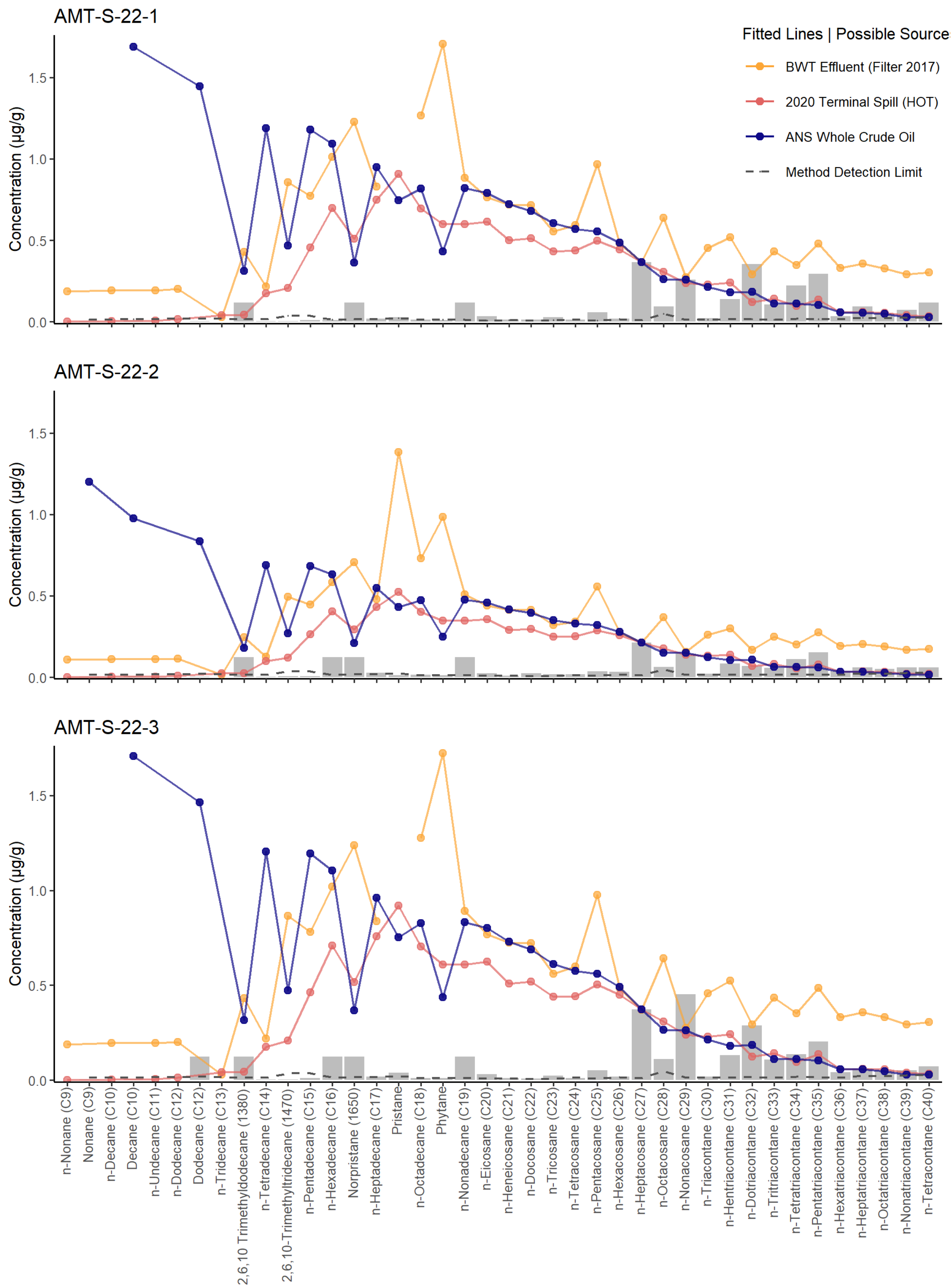

Figure 9. 2022 Saturated hydrocarbons (SHC) profiles from individual sediment samples at the Valdez Marine Terminal (AMT) with the duplicate replicate, three possible ANS-related source profiles, and the analyte specific method detection limit superimposed as different lines.

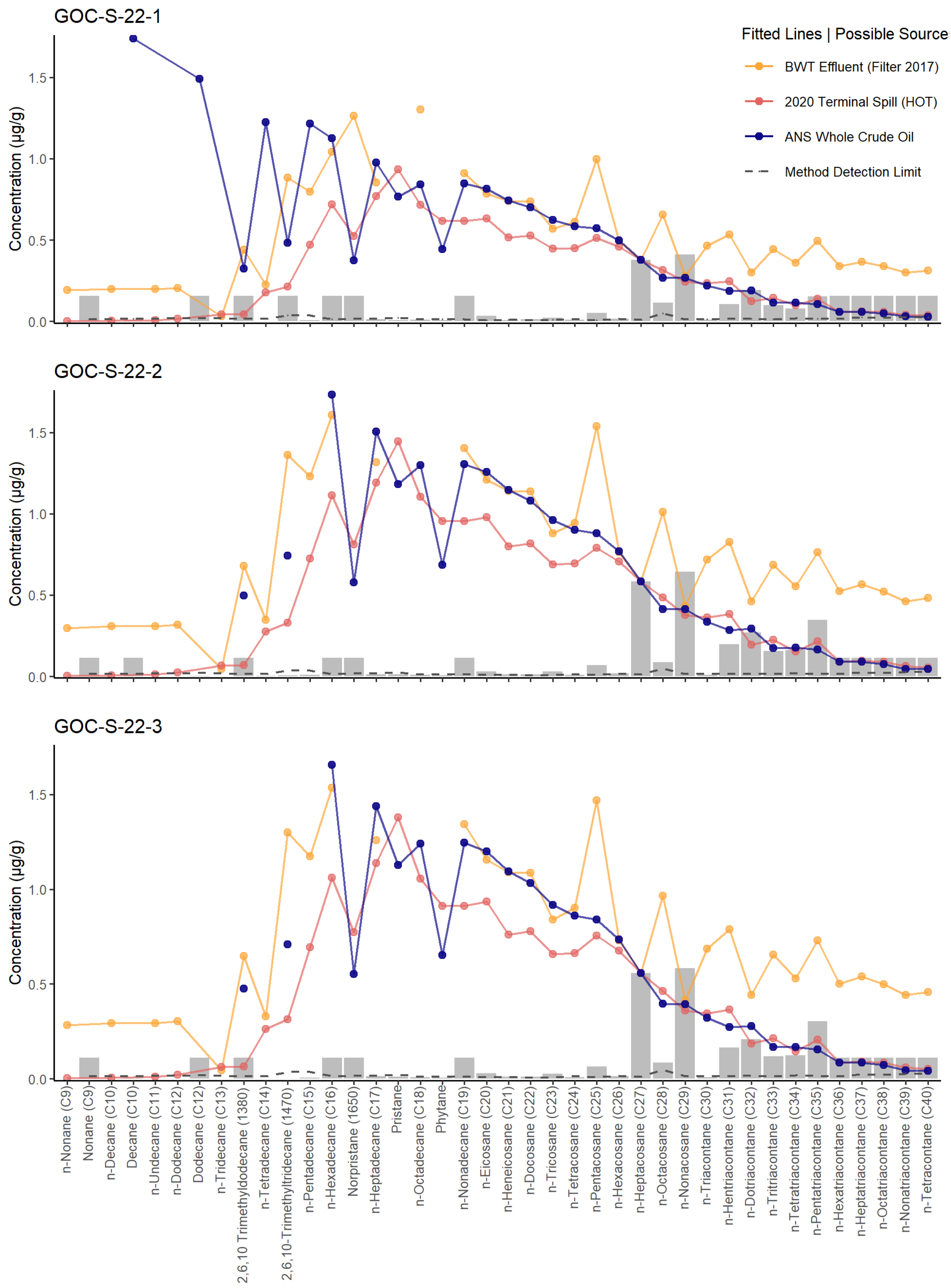

Figure 10. 2023 Saturated hydrocarbons (SHC) profiles from individual sediment samples at Gold Creek (GOC) with three possible ANS-related source profiles and the analyte specific method detection limit superimposed as different lines.

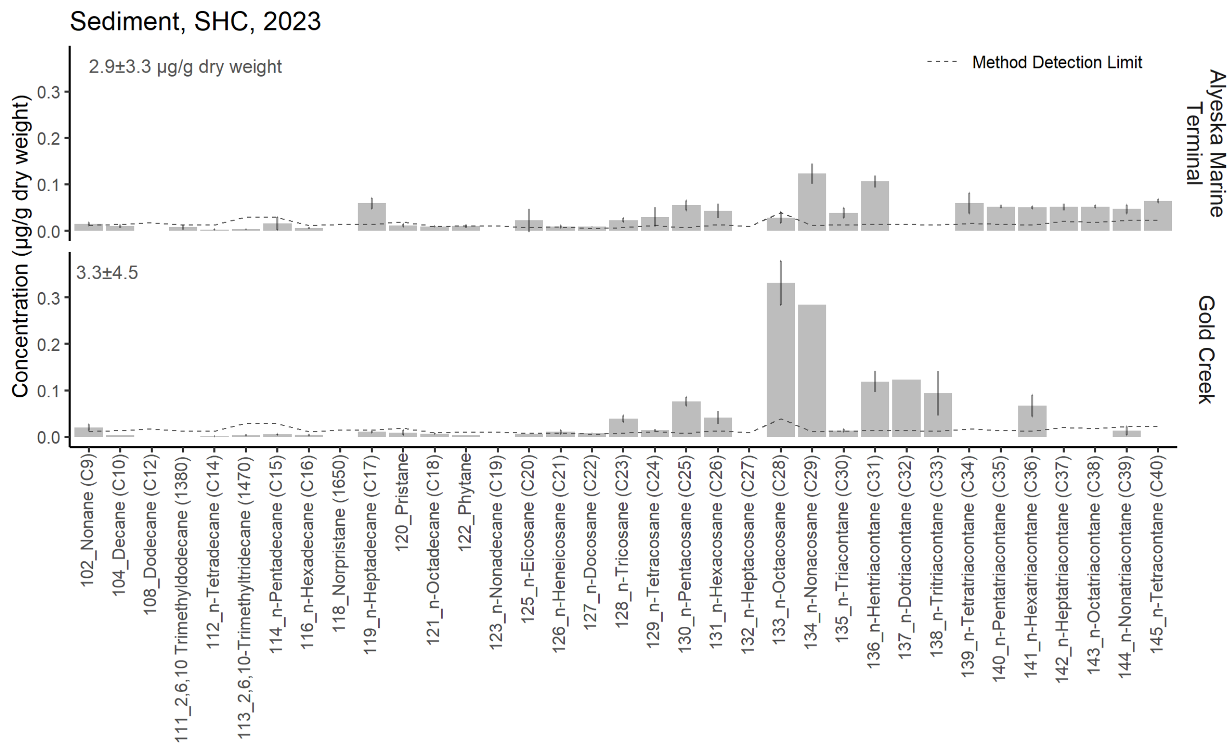

Figure 11. 2023 Saturated hydrocarbons (SHC) profiles from sediment samples plotted by mean ± 1 standard deviation. The analyte specific method detection limit is superimposed as a dashed line. Sum SHC values (mean ± 1 standard deviation) are found in the upper left corner of each site profile.

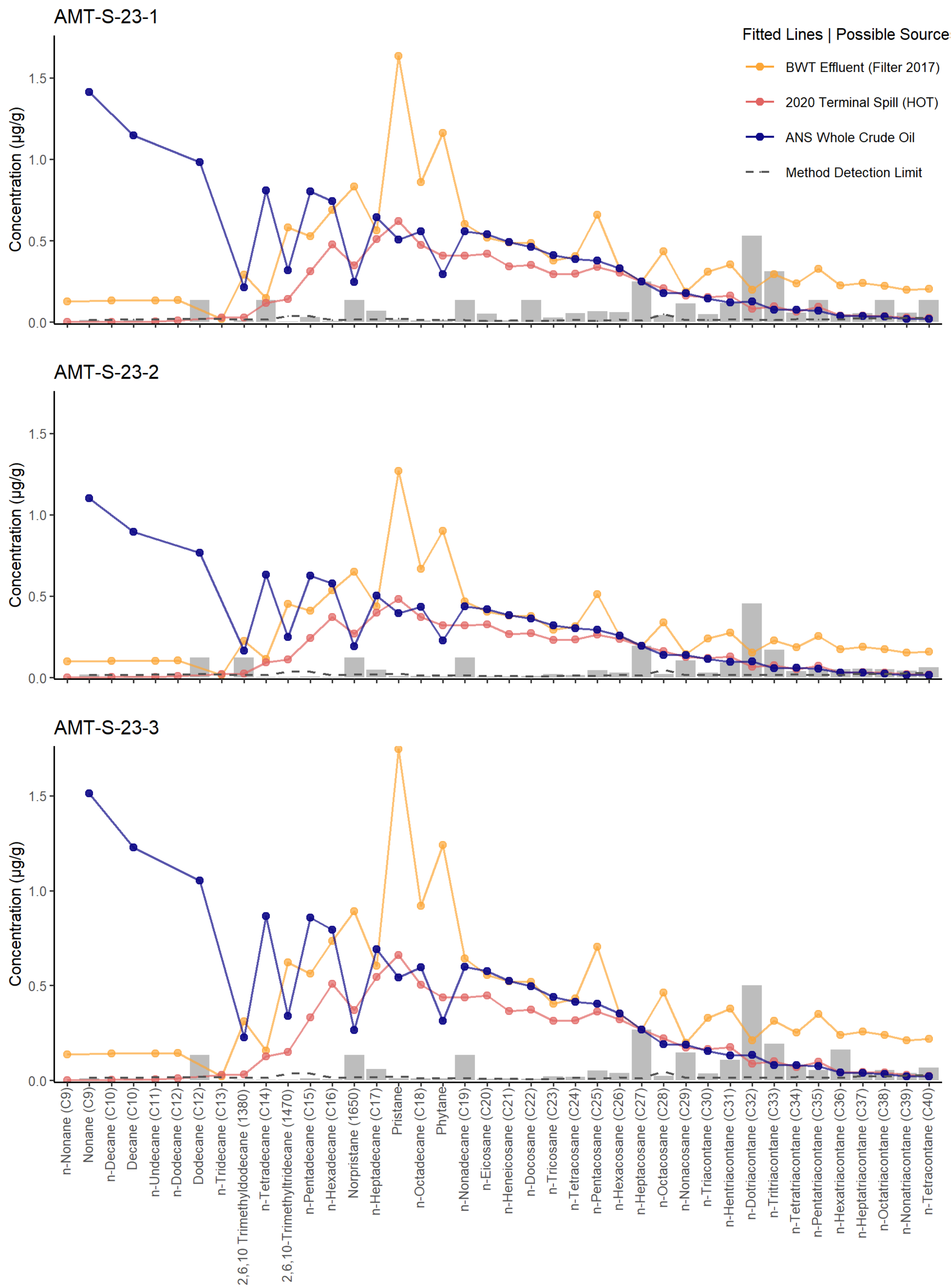

Figure 12. 2023 Saturated hydrocarbons (SHC) profiles from individual sediment samples at the Valdez Marine Terminal (AMT) with three possible ANS-related source profiles and the analyte specific method detection limit superimposed as different lines.

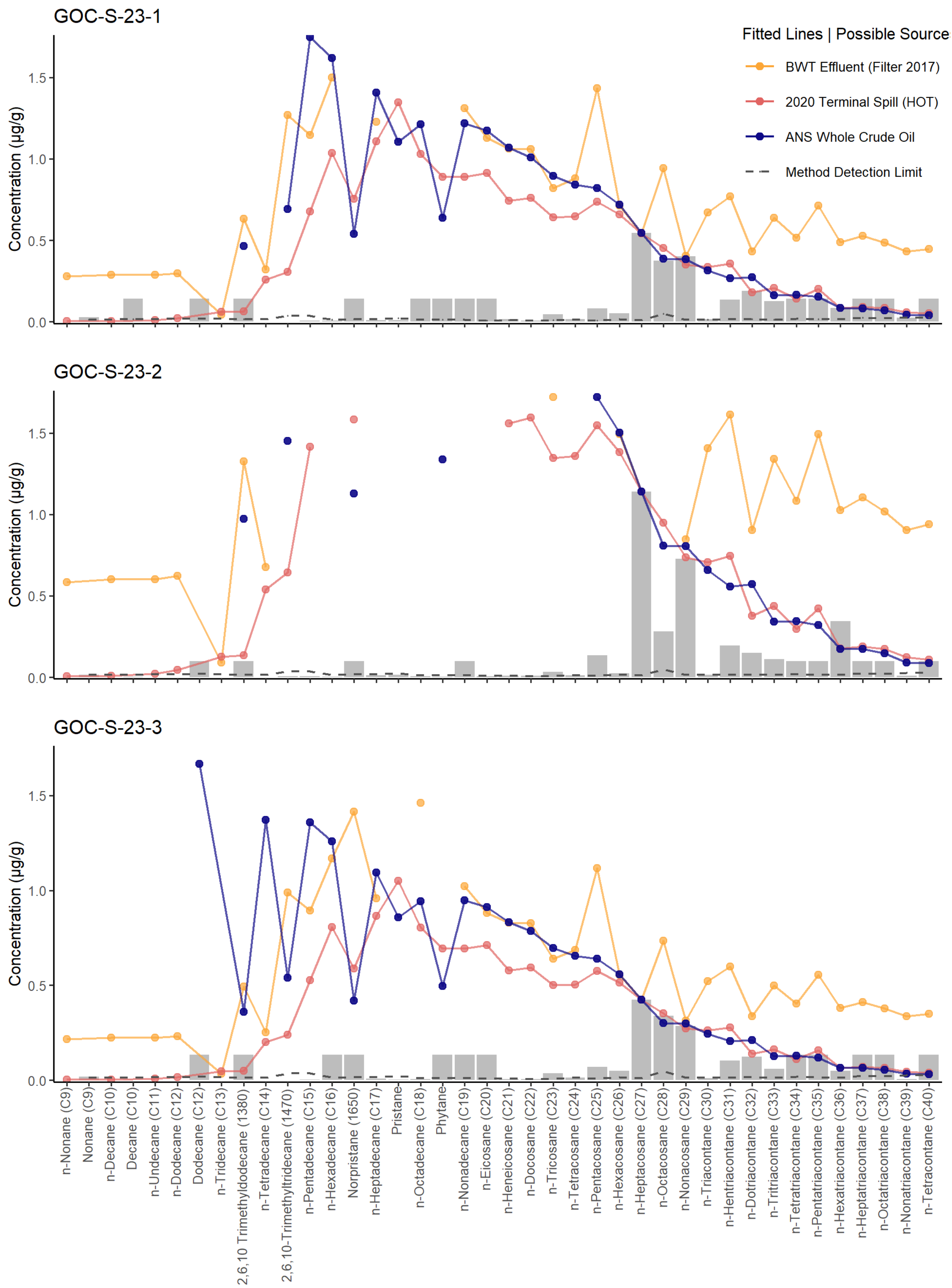

Figure 13. 2023 Saturated hydrocarbons (SHC) profiles from individual sediment samples at Gold Creek (GOC) with three possible ANS-related source profiles and the analyte specific method detection limit superimposed as different lines.

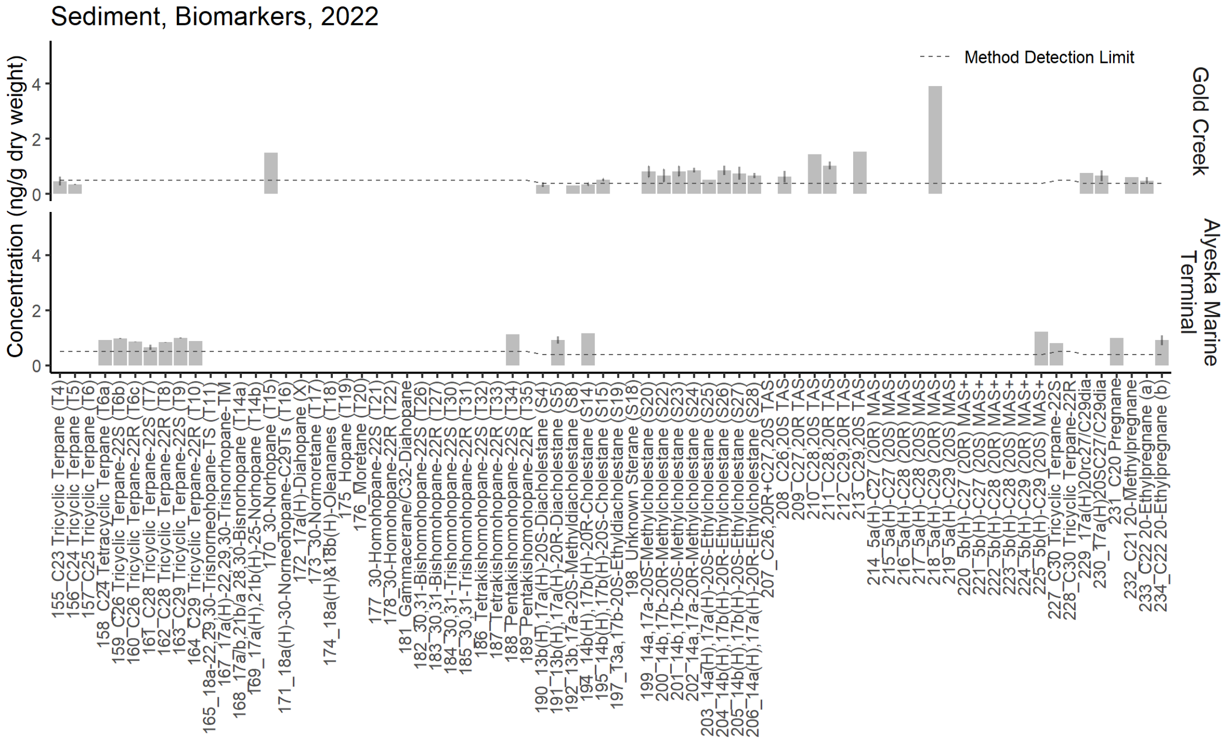

Figure 14. 2022 Petroleum chemical biomarker profiles from sediment samples plotted by mean ± 1 standard deviation. The analyte specific method detection limit is superimposed as a dashed line.

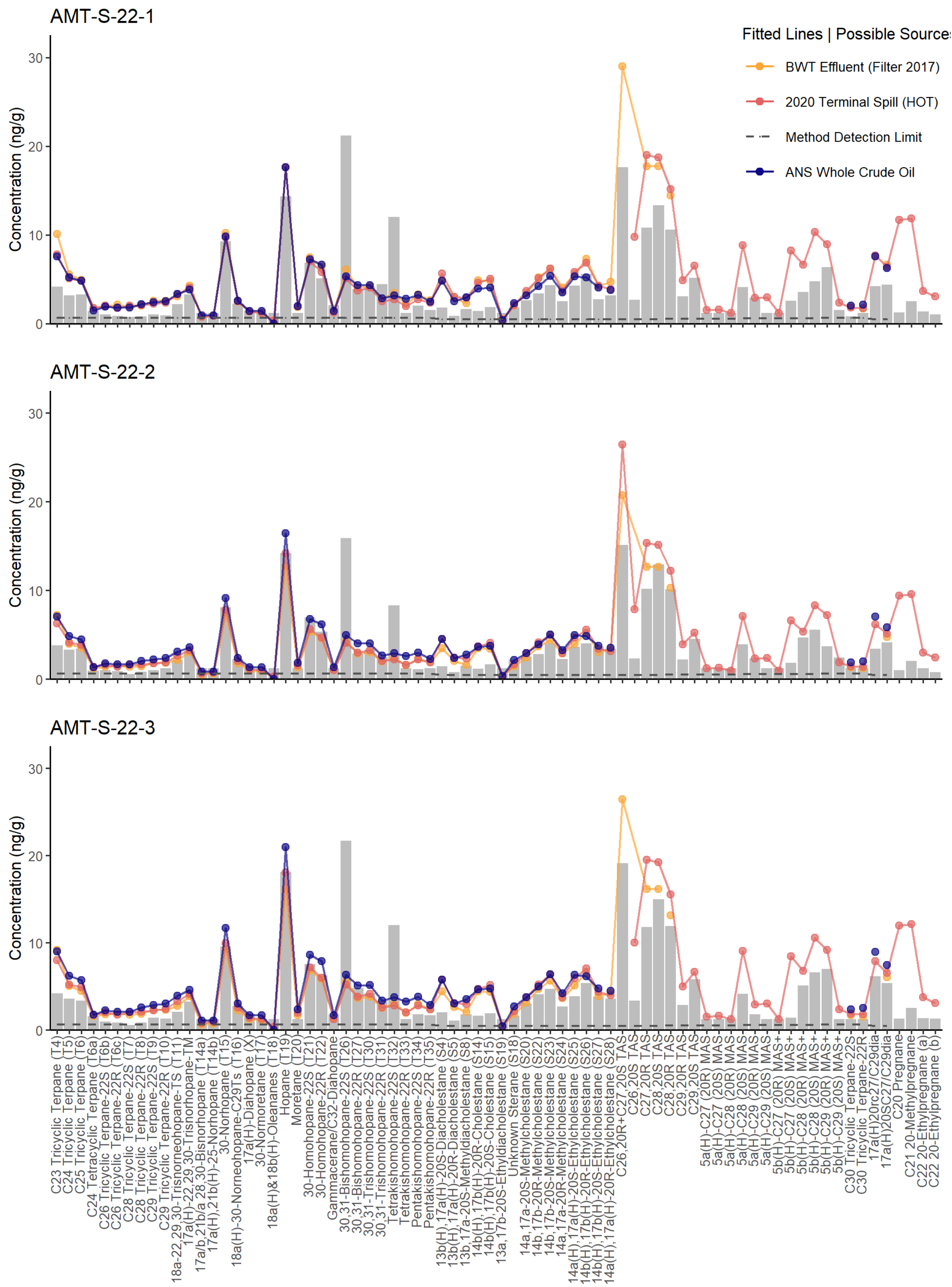

Figure 15. 2022 Petroleum chemical biomarker profiles from individual sediment samples at the Valdez Marine Terminal (AMT) with three possible ANS-related source profiles and the analyte specific method detection limit superimposed as different lines.

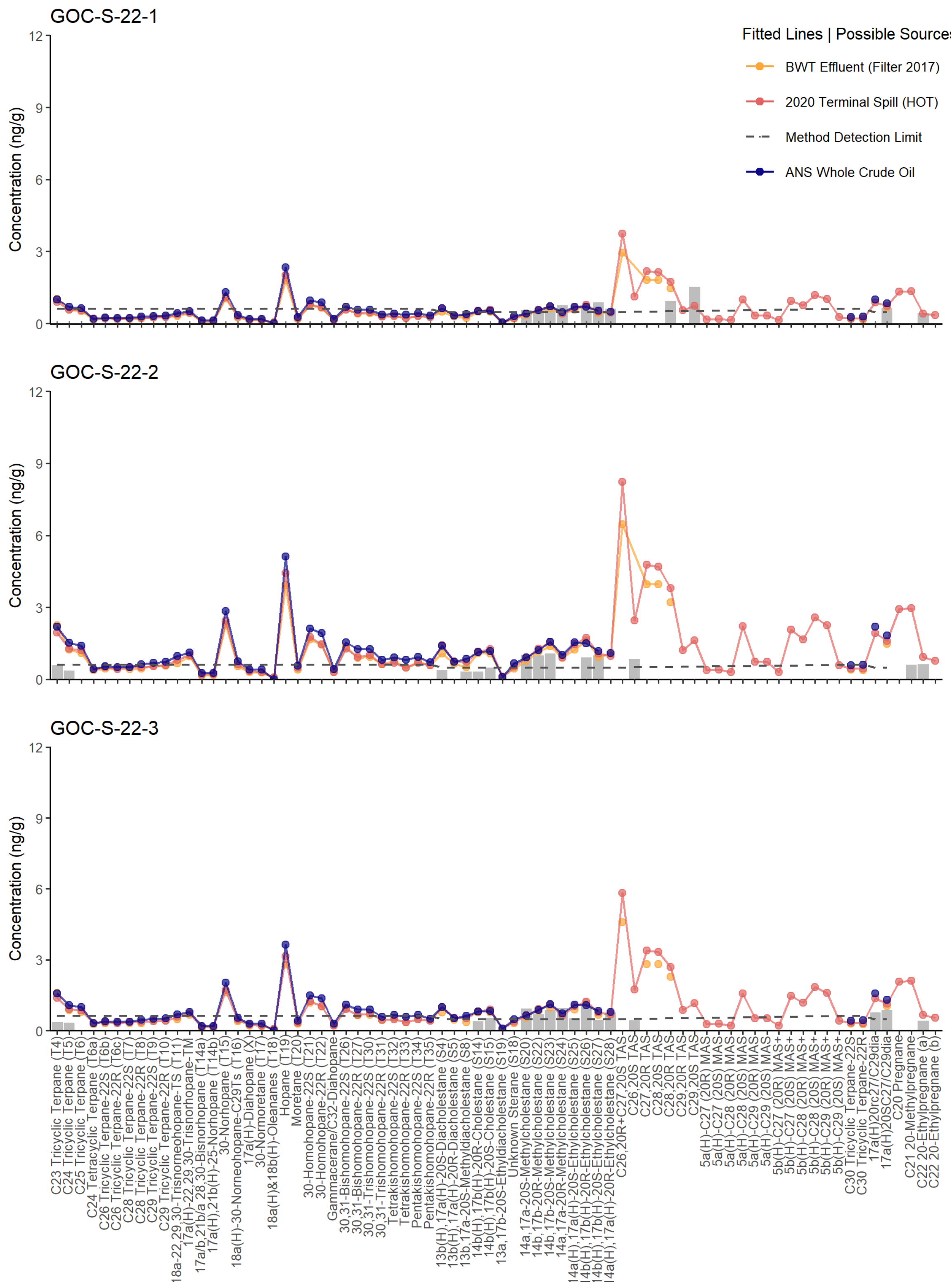

Figure 16. 2022 Petroleum chemical biomarker profiles from individual sediment samples at Gold Creek with (GOC) three possible ANS-related source profiles and the analyte specific method detection limit superimposed as different lines.

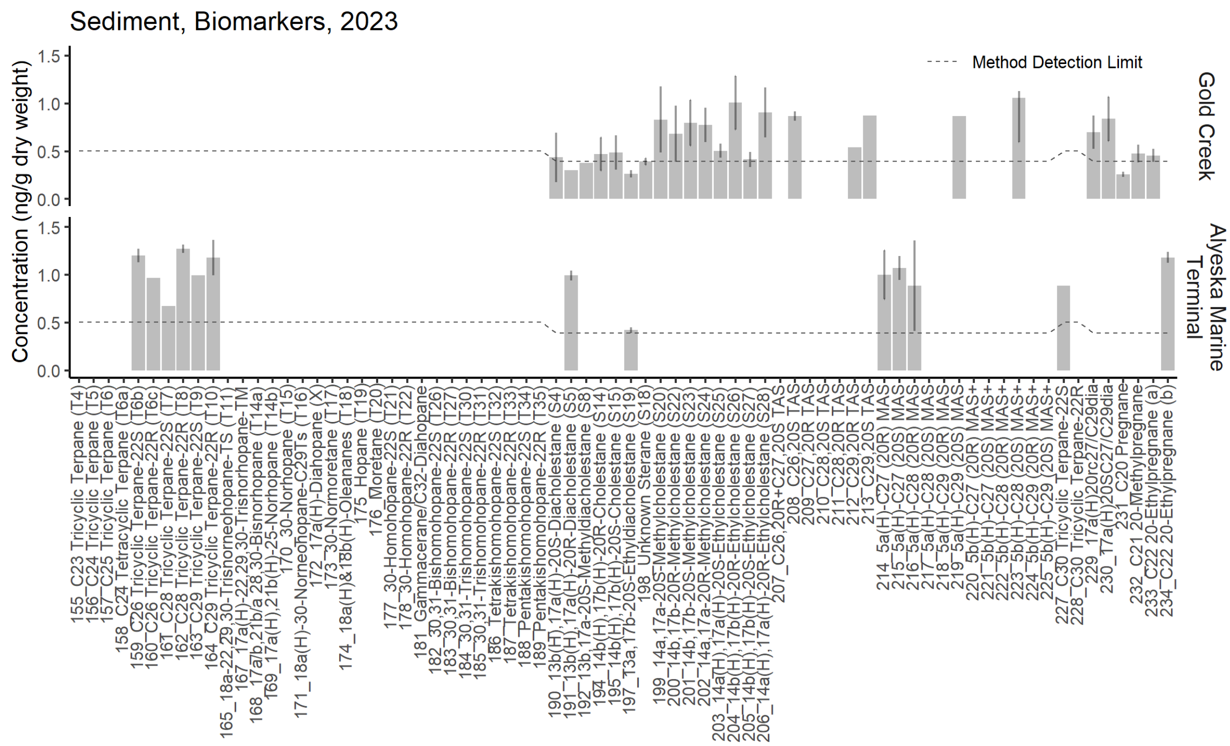

Figure 17. 2023 Petroleum chemical biomarker profiles from sediment samples plotted by mean ± 1 standard deviation. The analyte specific method detection limit is superimposed as a dashed line.

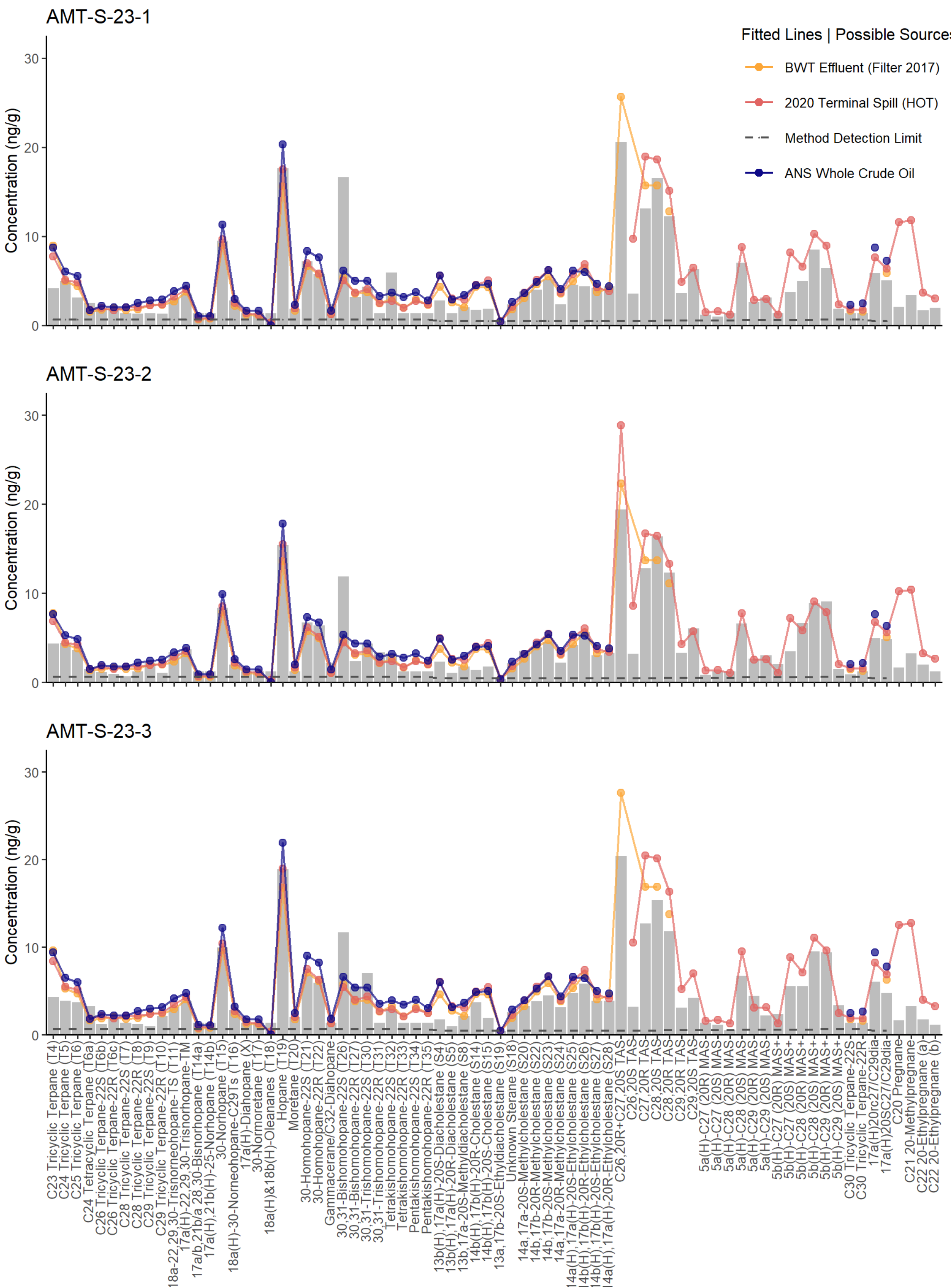

Figure 18. 2023 Petroleum chemical biomarker profiles from individual sediment samples at the Valdez Marine Terminal (AMT) with three possible ANS-related source profiles and the analyte specific method detection limit superimposed as different lines.

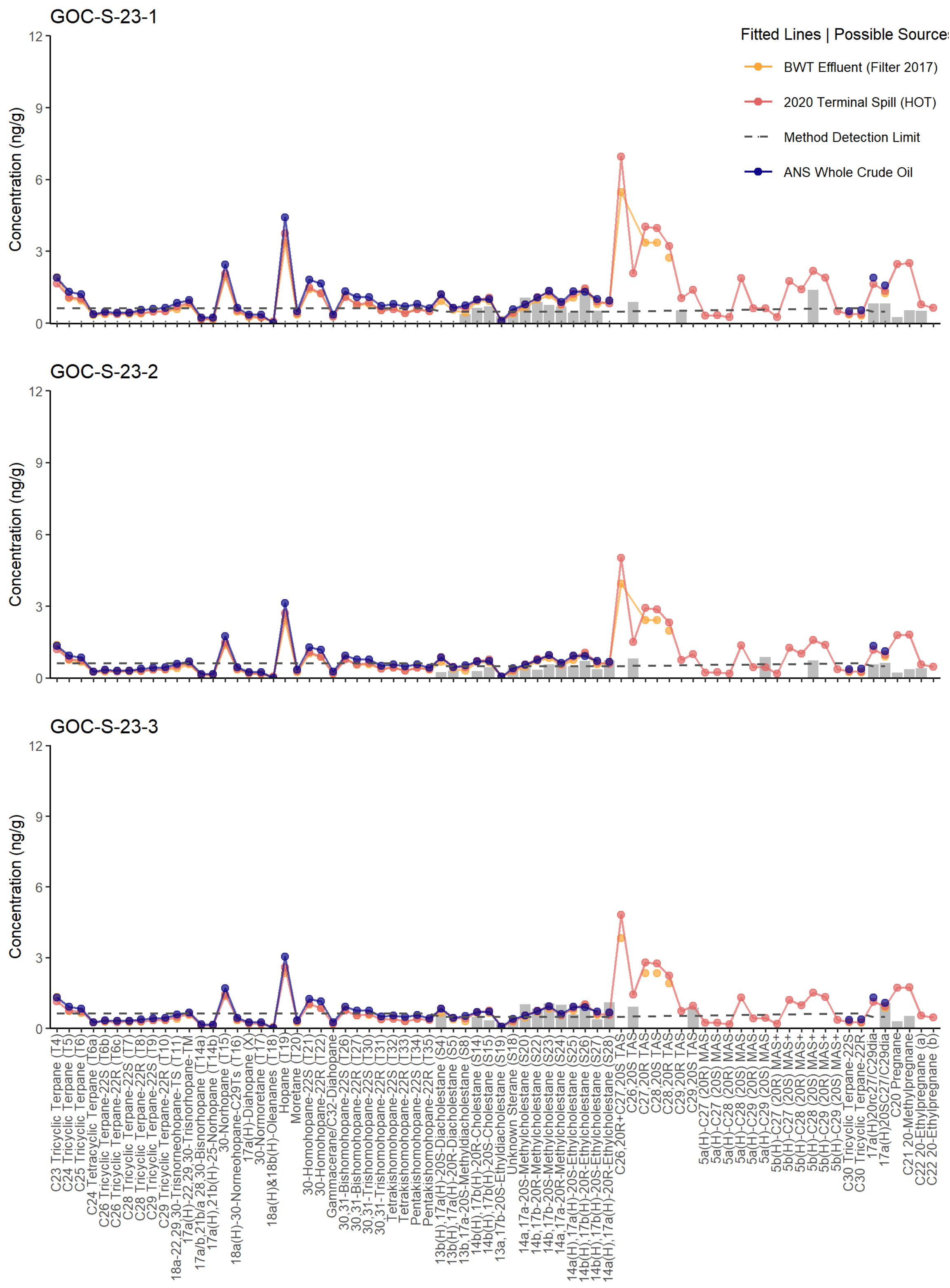

Figure 19. 2023 Petroleum chemical biomarker profiles from individual sediment samples at Gold Creek (GOC) with three possible ANS-related source profiles and the analyte specific method detection limit superimposed as different lines.

Mussel Tissue Data

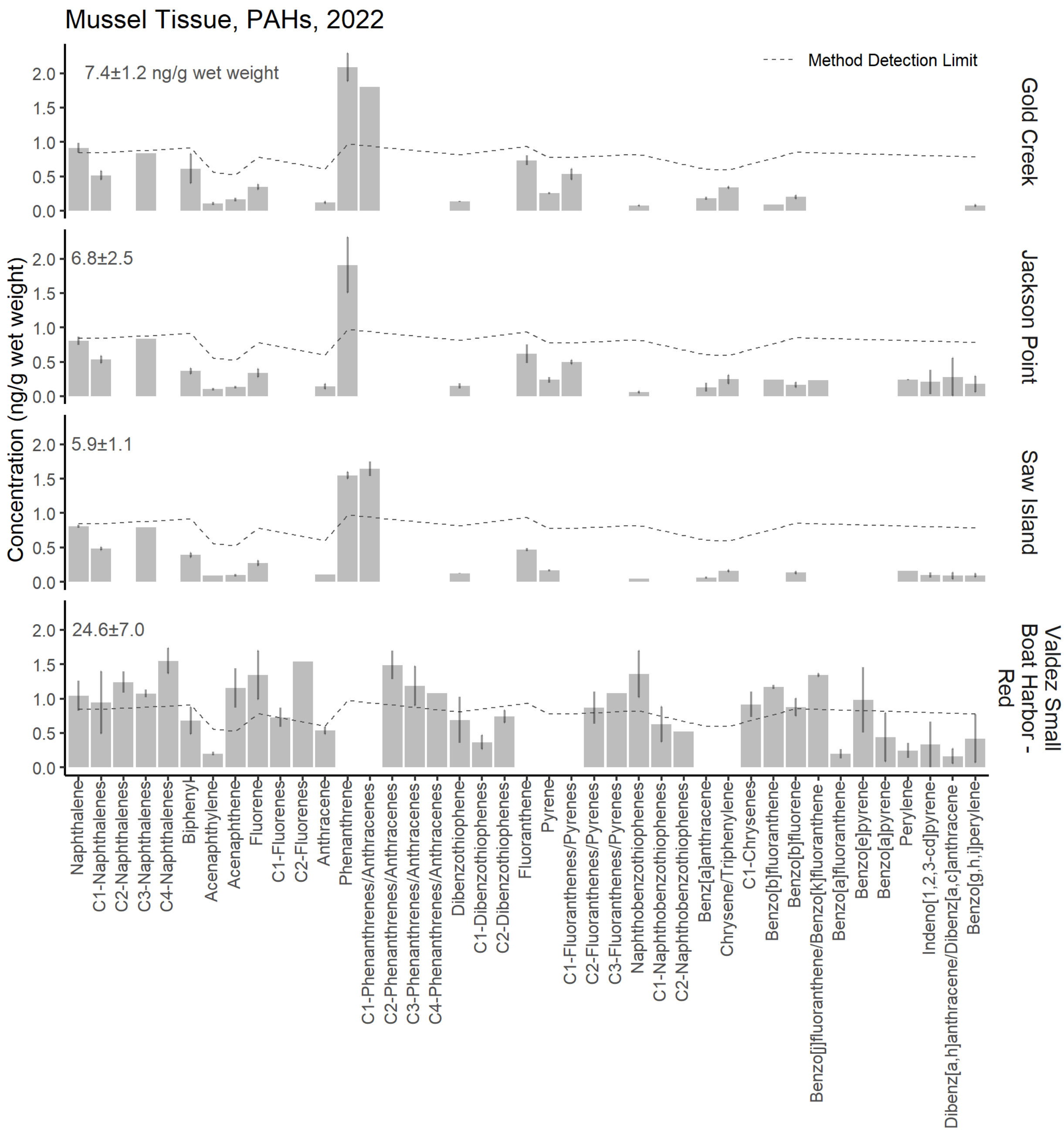

Figure 20. PAH profiles from 2022 mussel tissue samples plotted by mean ± 1 standard deviation. The analyte specific method detection limit is superimposed as a dashed line. Sum 42 PAH values (mean ± 1 standard deviation) are found in the upper left corner of each site profile.

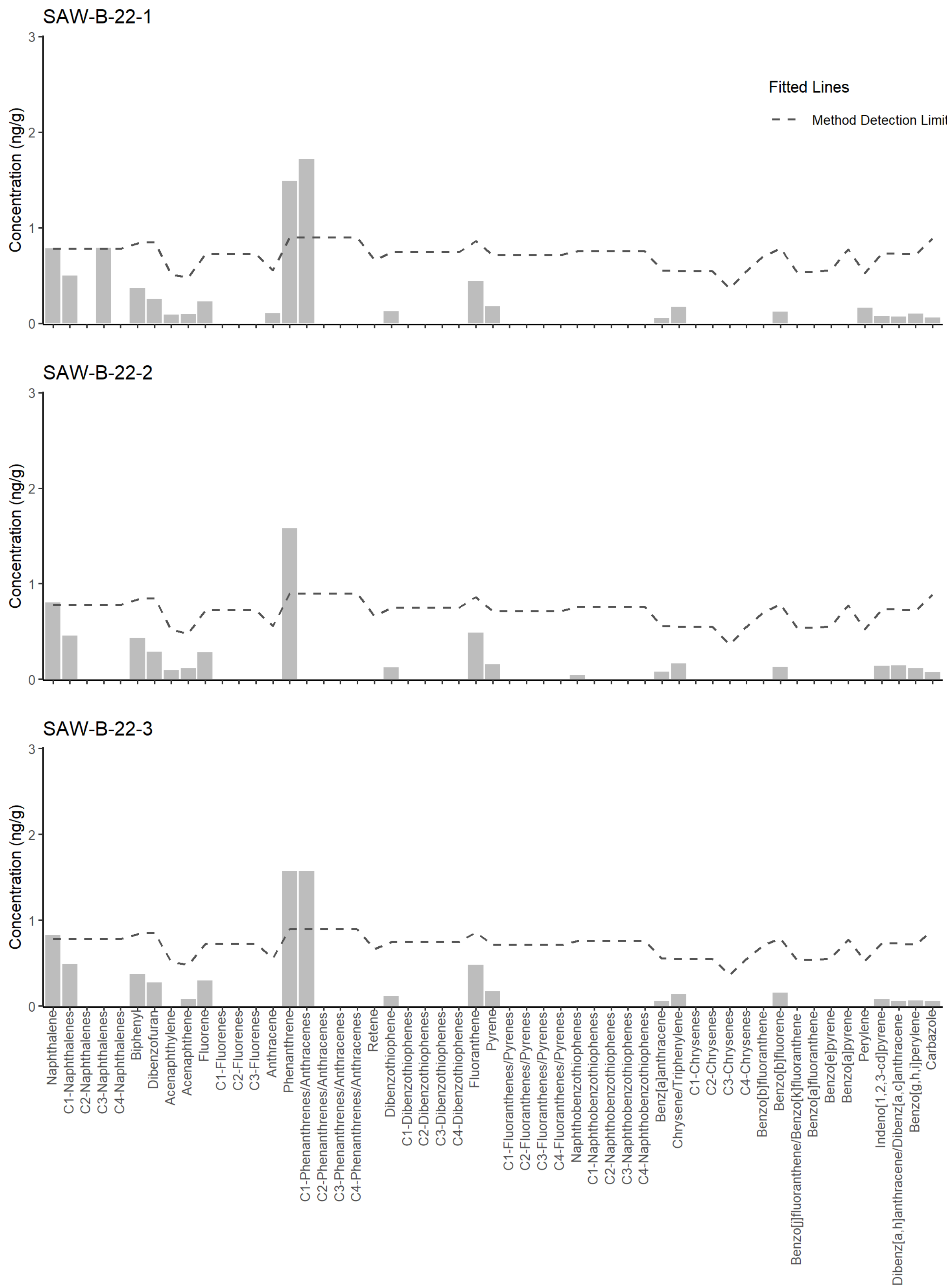

Figure 21. 2022 PAH profiles from individual mussel tissue samples at Saw Island (SAW) with the analyte specific method detection limit superimposed as a dashed line.

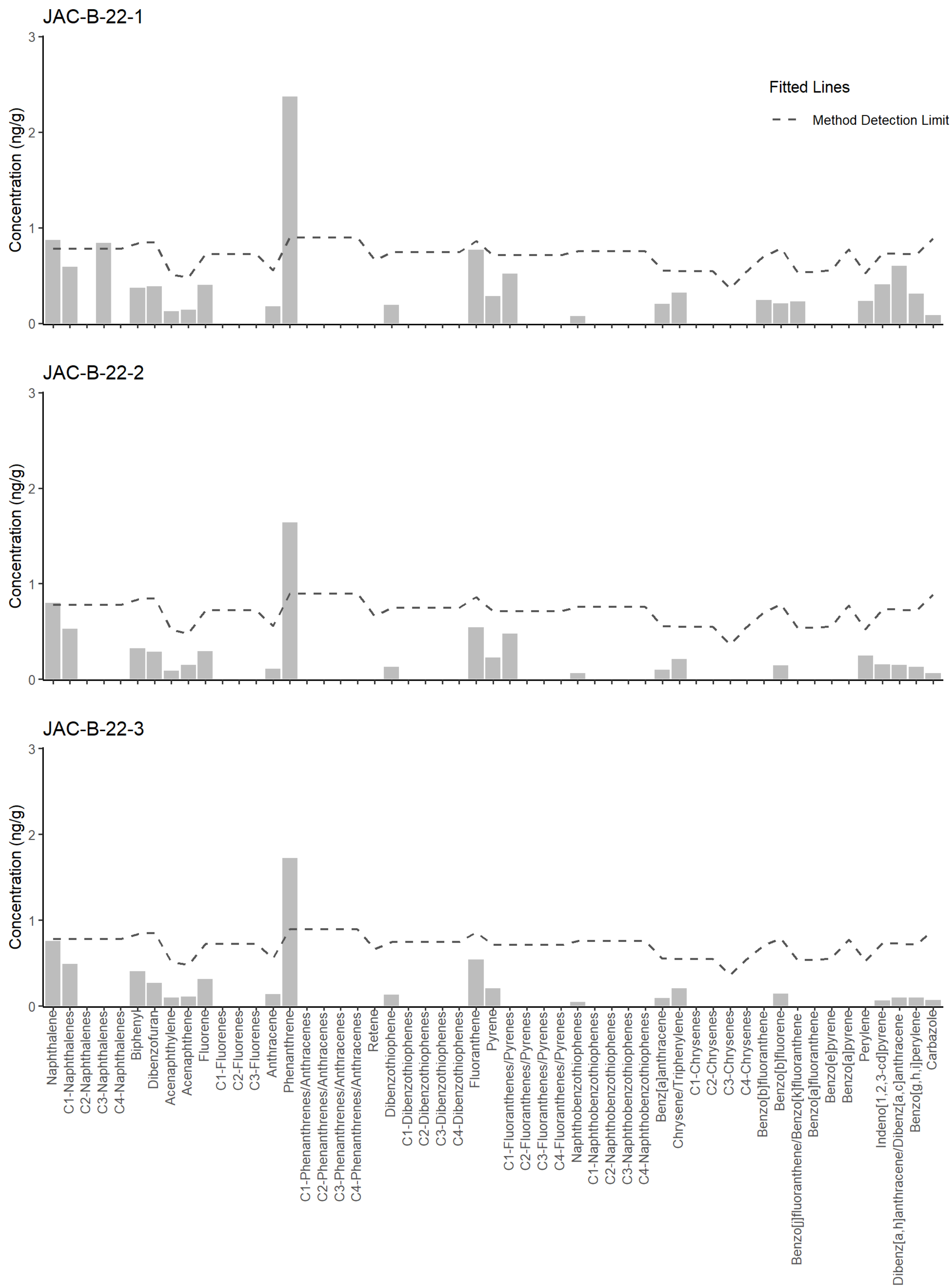

Figure 22. 2022 PAH profiles from individual mussel tissue samples at Jackson Point (JAC) with the analyte specific method detection limit superimposed as a dashed line.

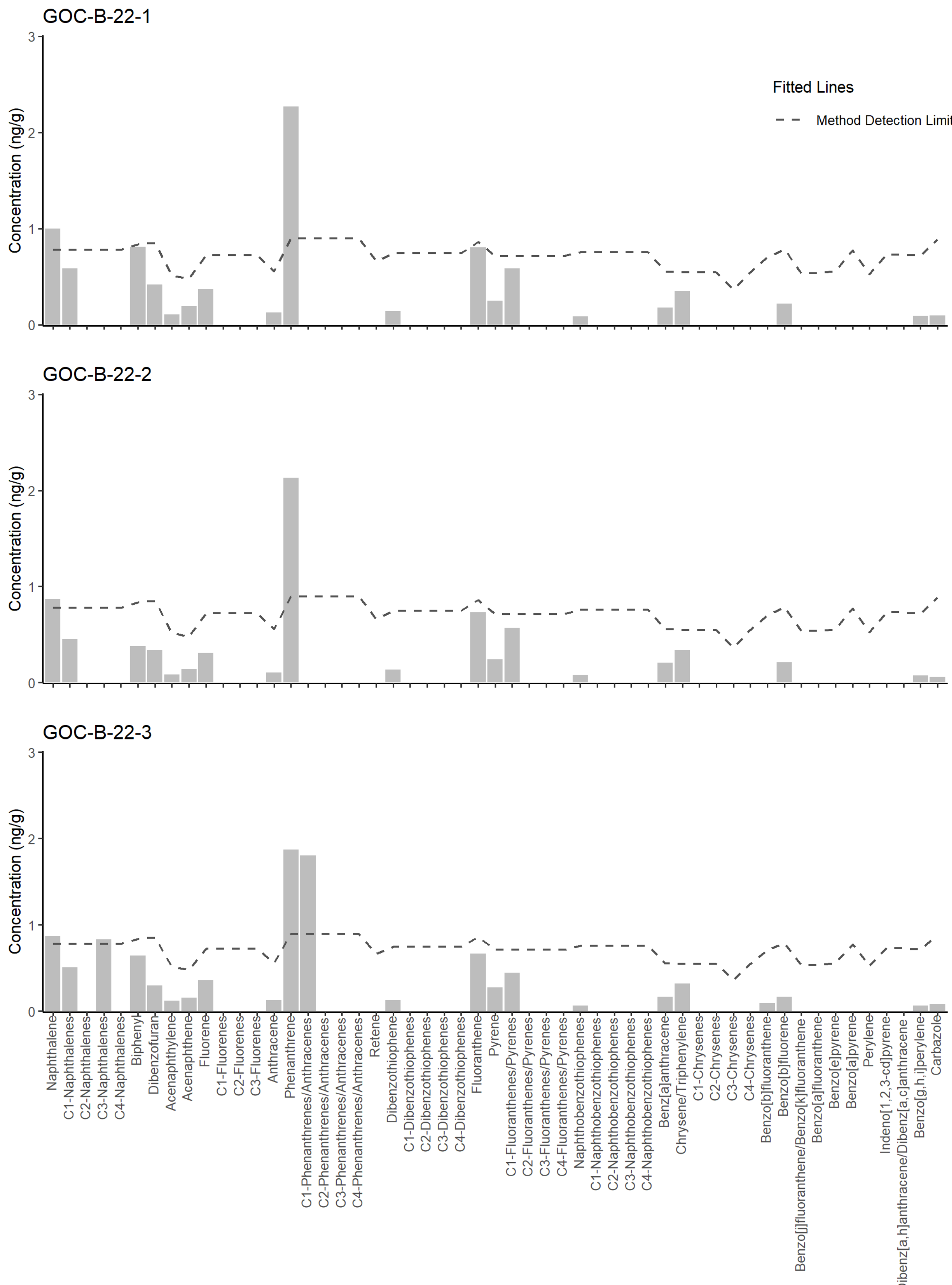

Figure 23. 2022 PAH profiles from individual mussel tissue samples at Gold Creek (GOC) with the analyte specific method detection limit superimposed as different lines.

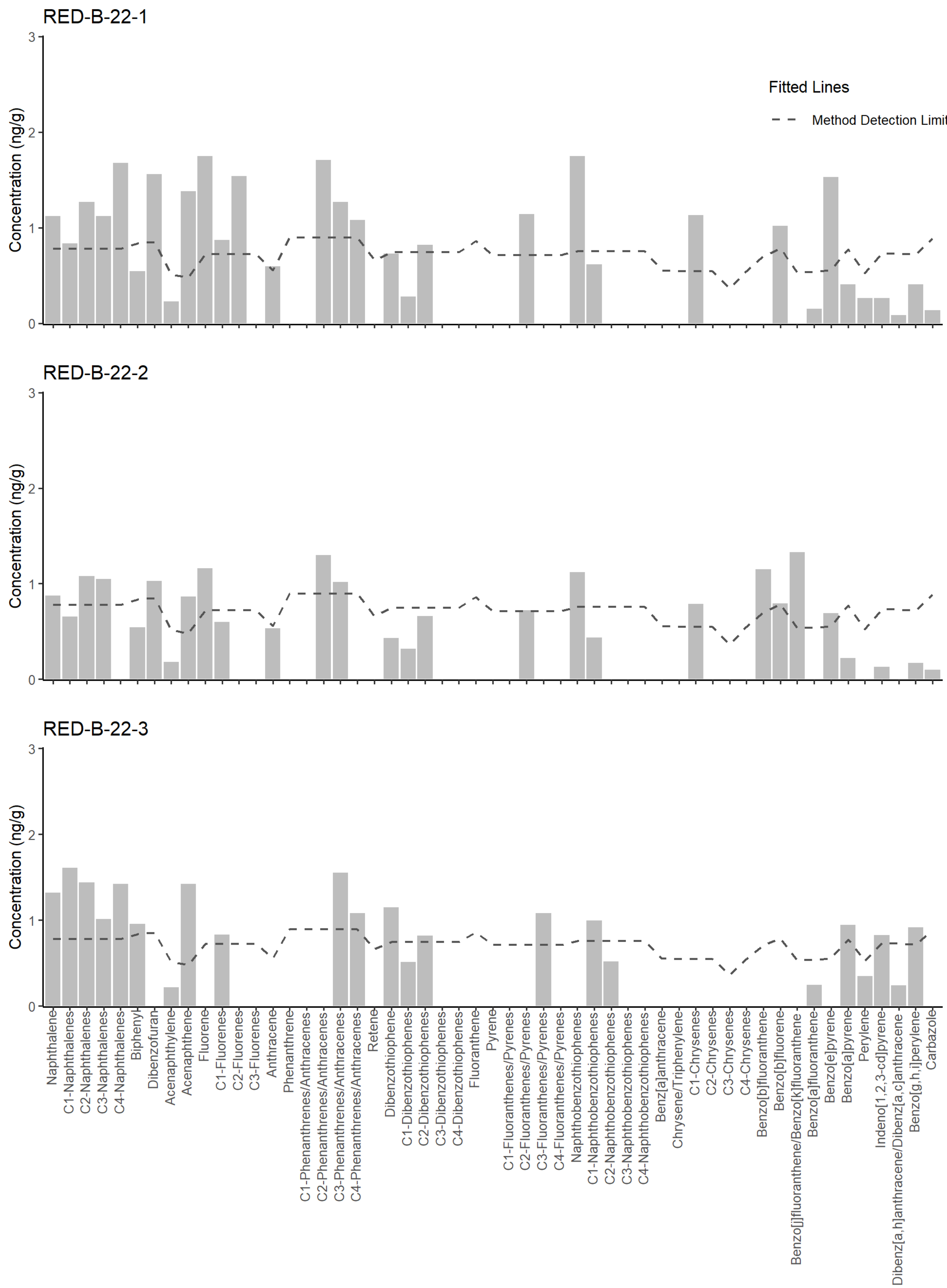

Figure 24. 2022 PAH profiles from individual mussel tissue samples at the Valdez Small Boat Harbor entrance (RED) with the analyte specific method detection limit superimposed as a dashed line.

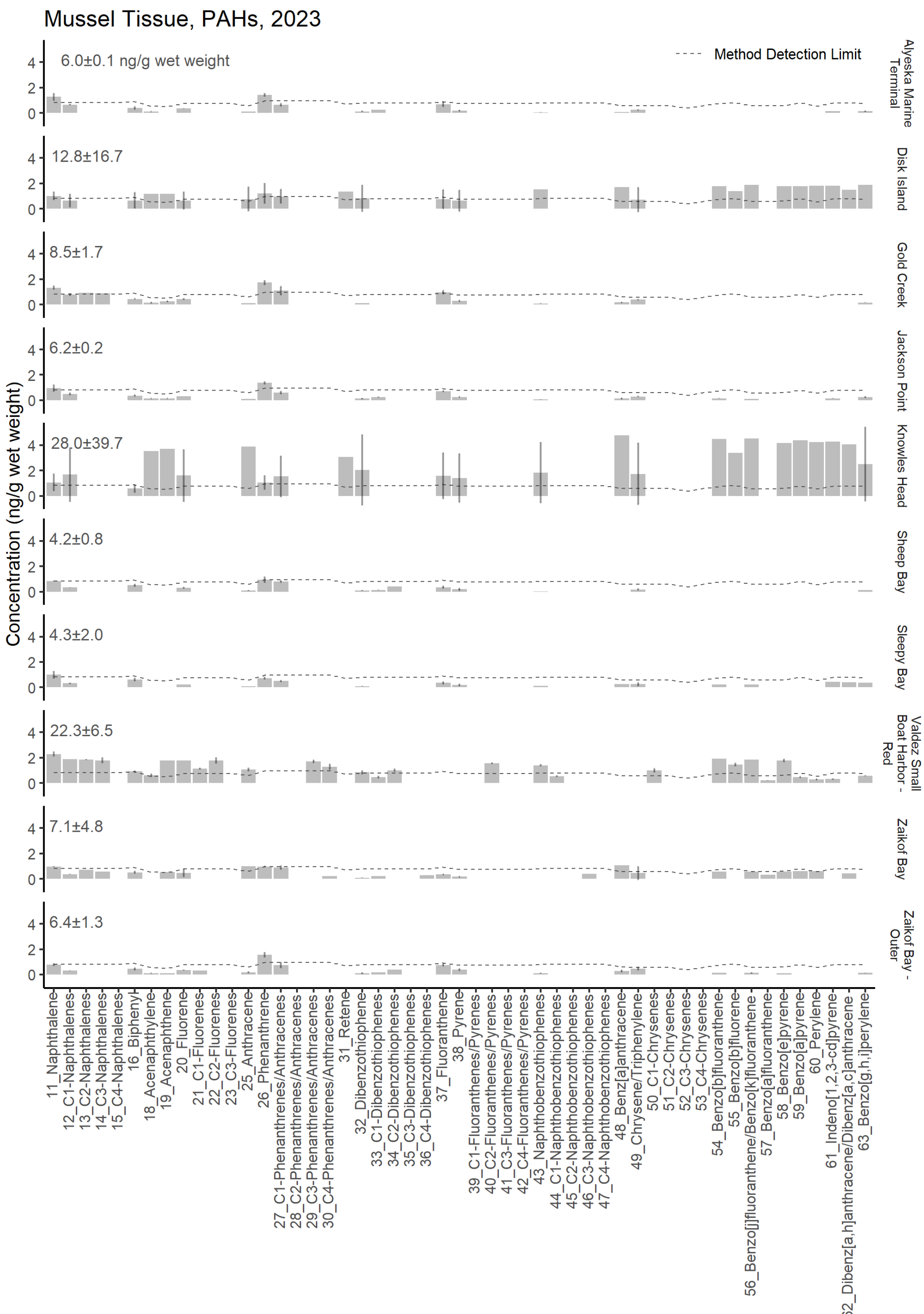

Figure 25. PAH profiles from 2023 mussel tissue samples plotted by mean ± 1 standard deviation. The analyte specific method detection limit is superimposed as a dashed line. Sum 42 PAH values (mean ± 1 standard deviation) are found in the upper left corner of each site profile.

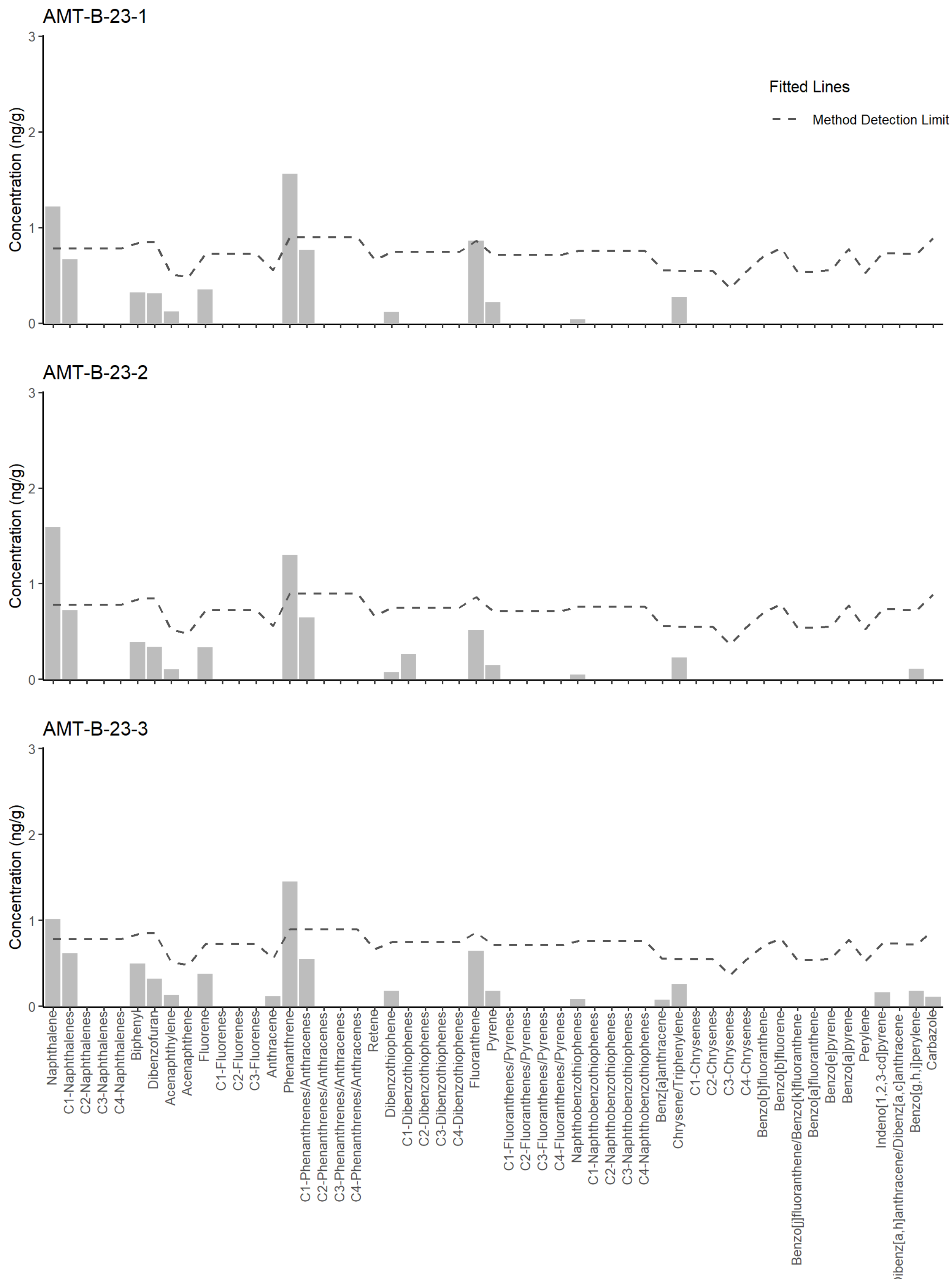

Figure 26. 2023 PAH profiles from individual mussel tissue samples at the Valdez Marine Terminal / Saw Island (AMT/SAW) with the analyte specific method detection limit superimposed as a dashed line.

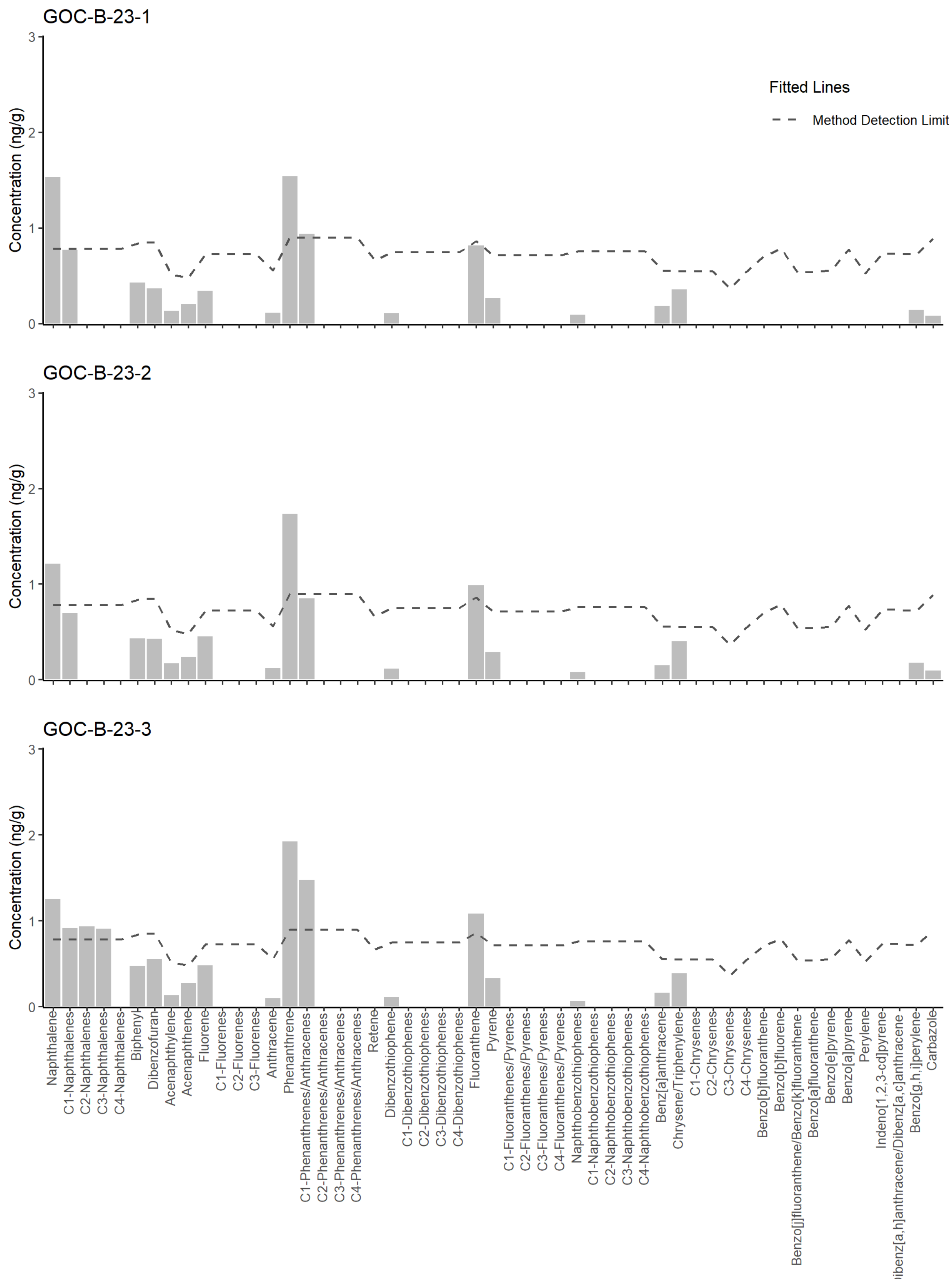

Figure 27. 2023 PAH profiles from individual mussel tissue samples at Gold Creek (GOC) with the analyte specific method detection limit superimposed as a dashed line.

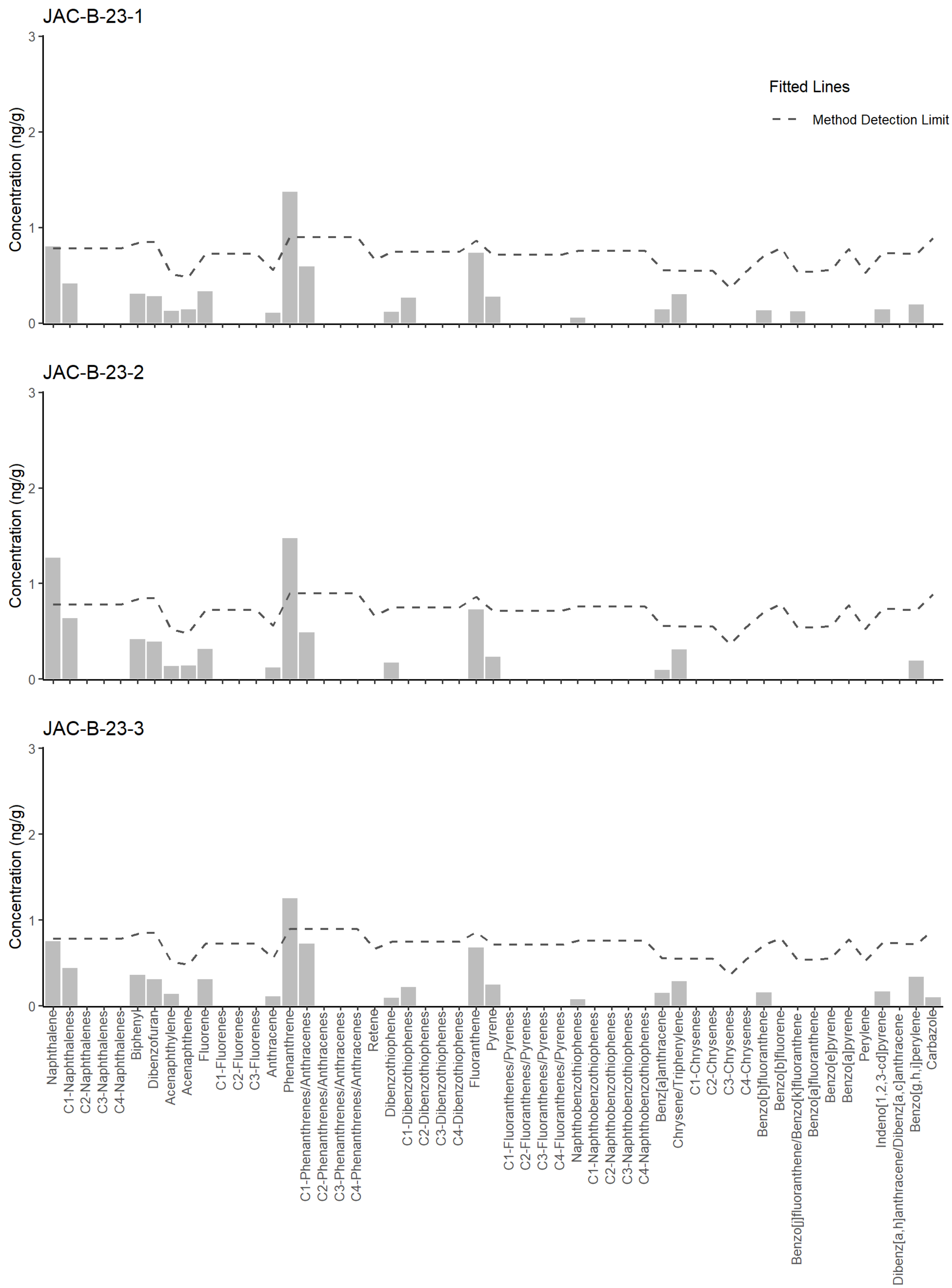

Figure 28. 2023 PAH profiles from individual mussel tissue samples at Jackson Point (JAC) with the analyte specific method detection limit superimposed as a dashed line.

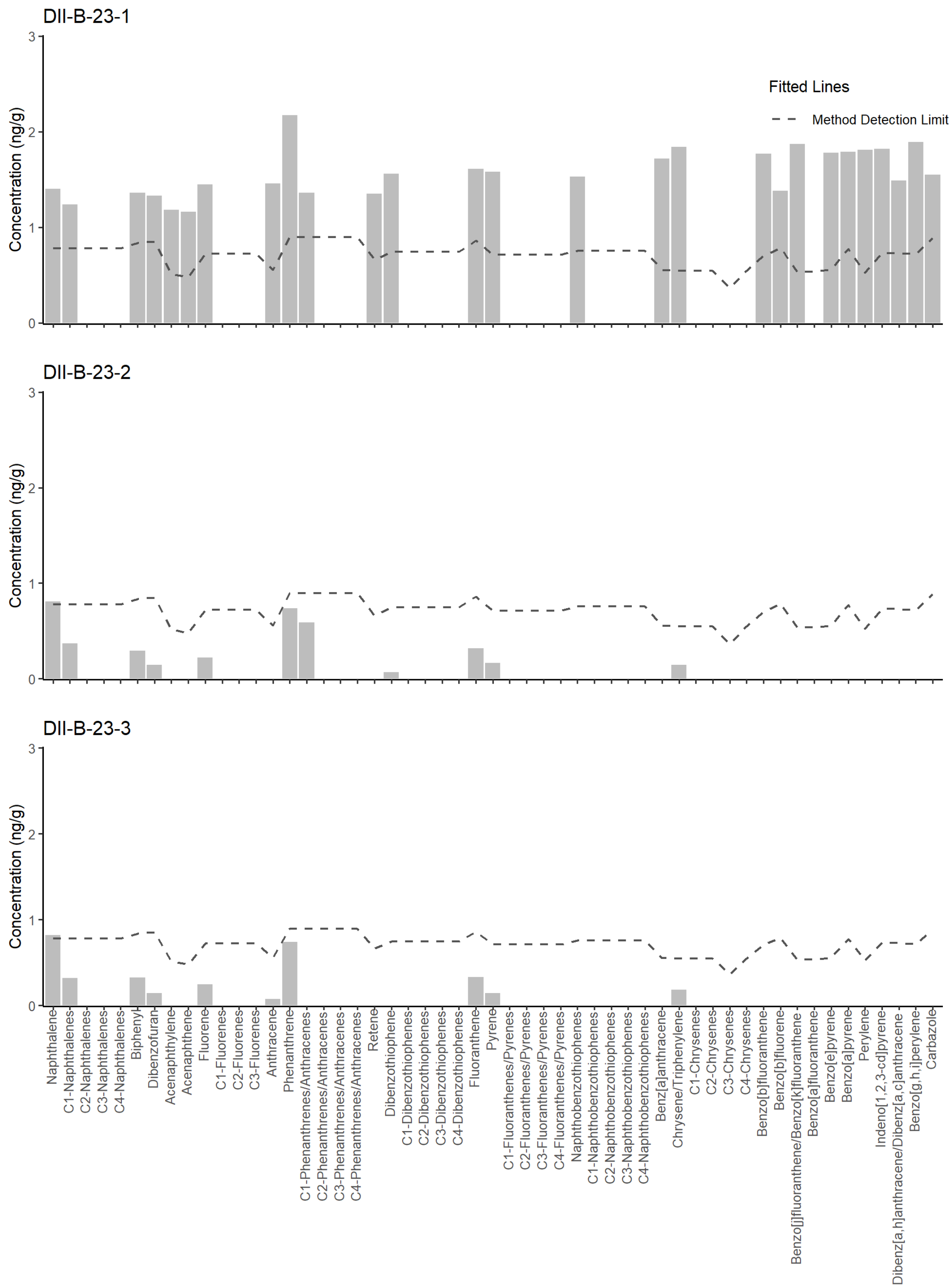

Figure 29. 2023 PAH profiles from individual mussel tissue samples at Disk Island (DII) with the analyte specific method detection limit superimposed as a dashed line.

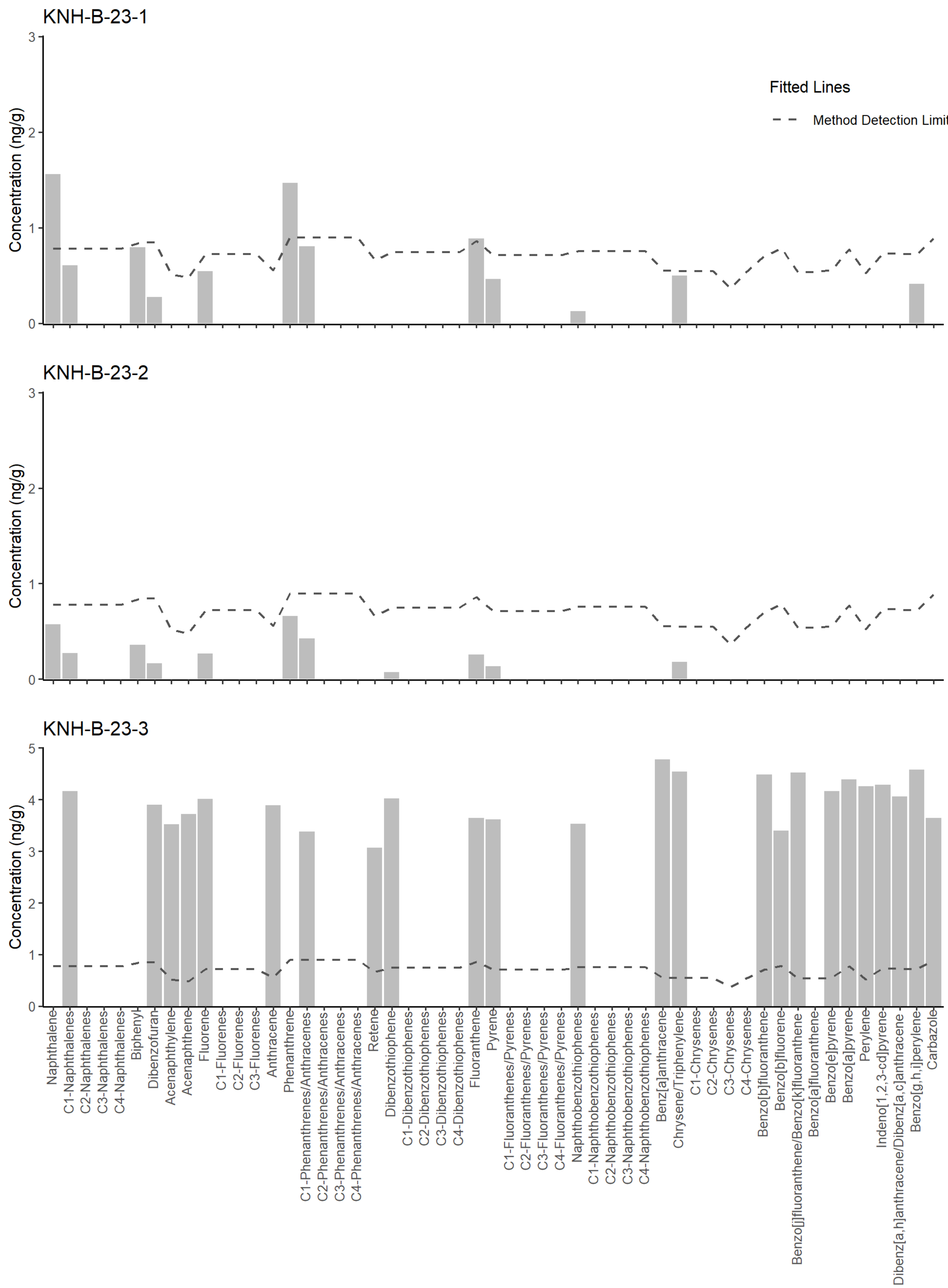

Figure 30. 2023 PAH profiles from individual mussel tissue samples at Knowles Head (KNH) with the analyte specific method detection limit superimposed as a dashed line.

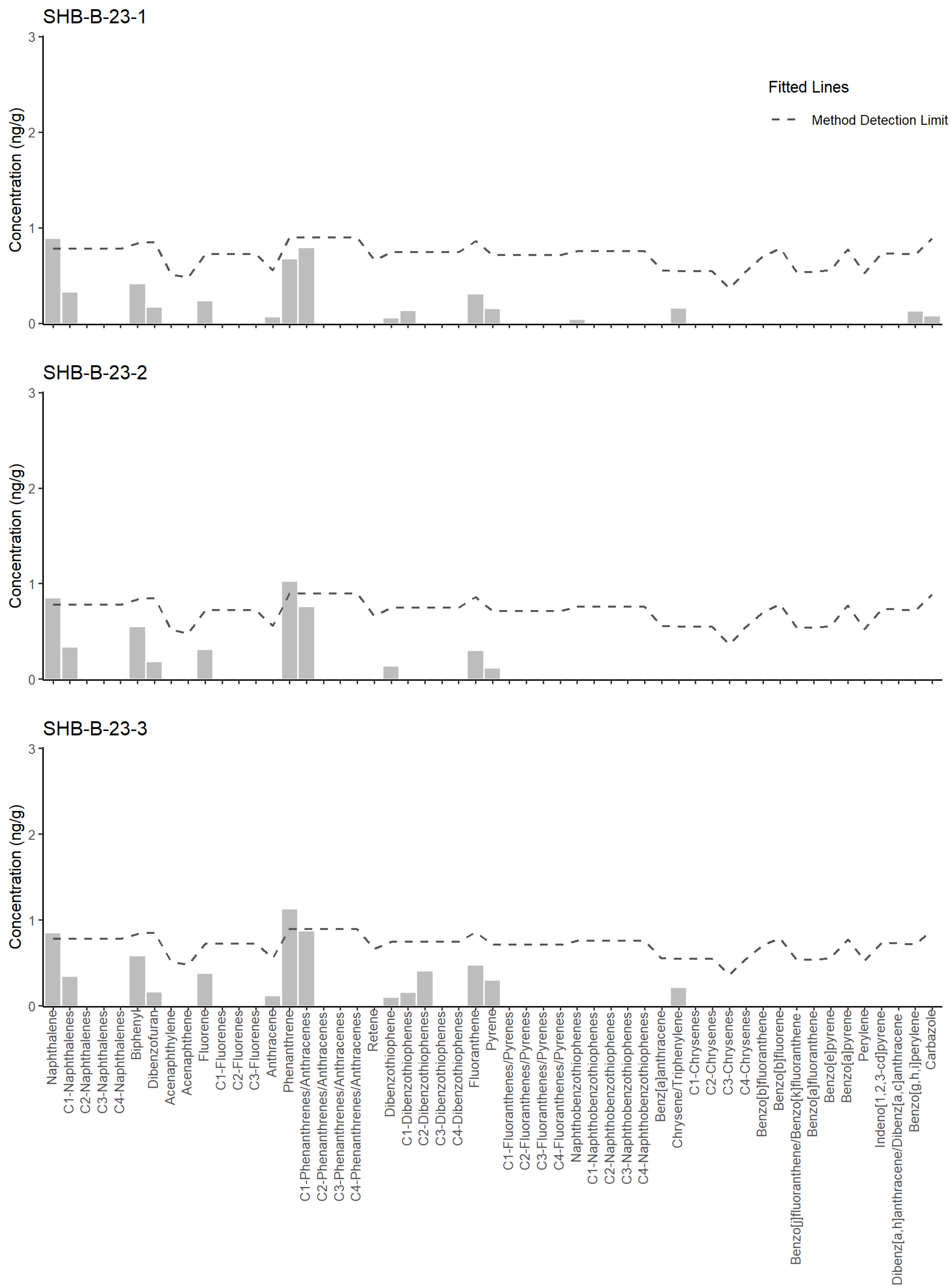

Figure 31. 2023 PAH profiles from individual mussel tissue samples at Sheep Bay (SHB) with the analyte specific method detection limit superimposed as a dashed line.

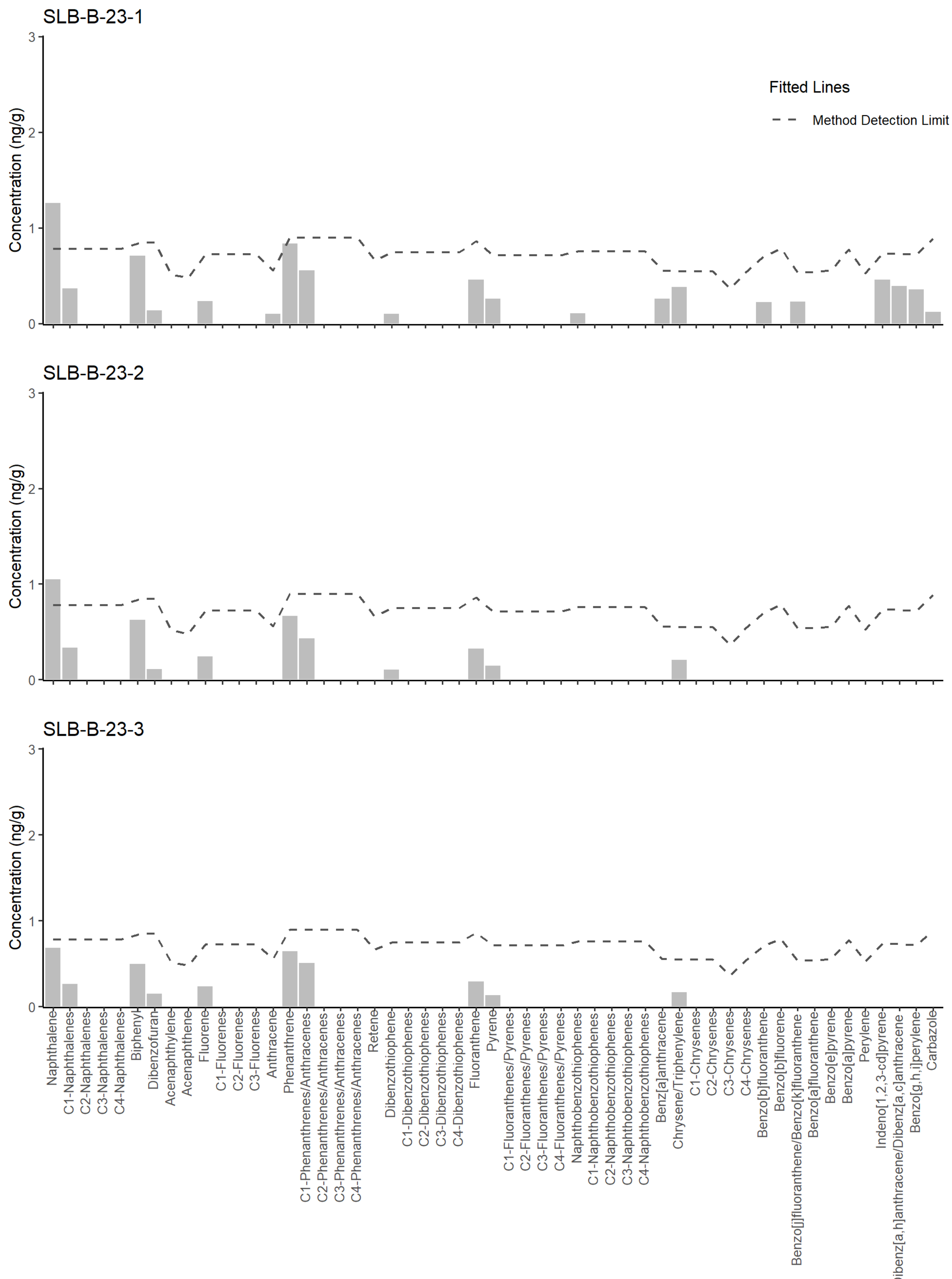

Figure 32. 2023 PAH profiles from individual mussel tissue samples at Sleepy Bay (SLB) with the analyte specific method detection limit superimposed as a dashed line.

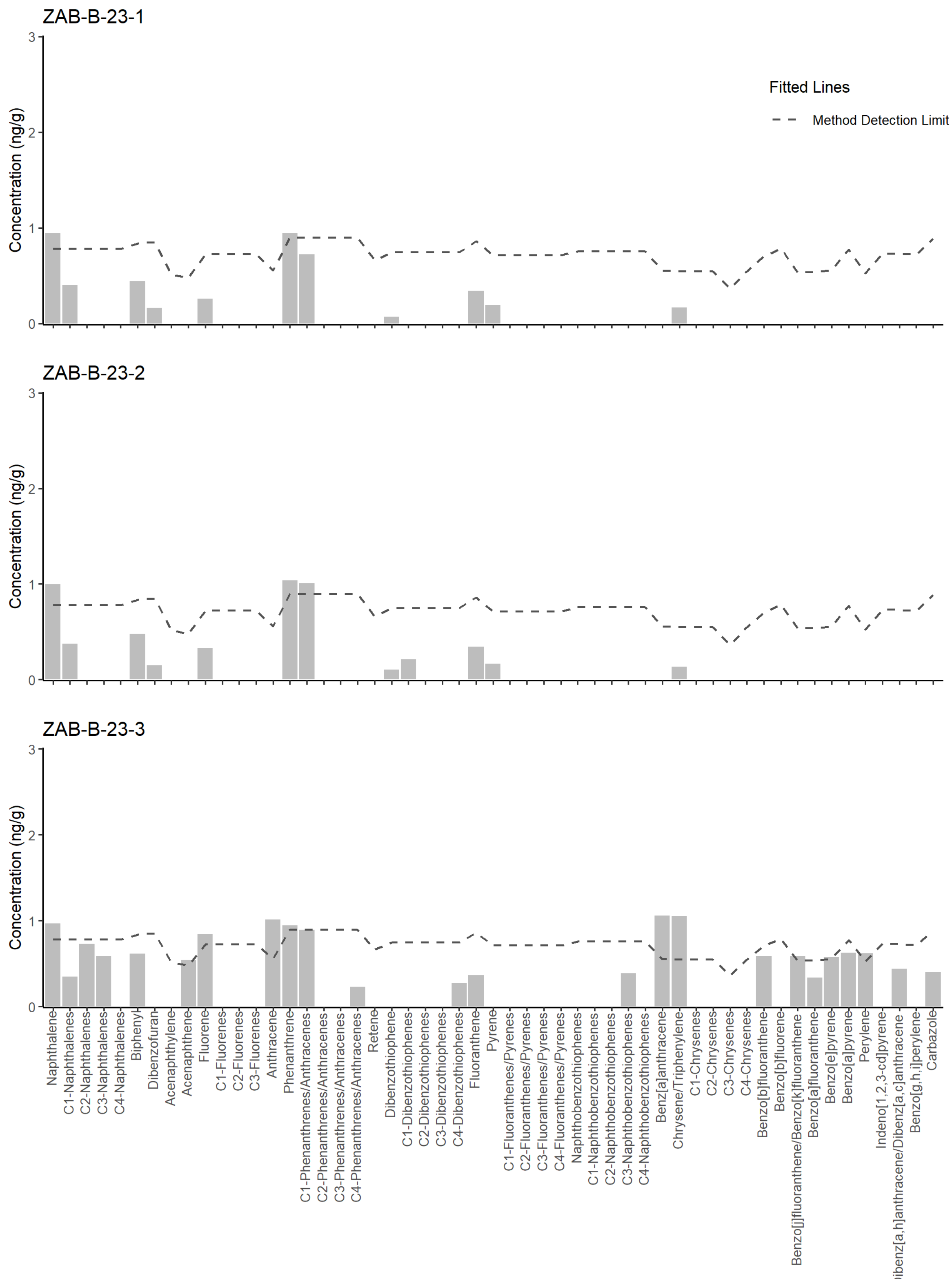

Figure 33. 2023 PAH profiles from individual mussel tissue samples Zaikof Bay (ZAB) with the analyte specific method detection limit superimposed as a dashed line.

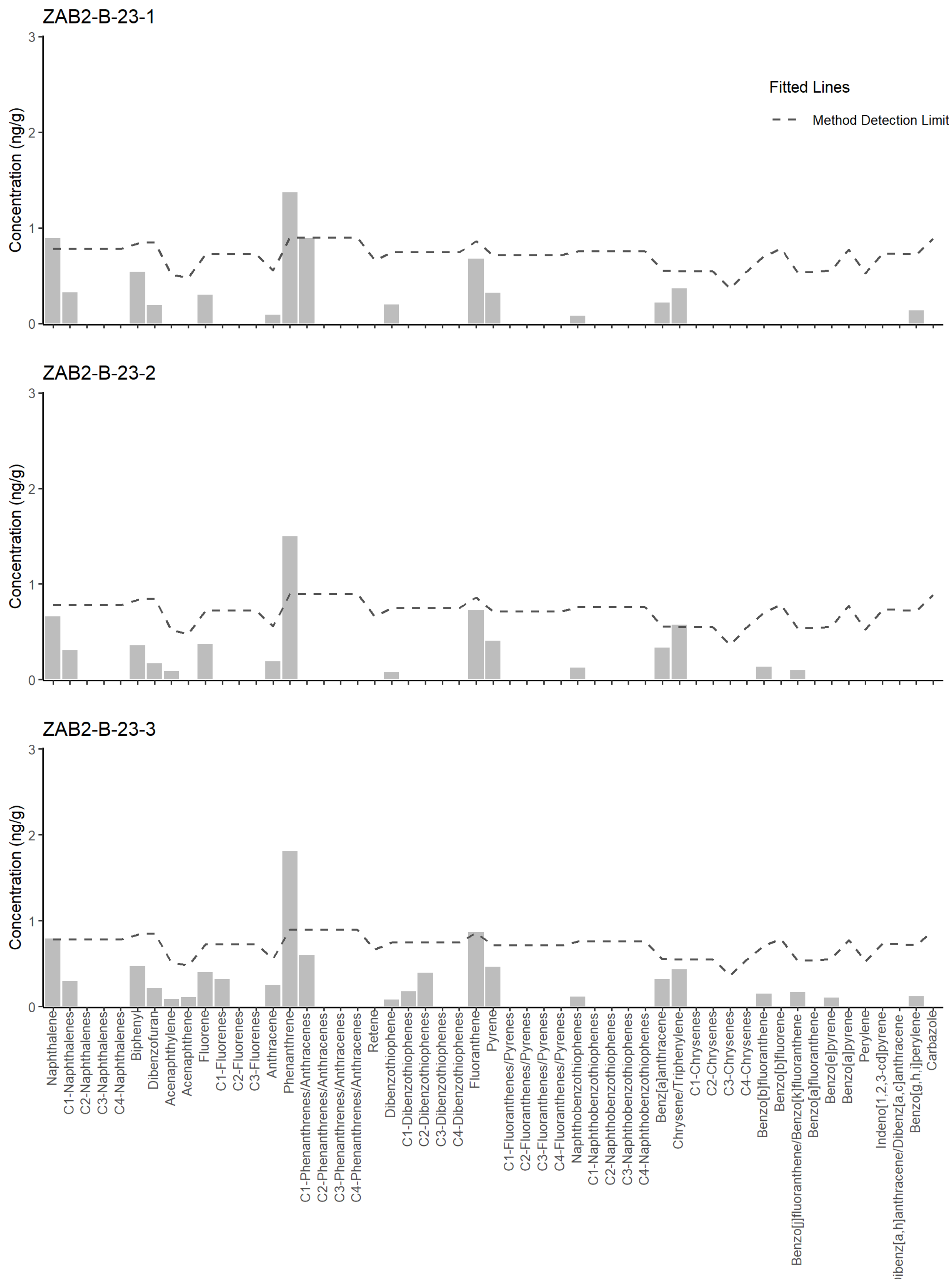

Figure 34. 2023 PAH profiles from individual mussel tissue samples at a new outer station in Zaikof Bay (ZAB) with the analyte specific method detection limit superimposed as a dashed line.

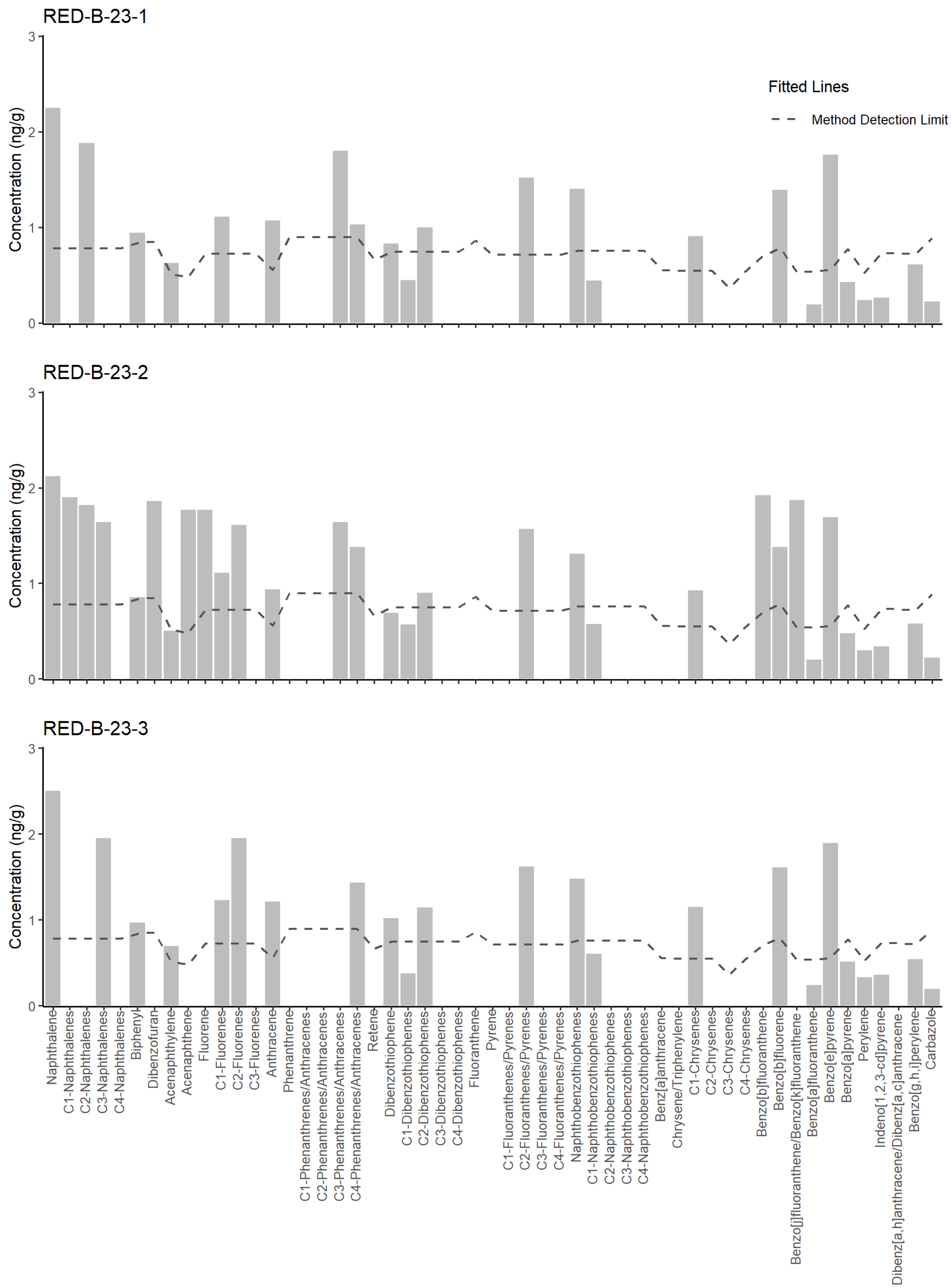

Figure 35. 2023 PAH profiles from individual mussel tissue samples at the Valdez Small Boat Harbor Red light (RED) with the analyte specific method detection limit superimposed as a dashed line.

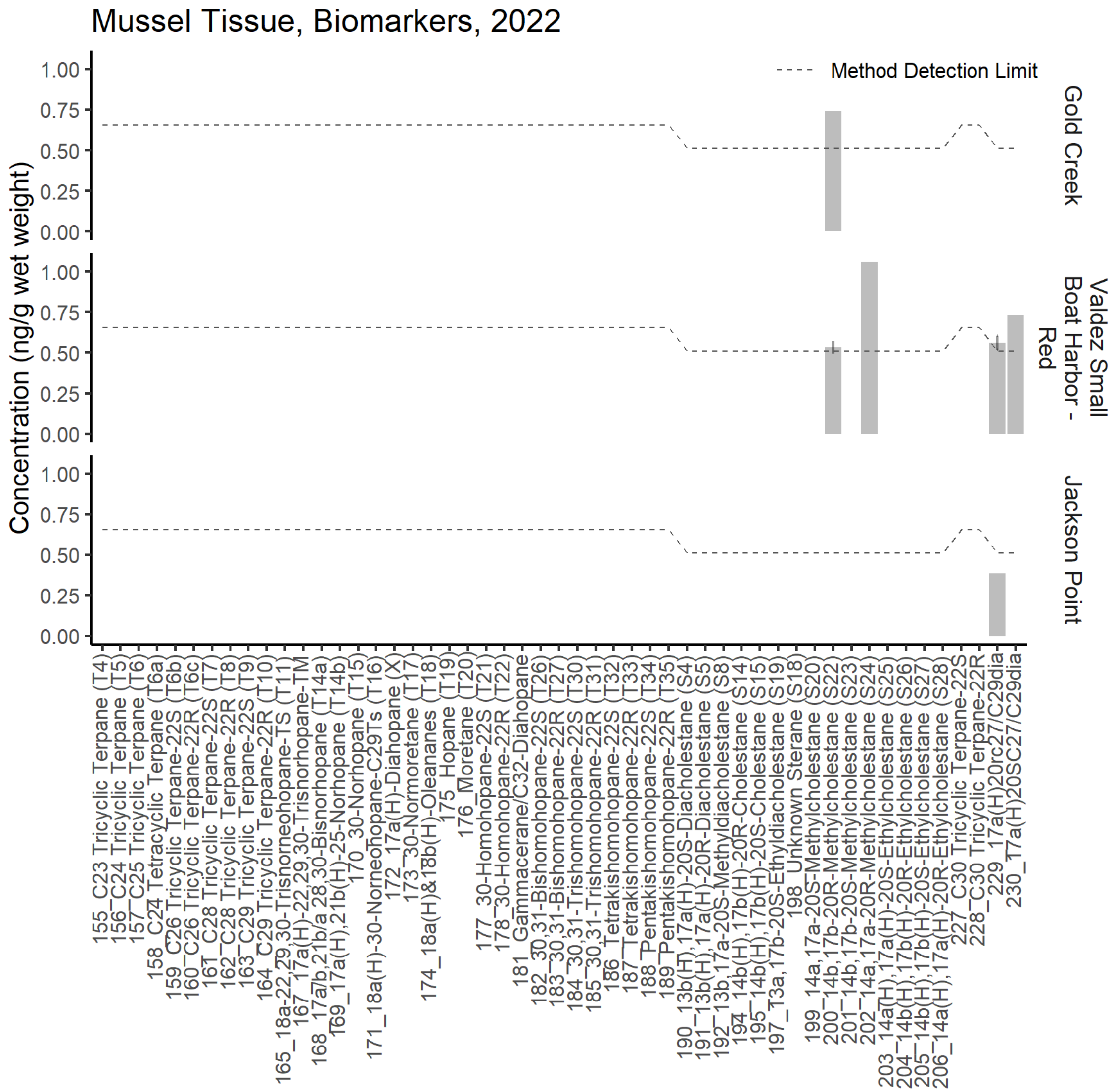

Figure 36. 2022 Petroleum chemical biomarker profiles from mussel tissue samples plotted by mean ± 1 standard deviation. The analyte specific method detection limit is superimposed as a dashed line.

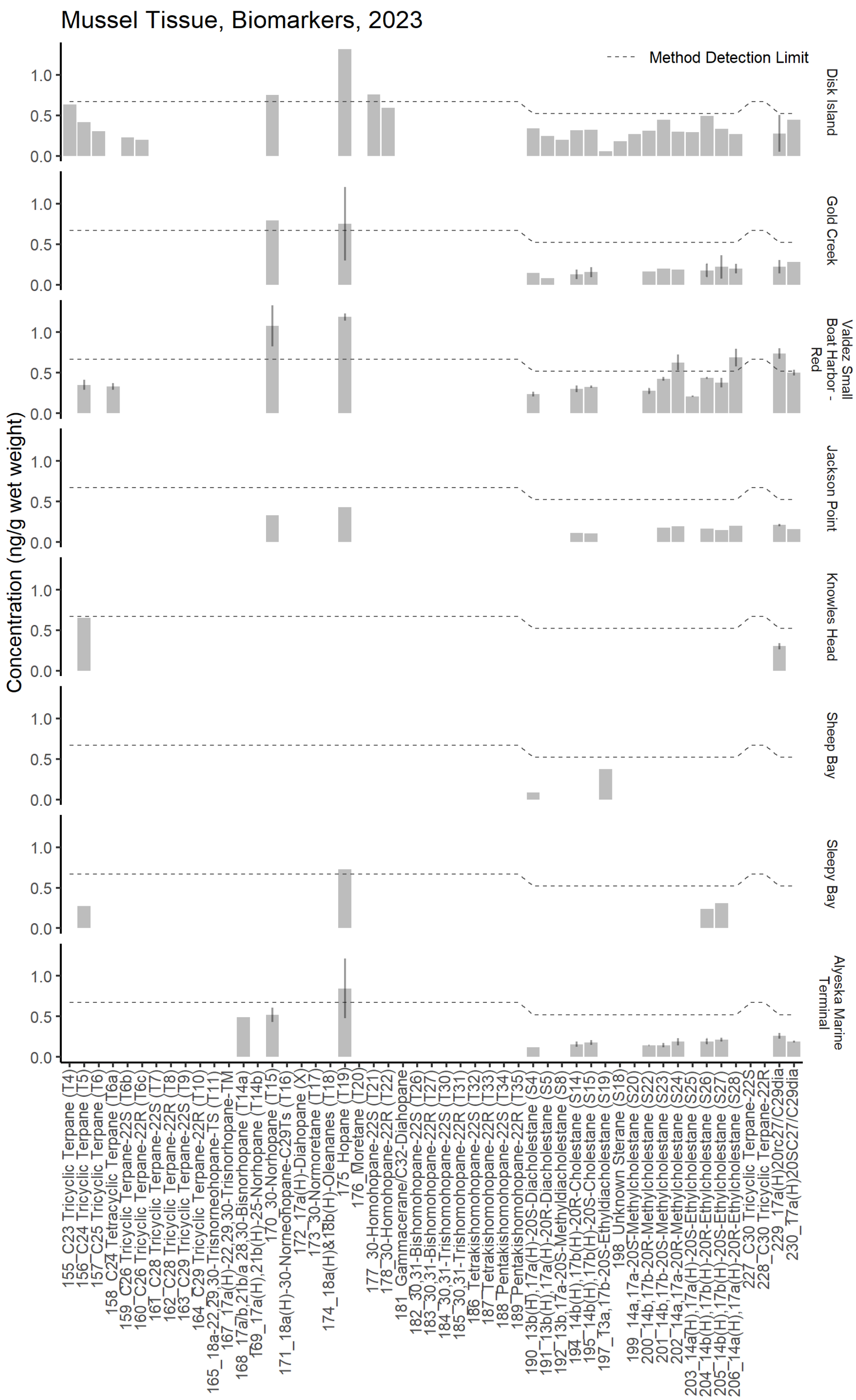

Figure 37. 2023 Petroleum chemical biomarker profiles from mussel tissue samples plotted by mean ± 1 standard deviation. The analyte specific method detection limit is superimposed as a dashed line.

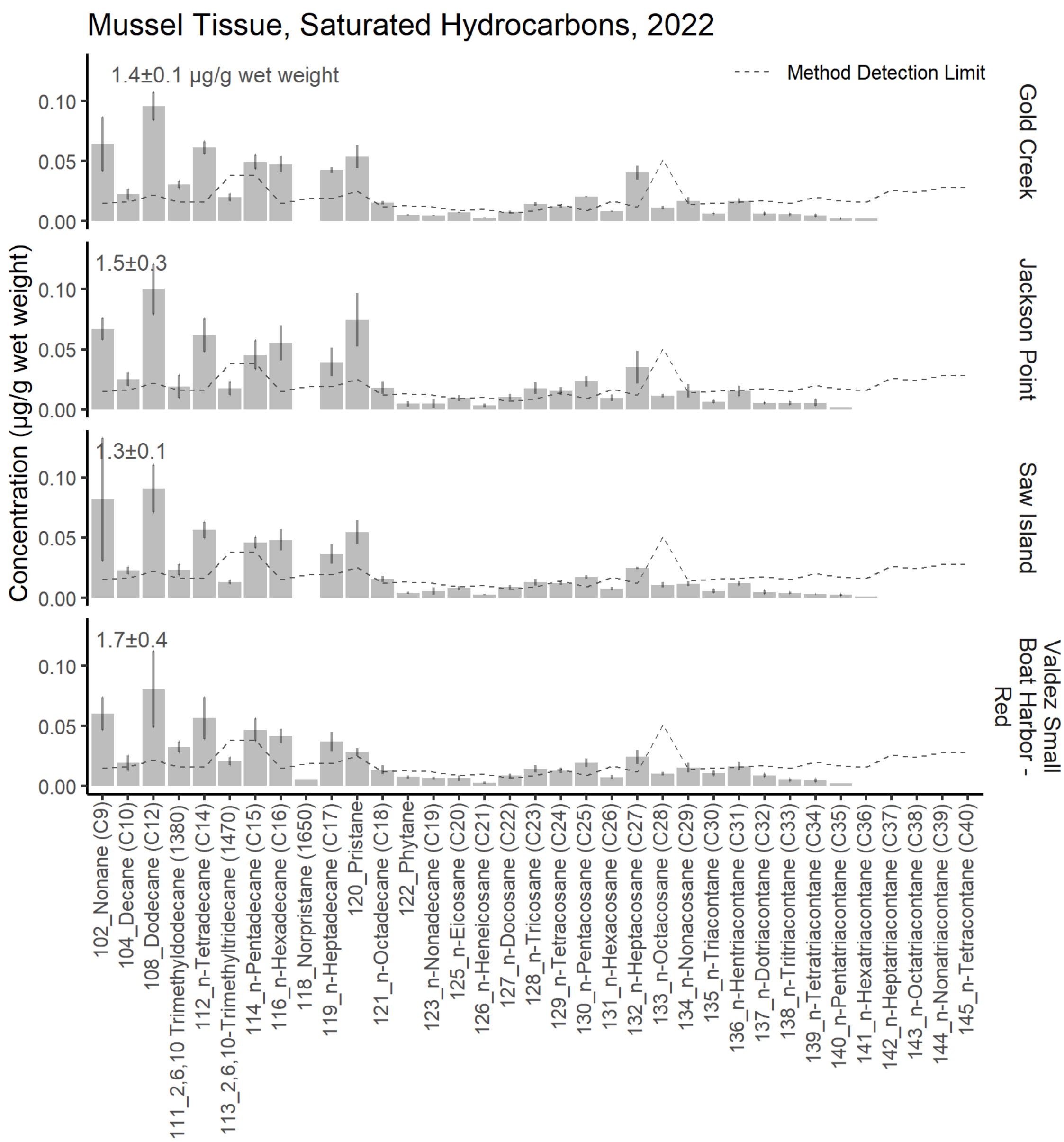

Figure 38. 2022 Saturated hydrocarbons (SHC) profiles from mussel tissue samples plotted by mean ± 1 standard deviation. The analyte specific method detection limit is superimposed as a dashed line. Sum SHC values (mean ± 1 standard deviation) are found in the upper left corner of each site profile.

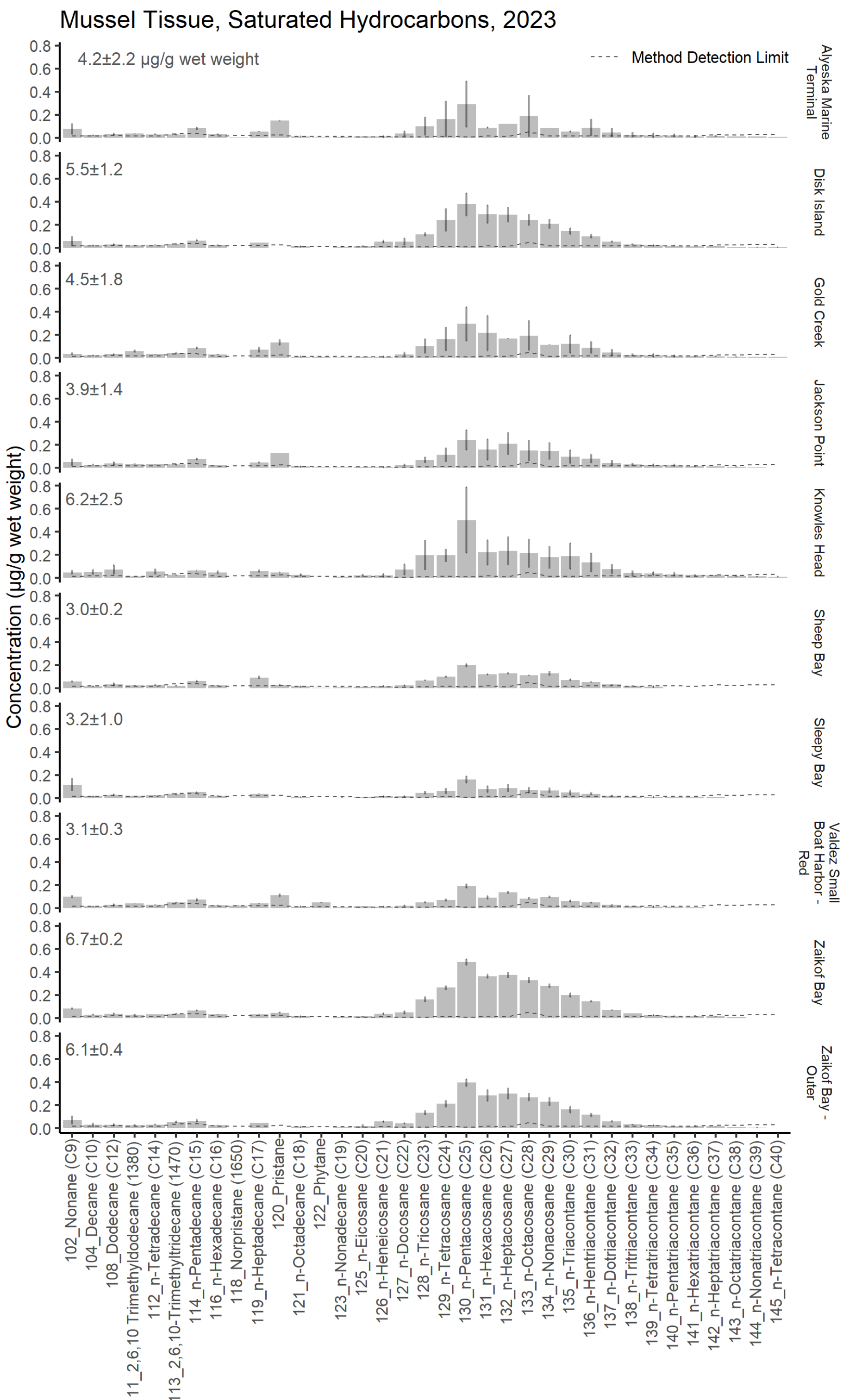

Figure 39. 2023 Saturated hydrocarbons (SHC) profiles from mussel tissue samples plotted by mean ± 1 standard deviation. The analyte specific method detection limit is superimposed as a dashed line. Sum SHC values (mean ± 1 standard deviation) are found in the upper left corner of each site profile.

Laboratory Data

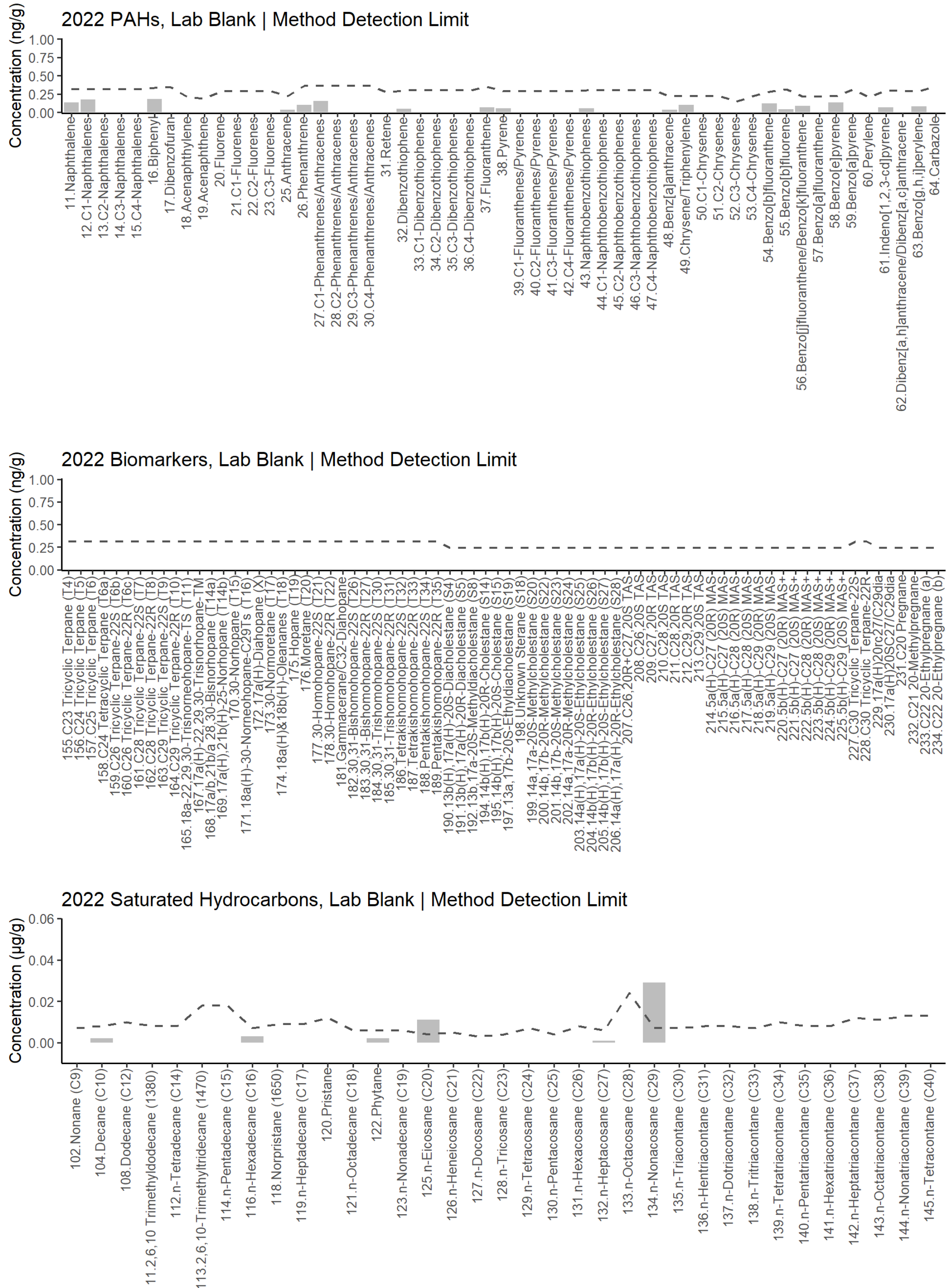

Figure 40. 2022 PAH, biomarker, and saturated hydrocarbon (SHC) profiles from the NewFields laboratory blanks with the analyte specific method detection limit superimposed as a dashed line.

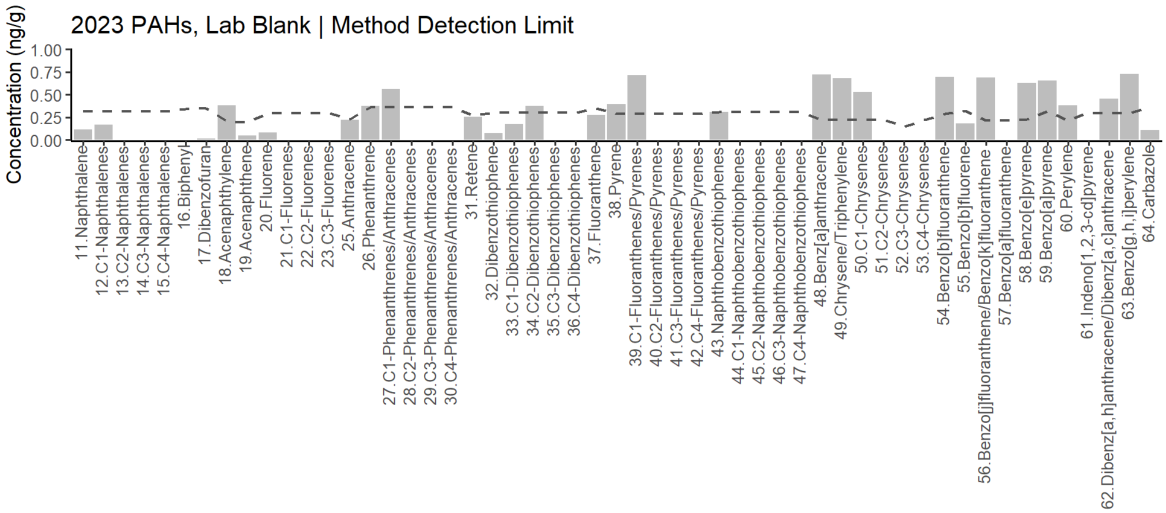

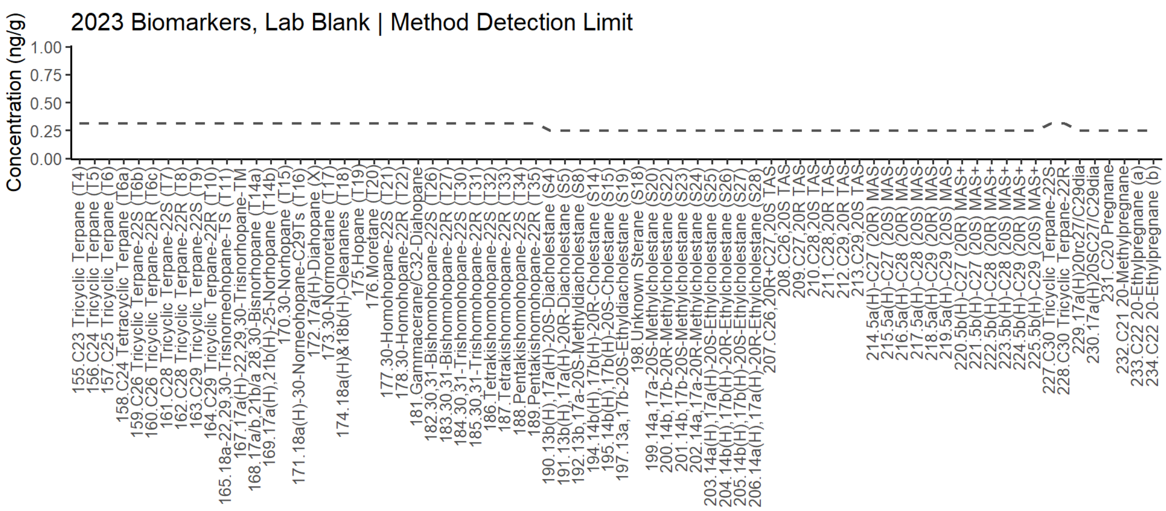

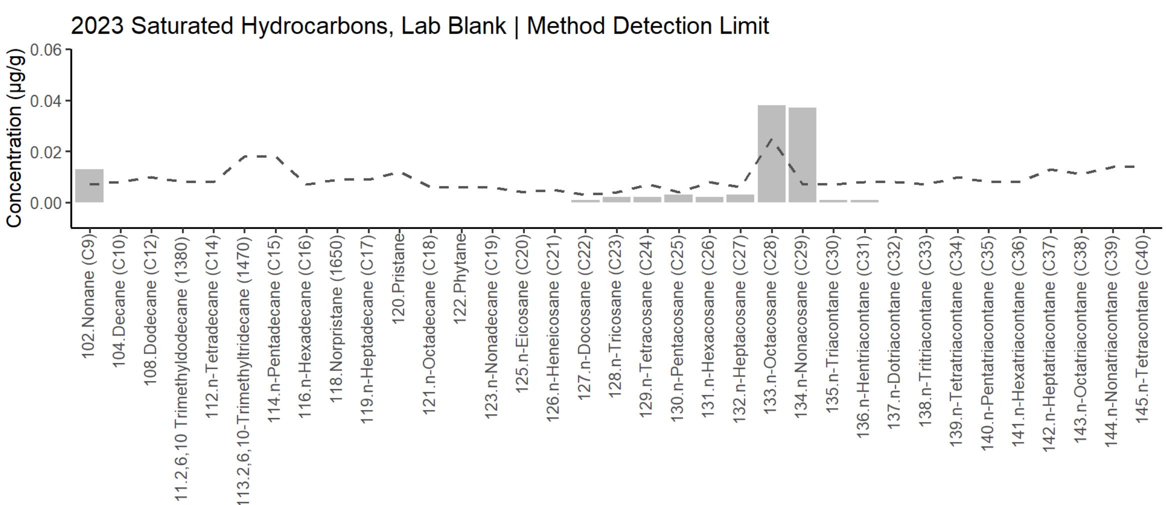

Figure 41. 2023 PAH, biomarker, and saturated hydrocarbon (SHC) profiles from the Alpha Analytical laboratory blanks with the analyte specific method detection limit superimposed as a dashed line.

Water via Passive Sampler Data

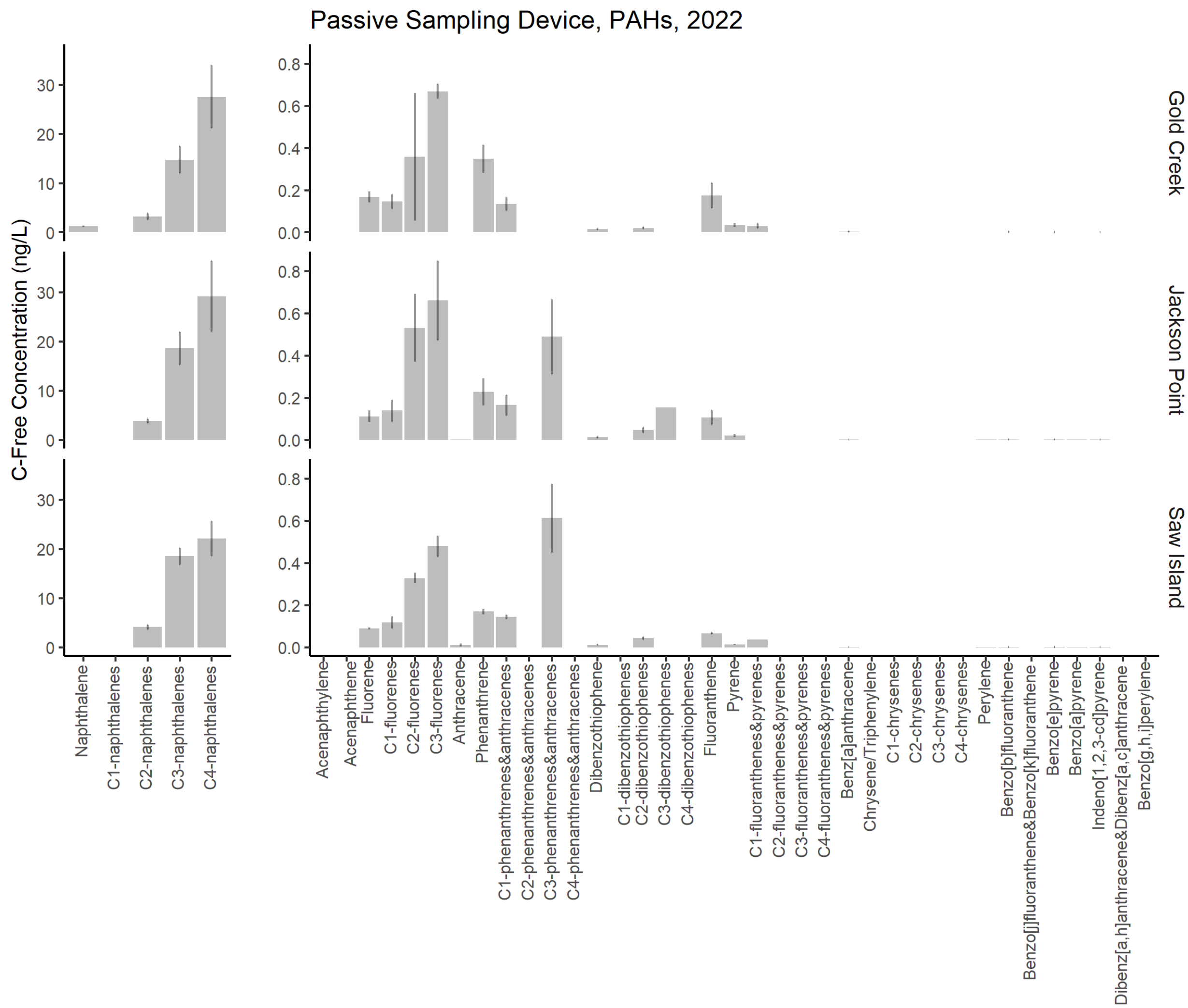

Figure 42. PAH profiles from water sampled via passive sampling devices deployed during LTEMP 2022 at Gold Creek, Jackson Point, and Saw Island plotted by mean value ± standard deviation.

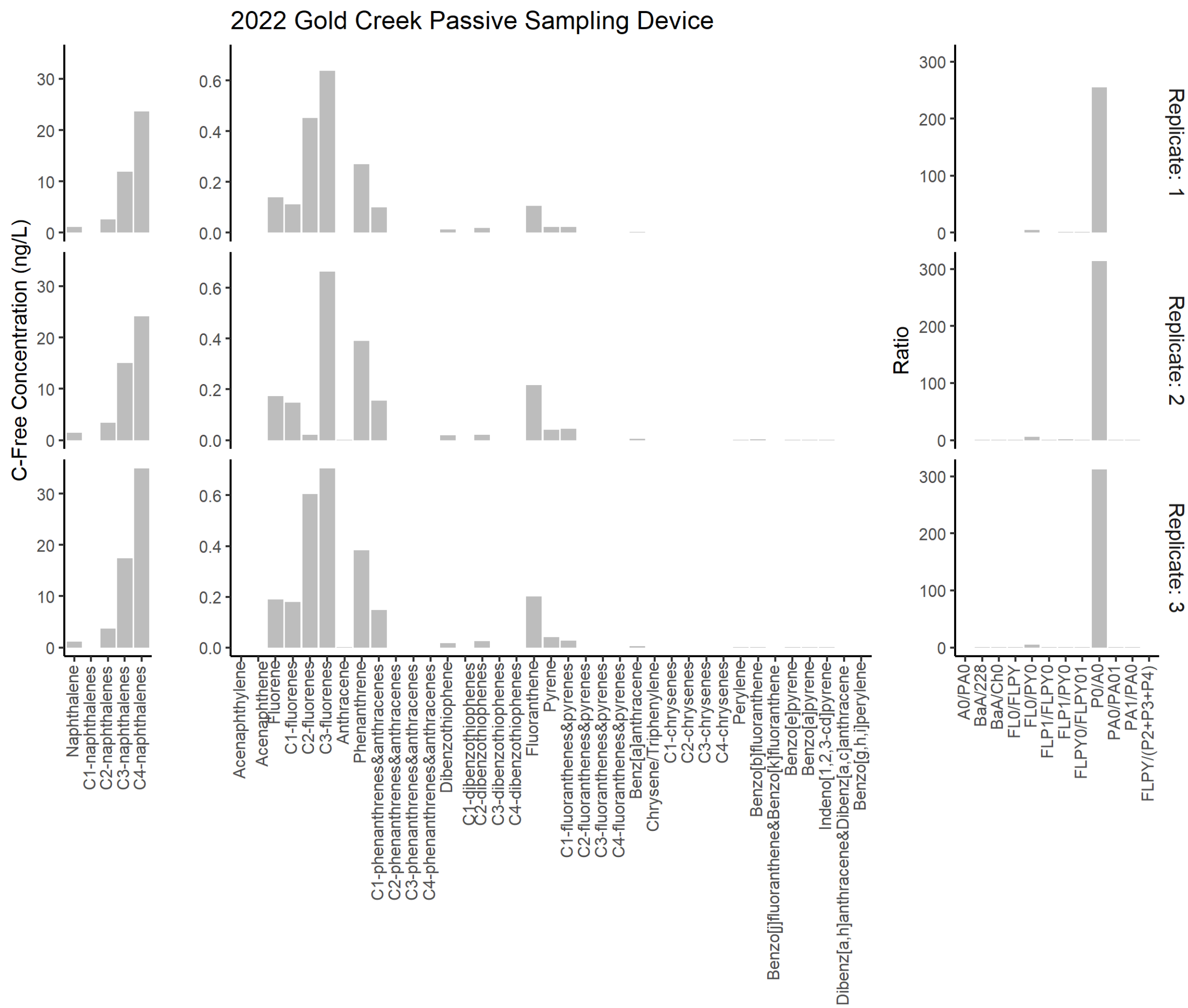

Figure 43. 2022 water PAH profiles and laboratory diagnostic ratios from individual passive sampling devices deployed at Gold Creek.

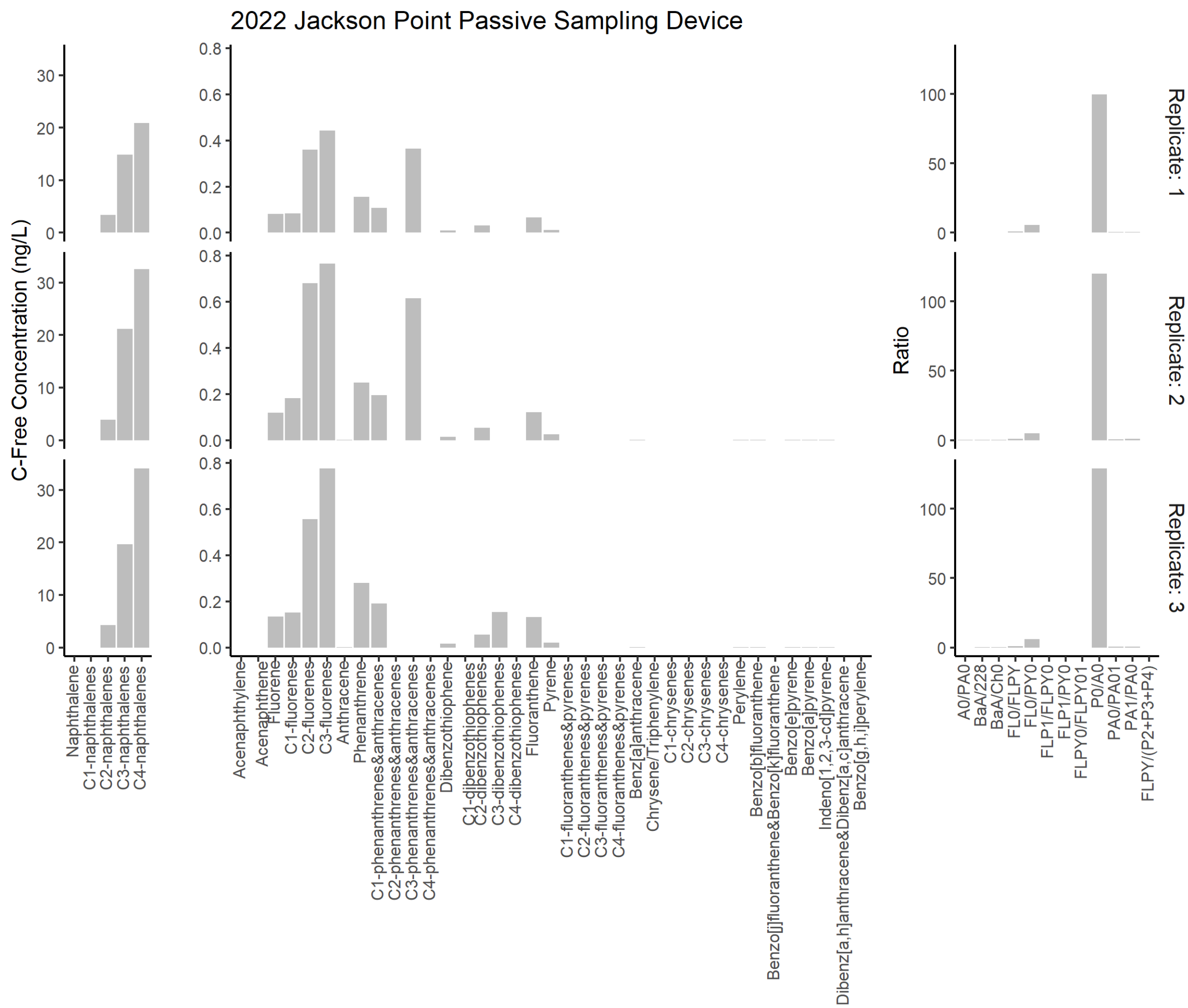

Figure 44. 2022 water PAH profiles and laboratory diagnostic ratios from individual passive sampling devices deployed at Jackson Point.

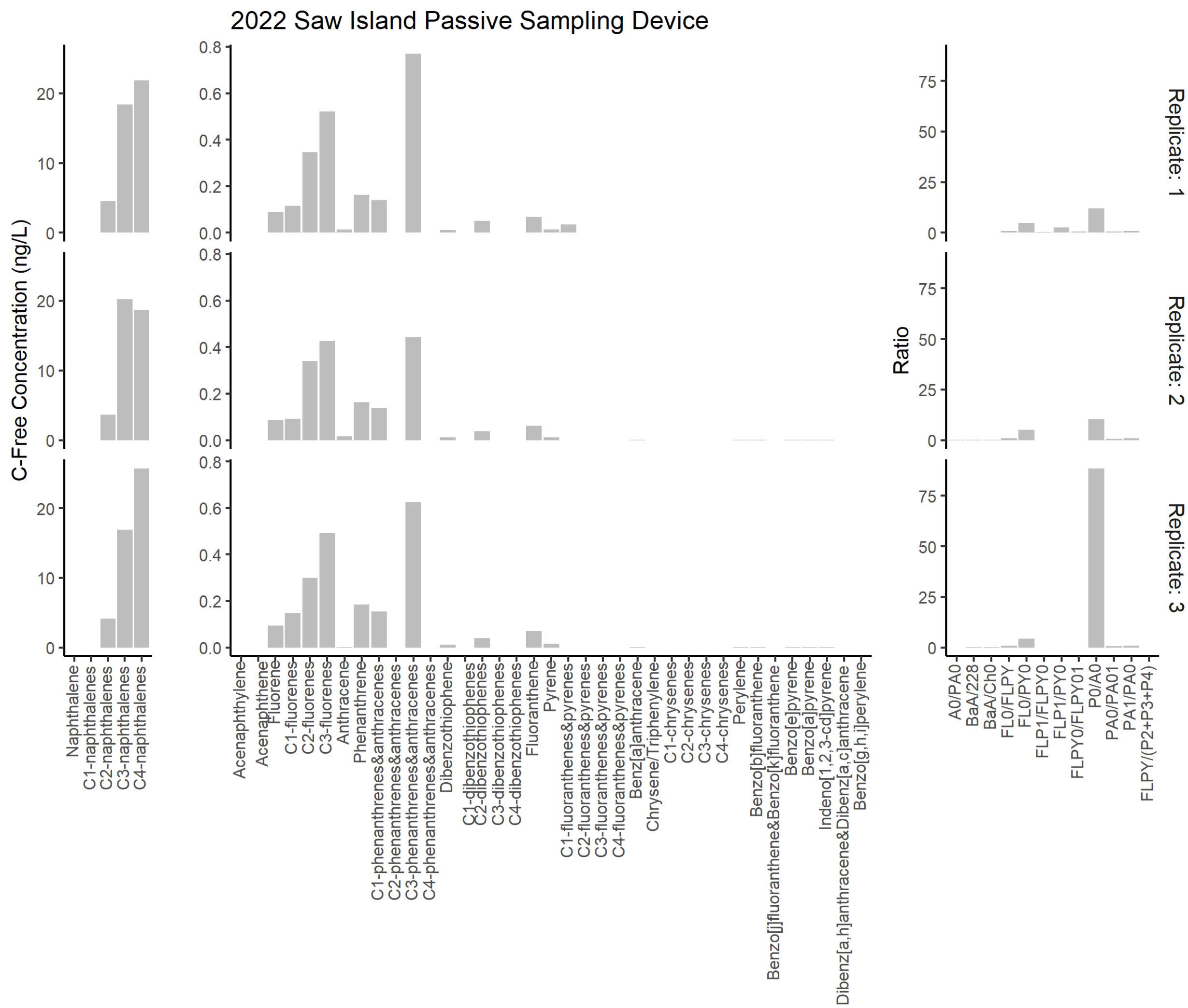

Figure 45. 2022 water PAH profiles and laboratory diagnostic ratios from individual passive sampling devices deployed at Saw Island.

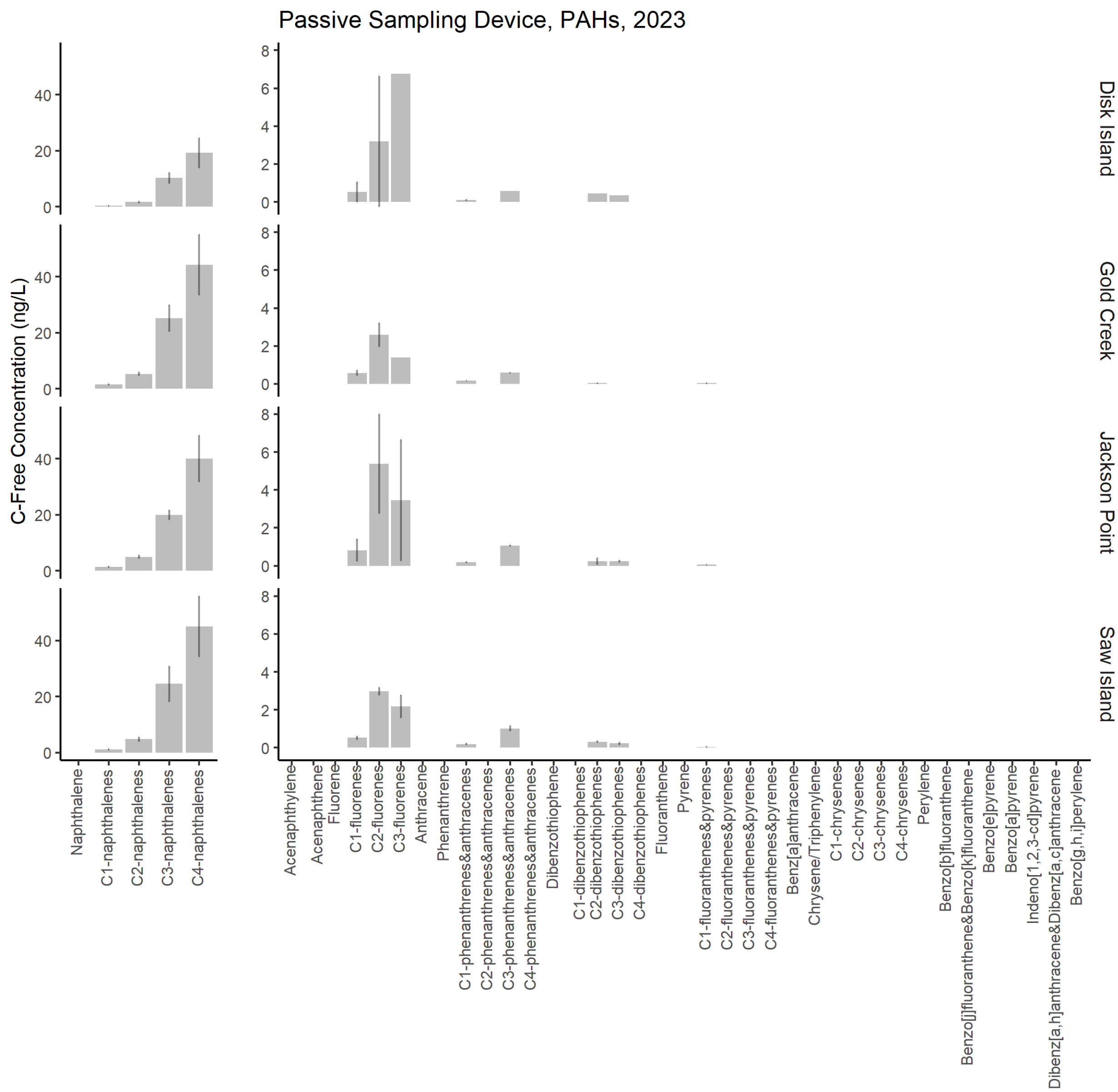

Figure 46. PAH profiles from water sampled via passive sampling devices deployed during LTEMP 2023 at Disk Island, Gold Creek, Jackson Point, and Saw Island plotted by mean value ± standard deviation.

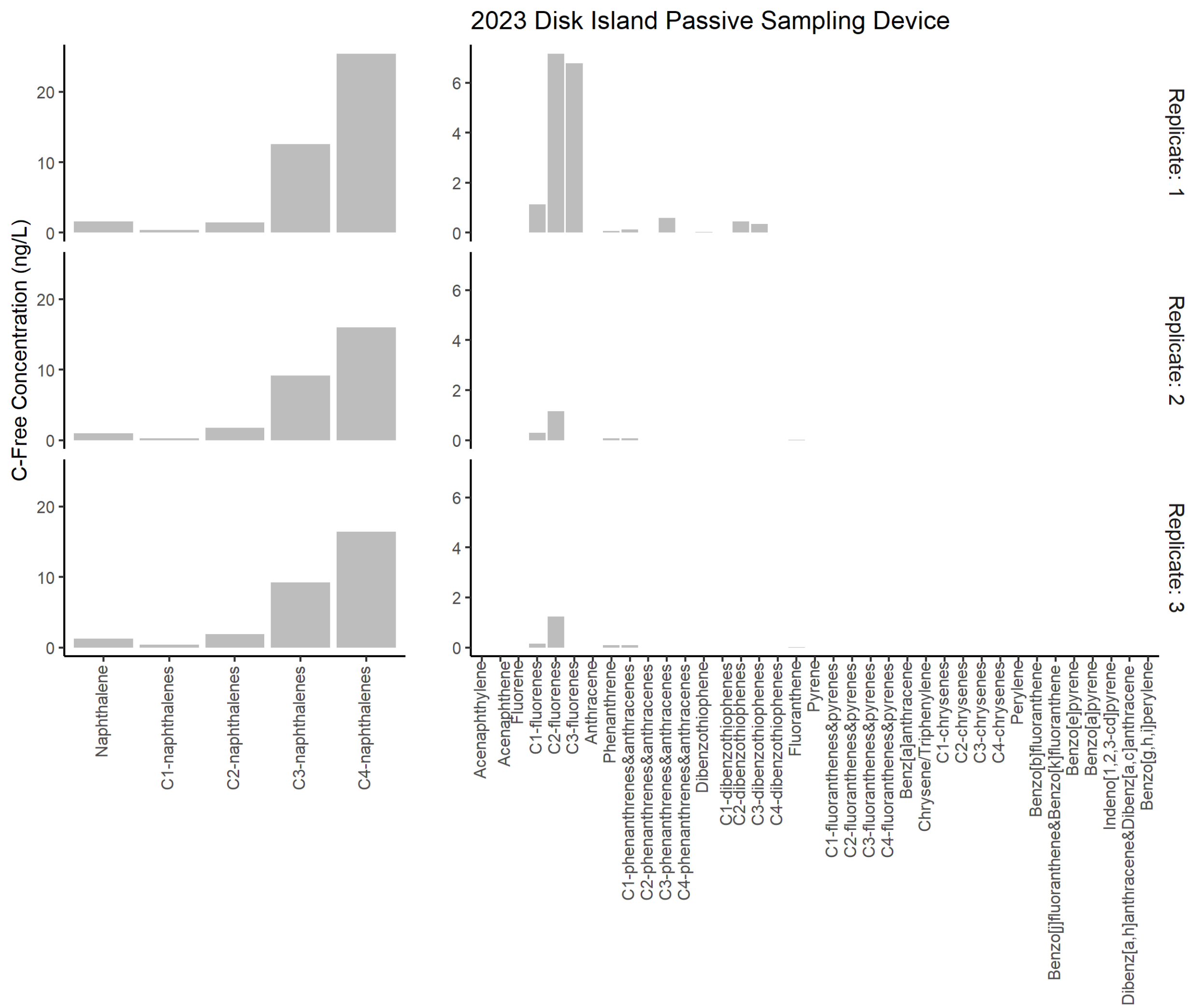

Figure 47. 2023 water PAH profiles from individual passive sampling devices deployed at Disk Island.

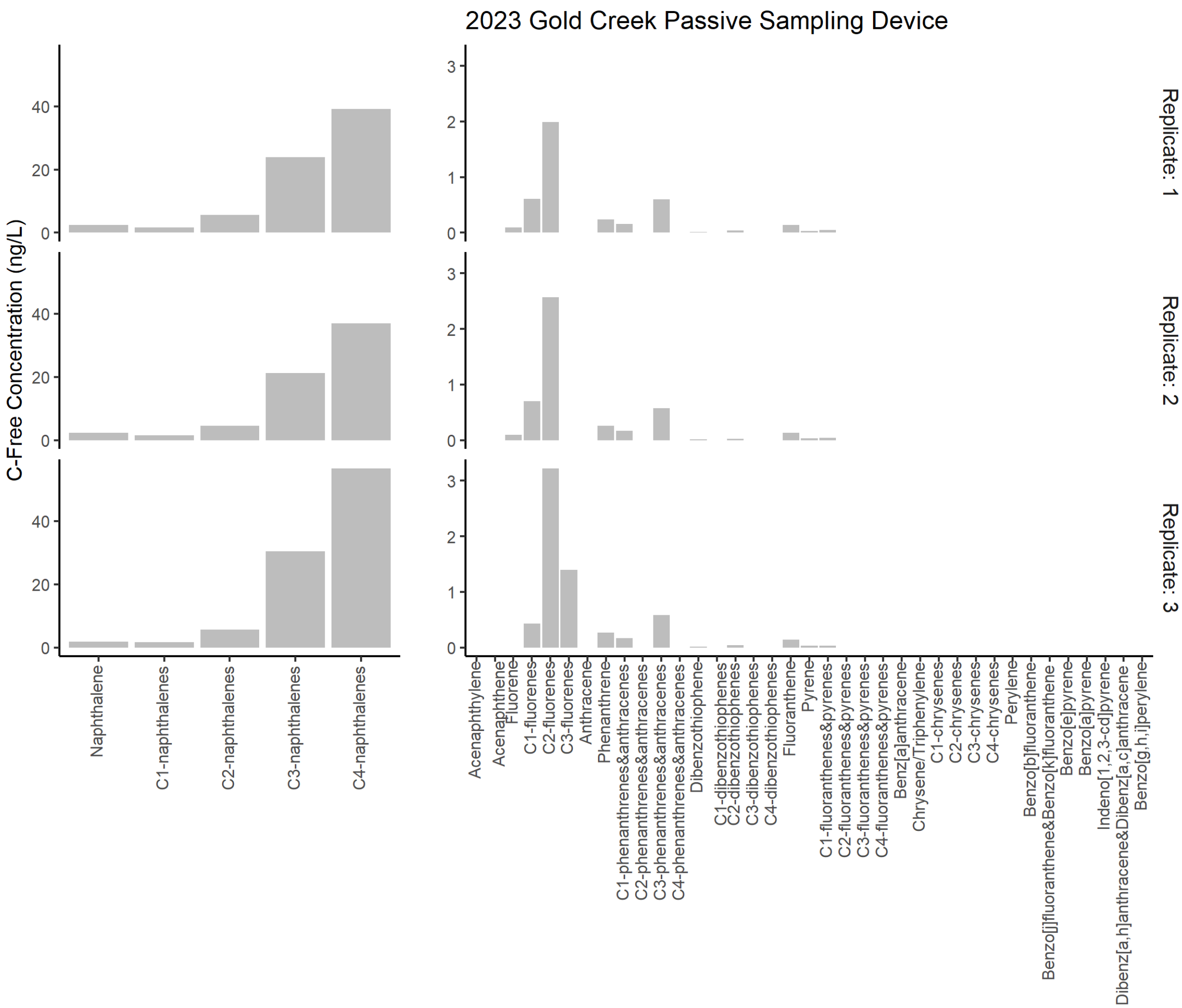

Figure 48. 2023 water PAH profiles from individual passive sampling devices deployed at Gold Creek.

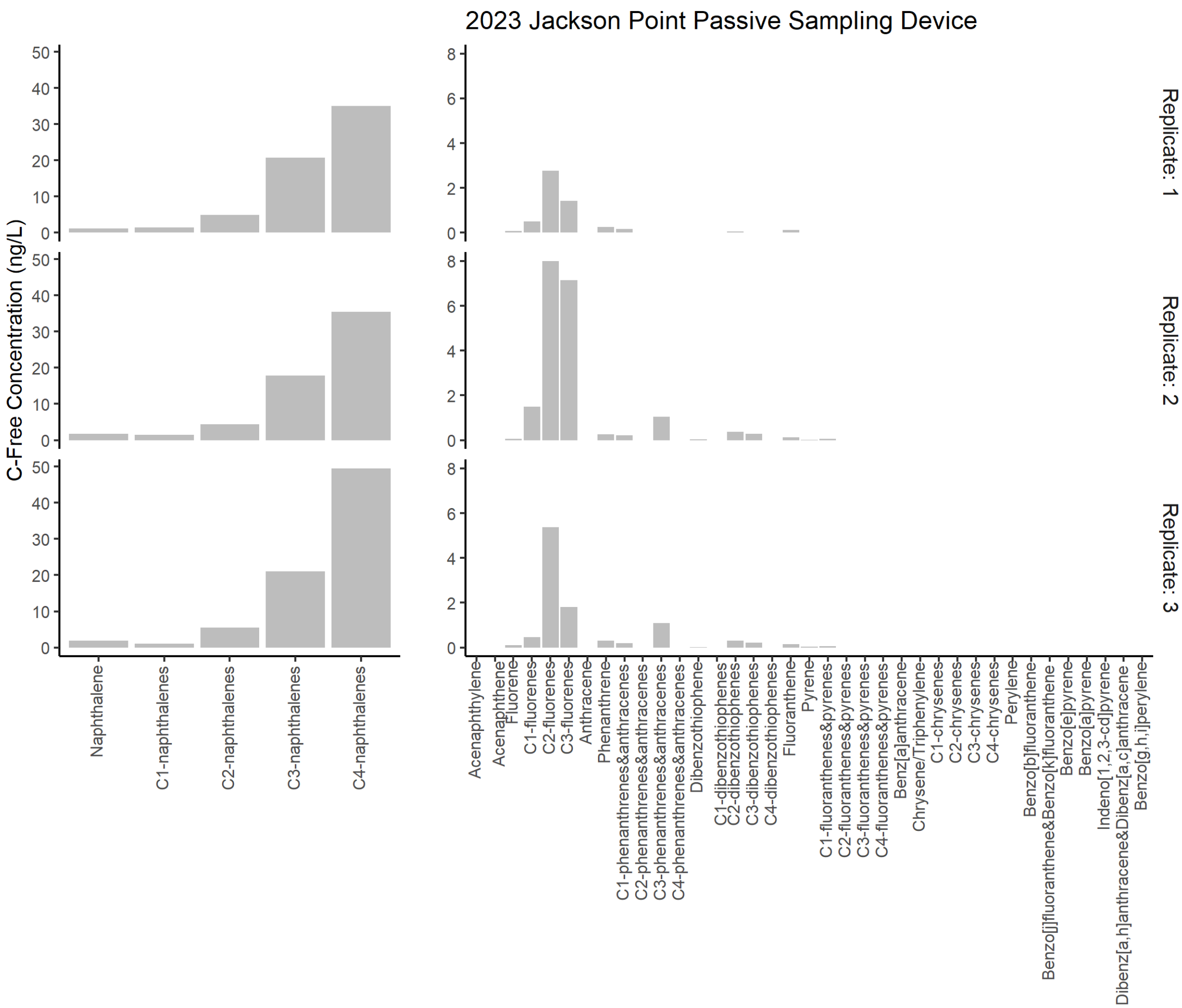

Figure 49. 2023 water PAH profiles from individual passive sampling devices deployed at Jackson Point.

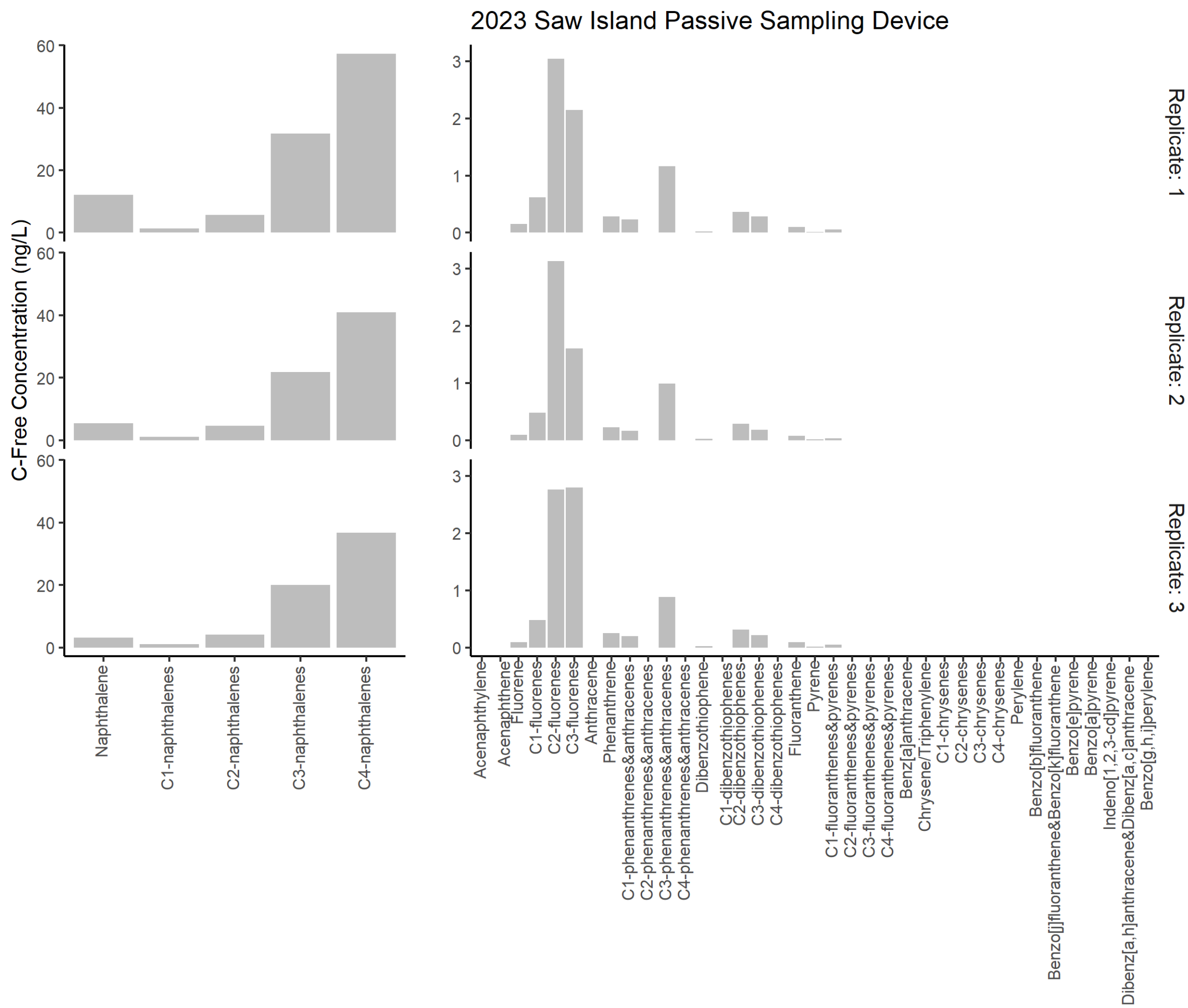

Figure 50. 2023 water PAH profiles from individual passive sampling devices deployed at Saw Island.